ANCHORAGE ZONE BEHAVIOR OF POST-TENSIONED BRIDGE DECKS WITH CLOSELY-SPACED ANCHORAGES

APPROVED:

_____

_____

To my wife,

Deeda

ANCHORAGE ZONE BEHAVIOR OF POST-TENSIONED BRIDGE DECKS WITH CLOSELY-SPACED ANCHORAGES

by

JOHN ALAN BURGESS, BSCE

REPORT

Presented to the Faculty of the Graduate School of
The University of Texas at Austin
in Partial Fulfillment
of the Requirements
for the Degree of

MASTER OF SCIENCE IN ENGINEERING

THE UNIVERSITY OF TEXAS AT AUSTIN

August 1986

ACKNOWLEDGMENTS

The author wishes to express his sincere gratitude to Dr. John E. Breen for his encouragement, wisdom, and assistance throughout this research project. Additional thanks to Dr. Ned Burns for his guidance and knowledge.

The author would like to thank to his parents for all of their support from the beginning. Finally, the author wishes express his love to his wife, Deeda for her patience, love, and understanding throughout this endeavor.

John Alan Burgess

The University of Texas
June 1986

TABLE OF CONTENTS

Chapter Page

Chapter Page

LIST OF TABLES

LIST OF FIGURES

CHAPTER 1

INTRODUCTION

1.1 Introduction

Deteriorating bridge decks are a national problem. Billions of dollars will be spent rehabilitating existing bridge decks and researching techniques to improve the durability of future ones. One promising method studied at the University of Texas at Austin by Poston and Phipps [1] was transverse post-tensioning. Cracked concrete provides a potential path for moisture and salts to penetrate the bridge deck and cause frost and corrosion damage. Transverse post-tensioning can essentially eliminate cracking in the bridge deck under service loading, thus improving the durability of the deck.

The success of a post-tensioned slab relies on the critical transfer of load from the high strength steel strands to the concrete through a small localized anchorage zone. Stresses induced by anchoring a prestressed tendon at the edge of a thin concrete slab, where it is uneconomical to have enlarged end blocks with substantial additional reinforcement to resist anchorage zone stresses, may lead to cracking or even failure of the concrete in the anchorage zone.

In their study of transverse post-tensioned bridge decks for composite slab-girder systems, Poston and Phipps [1] determined extra tendons were required in the regions containing diaphrams.
If transverse tendons were equally spaced, the lateral restraining effect of the diaphrams tended to reduce the transverse stress in the bridge deck in the vicinity of diaphrams. To compensate for this stress reduction, Poston and Phipps found more closely-space tendons would be required in the diaphram regions to achieve a uniform state of transverse stress in the slab. Figure 1.1 shows a bridge deck with

(a) Transversely post-tensioned bridge deck

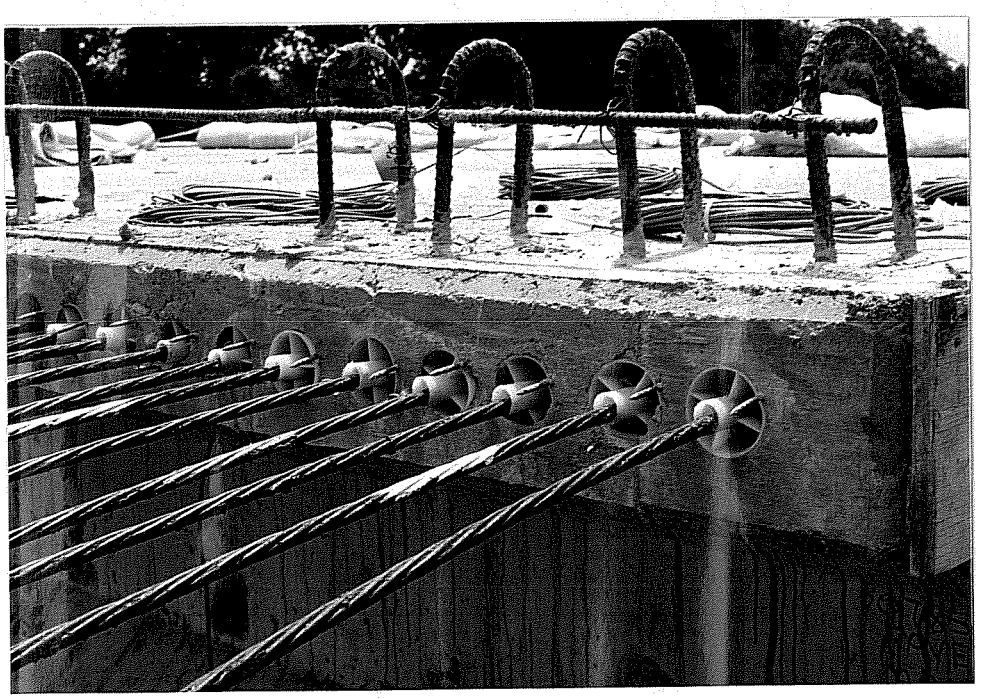

(b) Closely-spaced bridge deck anchorages

Fig. 1.1 Transversely post-tensioned bridge deck with closely-spaced anchorages

closely-spaced anchorages. In preliminary investigations to ensure cracking in the anchorage zone would not be a controlling factor in the bridge deck design, Poston and Phipps found current design provisions provided little guidance for the design of post-tensioned anchorage zones with closely-spaced tendons.

The accurate determination of stresses in the vicinity of a single end anchorage is complex. When many anchorages are placed side by side to provide the force level required to prestress a slab, the difficultly of anchorage zone analysis is compounded. The complex and expensive three dimensional finite element analyses [2] required to accurately predict anchorage zone cracking stress levels have led ACI, AASHTO, and PTI to base their design provisions more on an accumulation of past experience and test data than on published analyses. In addition, current design recommendations do not give sufficient guidance for thin post-tensioned slabs with closely-spaced anchorages where large reinforced end blocks are not economical but where considerable structural reinforcement is present as in bridge decks. Thus, this study of the anchorage zone behavior of post-tensioned bridge decks with closely-spaced anchorages was undertaken. The objective and scope of the study is outlined in the following sections.

1.2 Objective

The principal objective of this study was to document the anchorage zone behavior of a typical reinforced and post-tensioned bridge deck with closely-spaced tendon anchorages, and to specifically determine if closely-spaced anchorages increase or decrease the cracking and ultimate load capacity of such post-tensioned bridge deck anchorage zones. A secondary objective was to examining the influence of supplementary spiral reinforcement on improving the performance of bridge deck anchorage zones. In addition, major building codes and

design specifications were reviewed to determine if current anchorage zone design provisions are applicable to multiple tendon anchorages in thin reinforced bridge slabs.

1.3 Scope

The scope of this study was limited to heavily reinforced bridge decks. The intent of the study was not to investigate the broad range of thin post-tensioned slab applications such as typical commerical building slabs which contain minimal amounts of conventional bonded reinforcement but to focus primarily on heavily reinforced bridge deck slabs.

Also the scope was limited to a pilot study of twelve full scale anchorage zone models. The purpose here was to determine trends in the performance of post-tensioned bridge deck anchorage zones with closely-spaced anchorages and not to develop design provisions addressing such variables as slab thickness and tendon spacing. Throughout the experimental program an eight inch slab thickness was used. However, two types of tendon anchorages were investigated; a single strand and a four strand anchorage.

1.4 Nature of Slab Anchorage Zone Stresses

A fundamental difference in pre-tensioned and post-tensioned concrete lies in the method of transferring the large forces in the high-strength steel strands to the concrete. In pre-tensioning applications, before the concrete is cast, the strands are tensioned between two jacking points in a stressing bed. After casting the concrete bonds to the unprotected steel strands along their full length. Once the concrete reaches adequate strength, the jacking force is released. The strands try to return to their original unstretched length but because of the bond between the two materials, the concrete is

forced into compression. Thus in this method, the high pre-tensioned force in the strands is transferred to the concrete through bond over the length of the strand.

In post-tensioning, the strands are enclosed in a plastic or metal tube to prevent bonding between the concrete and steel strands. After the concrete has attained sufficient strength, the strands are tensioned and anchored at the ends of the slab with anchorage hardware which apply load to the concrete through bearing plates. In some applications the tendons may be subsequently bonded by grouting but this does not relieve the heavy load at the anchorages during stressing. Thus the major difference in post-tensioning lies in transferring the large prestress force in the strands to the concrete through a small end bearing anchorage compared to distributing it throughout the length of the strand through bond.

The direct bearing of a large prestress force on the edge of the concrete slab results in a complex state of stress in the immediate vicinity of the anchorage. St. Venant's principle states that a concentrated force applied over a small localized area should exhibit an essentially uniform stress distribution at a distance approximately equal to the depth of the section. The region between the applied force and the zone which has a uniform stress distribution is called the lead-in zone or anchorage zone as illustrated in Figure 1.2a. The stress distribution in the zone is not uniform and cannot be analyzed by the usual laws of strength of materials.

Schlaich [3], using a "truss analogy," perceived the applied prestress force in the anchorage zone being resisted by a series of compression struts and tension ties in a truss-like action. If the compression flow lines in Figure 1.2a are replaced with compression struts as shown in Figure 1.2b, it is evident a tension tie between the compression struts is required for equilibrium to resist the transverse component of the compression flow. The magnitude of stress in the tension tie is directly related to the slope of the compression strut. This tensile stress tends to split or burst the section transversely

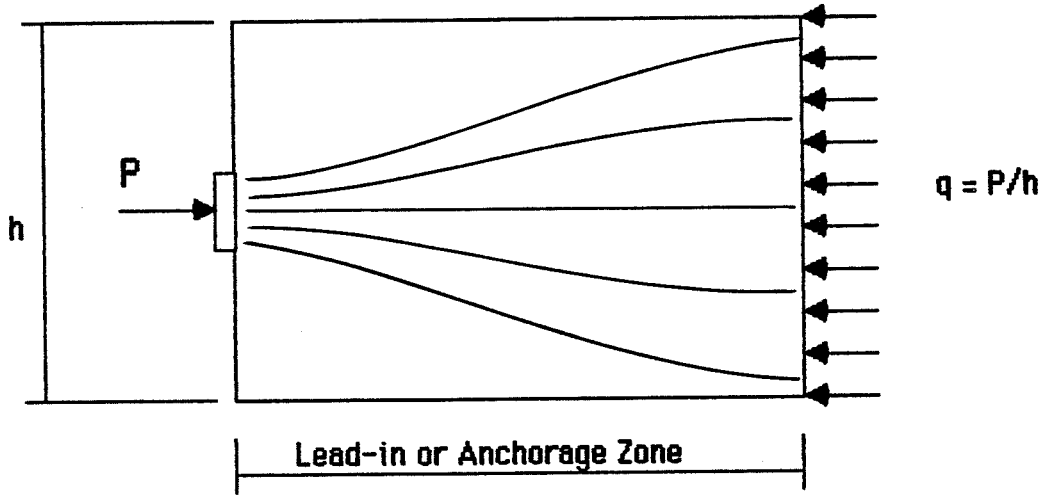

(a) Anchorage zone

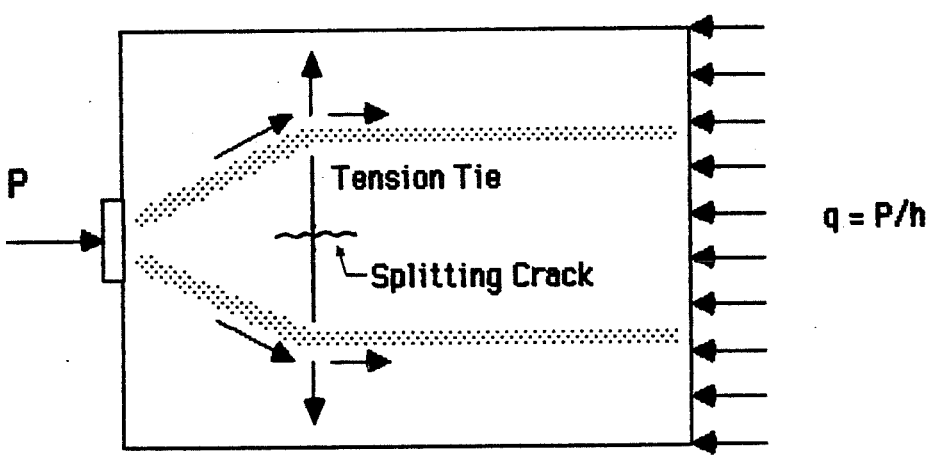

(b) Truss analogy for an anchorage zone

Fig. 1.2 Post-Tensioned slab anchorage zone with one anchorage

along the tendon path, as shown in Figure 1.2b, and is called bursting stress. The variation of stress from compression to tension along the tendon path is shown in Figure 1.3.

In addition to bursting stress, another tension stress occurs on the surface of the slab parallel to the loaded edge as illustrated in Figure 1.4. This surface tensile stress tends to cause the concrete cover to spall off and thus has been given the name spalling stress. Intuitively, a third zone of stress can be predicted to occur directly under the anchor plate. This compressive stress results from the direct bearing of the anchorage on the concrete and is known as bearing stress. Even though these three different types of stresses have been identified in the anchorage zone, the precise interaction of the stresses has yet to be fully understood for the single anchorage case or for the more complex case of several closely-spaced anchorages.

The "truss analogy" can also provide insight into the anchorage zone behavior when the prestress force of many closely-spaced anchorages are required at the edge of a thin slab. Figure 1.5a illustrates the compression flow lines for these anchorages and, Figure 1.5b, the compression struts and tension ties. With three anchorages, the stress distribution at the beginning of the anchorage zone is closer to uniform distribution than the single anchorage case. The effect of adjacent anchorages actually reduces the slope of the compression struts and in turn reduces the magnitude of the tensile bursting stresses. Thus the problems with multiple anchorages may not be as critical for bursting stresses as originally thought.

The accurate determination of stresses in the anchorage zone of post-tensioned slabs is complex. Three methods based on elasticity theory will be discussed in the next section. Although these methods provide insight into the state of stress in the anchorage zone, the actual behavior of the concrete surrounding the anchorage is not elastic. Compressive stresses in the immediate vicinity of the

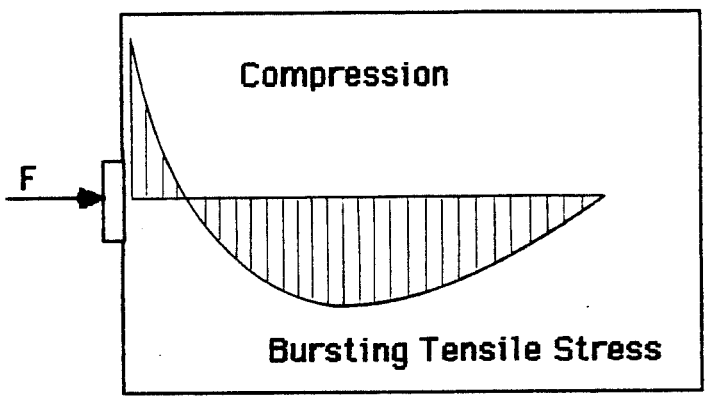

Fig. 1.3 Variation of Bursting Stress along the tendon path

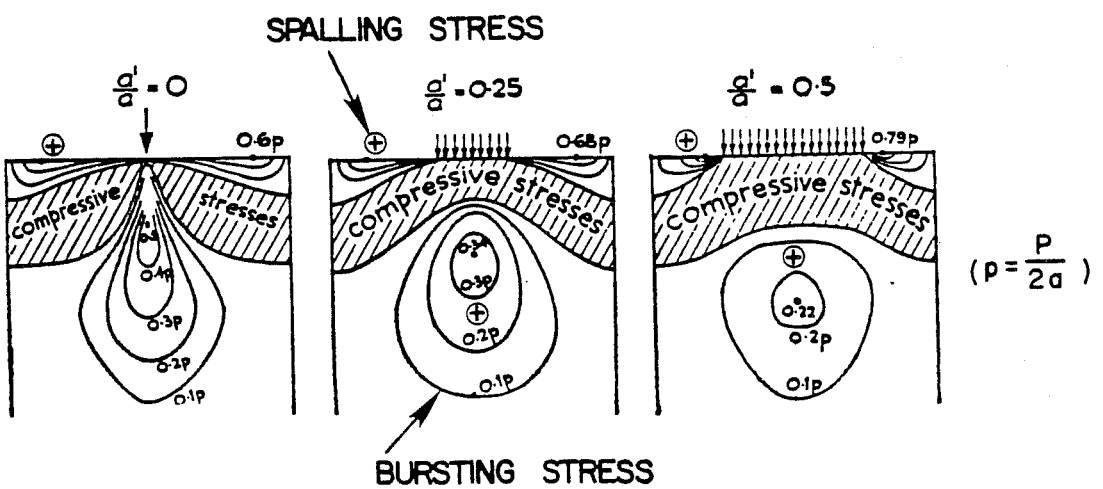

Fig. 1.4 Spalling and Bursting stresses (from Ref. #4)

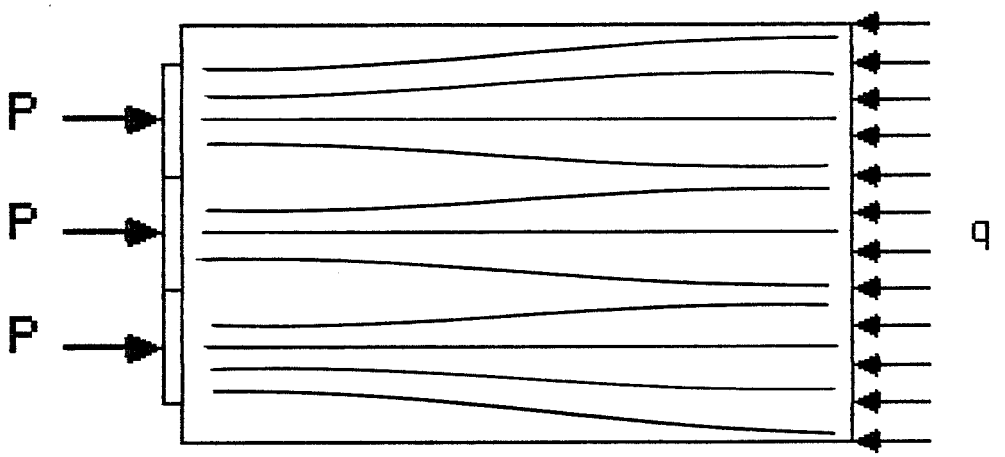

(a) Compression Flow Lines for three anchorages

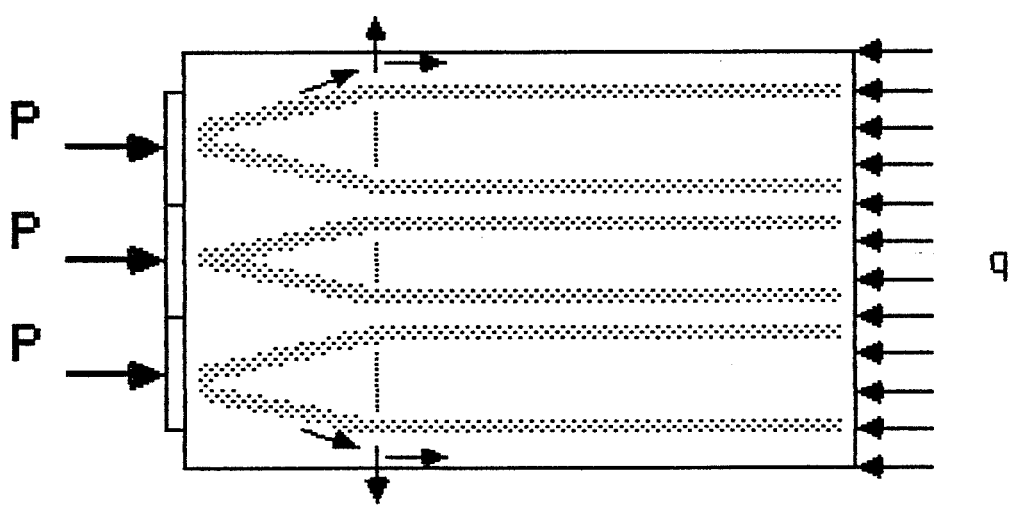

(b) Truss Analogy for three anchorages

Fig. 1.5 Post-Tensioned slab anchorage zone with three anchors

anchorage can approach or exceed the uniaxial compressive strength of the concrete thus are accompanied with high inelastic strains and deformations.

Three dimensional finite element modeling of the concrete-anchorage interaction has been used to compute stresses in post-tensioned girders that closely correlate with observed stresses in full scale tests [2]. However, the analysis is expensive and the input is so complex that it is generally beyond the scope of practical applications. Even though elastic theory results are only valid prior to cracking, they are useful in determining where the tensile stresses occur and consequently alert the designer to regions where anchorage zone reinforcement may be required. In the next section, provisions for the design of post-tensioned anchorage zones are reviewed.

1.5 Design Provisions

1.5.1 Guyon. The first major contribution in the study of anchorage zone stresses occurred in the early 1950's. Guyon [4], while investigating the tensile stresses responsible for cracking problems in early post-tensioning applications in Europe, found localized stresses at right angles to the line of action of the applied force which tended to burst the element transversely. Guyon developed a theoretical model based on two-dimensional elasticity to analyze the bursting stresses which he discovered in post-tensioned anchorage zones. His theorical analysis has been verified by photoelastic tests and by other elasticity solutions developed in the mid -1960's.

In addition to his elasticity solutions for symmetrical axial loads, Guyon derived the symmetrical prism analogy for eccentric axial loads and the successive resultants method for the case of multiple anchorages in a rectangular end block. Full development of these methods are found in Guyon texts [4, 5]. Guyon's anchorage zone design provisions were originally developed for post-tensioned girders with enlarged end blocks to resist the anchorage zone stresses. Caution

should be exercised in applying these methods to thin slabs where it is uneconomical to have enlarged end blocks to resist the high stress concentration. Guyon's two-dimensional elastic analyses were the basis of subsequent investigations by Leonhardt [6], Rhodes and Turner [7], and many others. Guyon's analyses are mentioned here for their important historical significance.

1.5.2 Leonhardt. Leonhardt [6] developed recommendations for the design of tensile reinforcement in the anchorage zone for single anchorages based on earlier work by Guyon [4]. For the two-dimensional problem, where the concentrically applied force is assumed to be spread over the entire width of the member, as shown in Figure 1.6, Leonhardt suggested the following expression for the total splitting force attributed to the bursting stresses:

$$Z = 0.3\,P\,(1 - a/h)$$

where

Z = total splitting or bursting force
P = tendon force
a = depth of the anchor plate
h = depth of the concrete section

Figure 1.7 from Leonhardt's text shows the distribution of the tensile stresses in a direction perpendicular to the tendon path. By integrating these curves, Leonhard derived the above expression. The reinforcement should be designed to resist the total splitting force, Z. Leondhardt suggested that "sufficient vertical reinforcement acting at a unit stress of 0.6 x reinforcement yield stress to resist the computed value of Z should be distributed within the distance of h/2 of the anchorage location." Leonhardt's expression only applies to single anchorages.

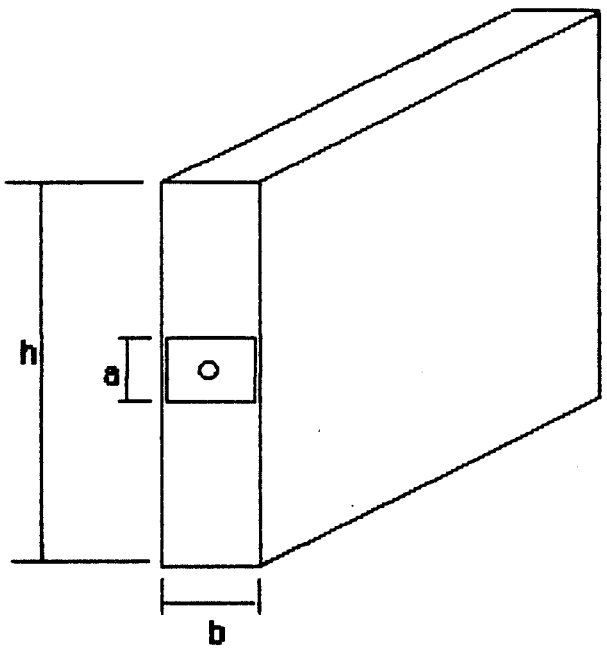

Fig. 1.6 Geometric Variables used in Leonhardt's Equation

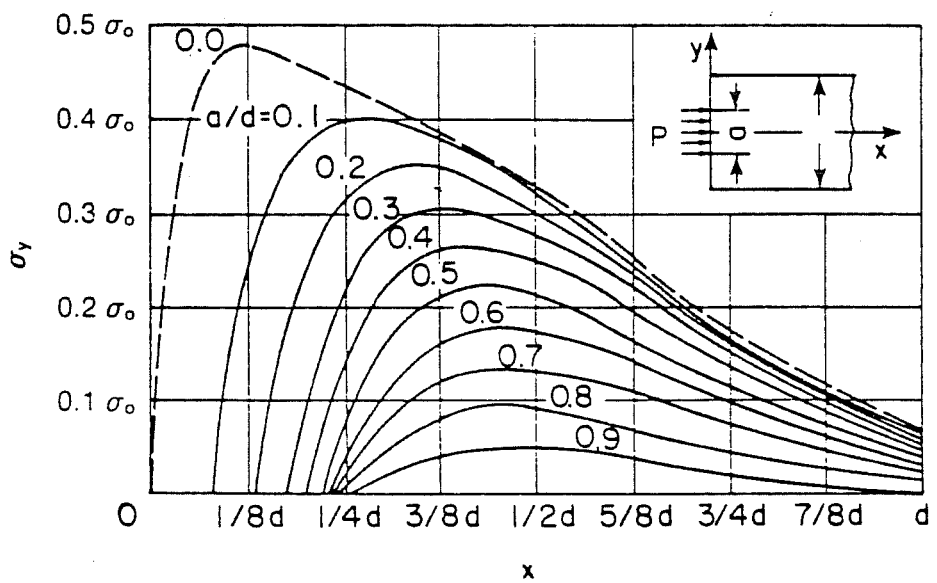

Fig. 1.7 Distribution of tensile stress perpendicular to tendon path (Ref. #6)

1.5.3 Rhodes and Turner. In 1966 Rhodes and Turner [7] developed a series of expressions where the total amount of reinforcement required to resist the bursting stresses could be easily calulated. They based these expressions on data from the extensive physical testing program of Zielinski and Rowe [8]. Rhodes and Turner's design equations will be developed fully in this section since they apply to both single and closely-spaced anchorages of square or rectangular design.

In an approach similar to Guyon, the first step in the Rhodes and Turner method is to determine the dimensions of the effective prism for each end anchorage. Examples are shown in Figure 1.8. A square anchor of side $2a_1$ is assumed to act on a prism of side and depth 2a. The dimension 2a is equal to the least distance between the center line of the anchor and the edge of the concrete or half clear distance to the neighboring anchor. If a rectangular anchor with a dimension of $2a_1$ by $2b_1$ is used, it is assumed to act on a rectangular prism of cross section 2a by 2b. In this case, two ratios a_1/a and b_1/b can be computed, giving different tensile forces in two perpendicular directions. For each prism, the uniform direct stress in the prism is

$$f_c = P/A_c$$

where

P = the maximum prestressing force

A_c = the cross-sectional area of the prism minus the area of the tendon duct

The maximum bursting tensile stress is

$$f_n = Bf_c$$

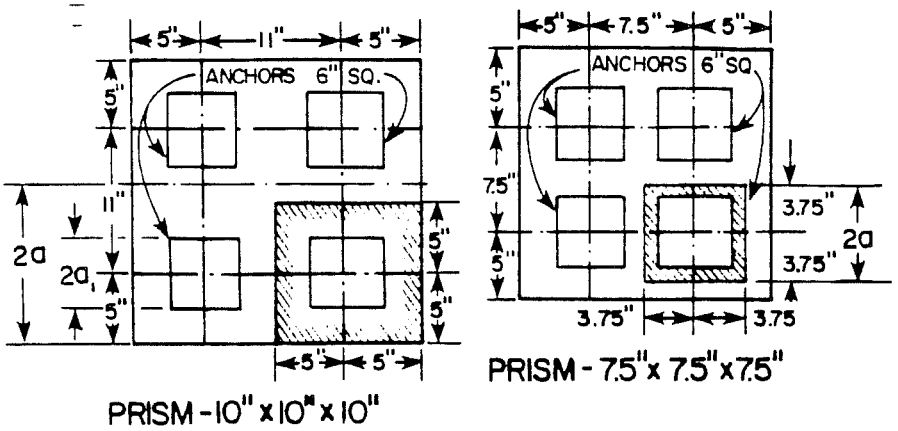

Fig. 1.8 Determination of prisms for end blocks (from Ref #7)

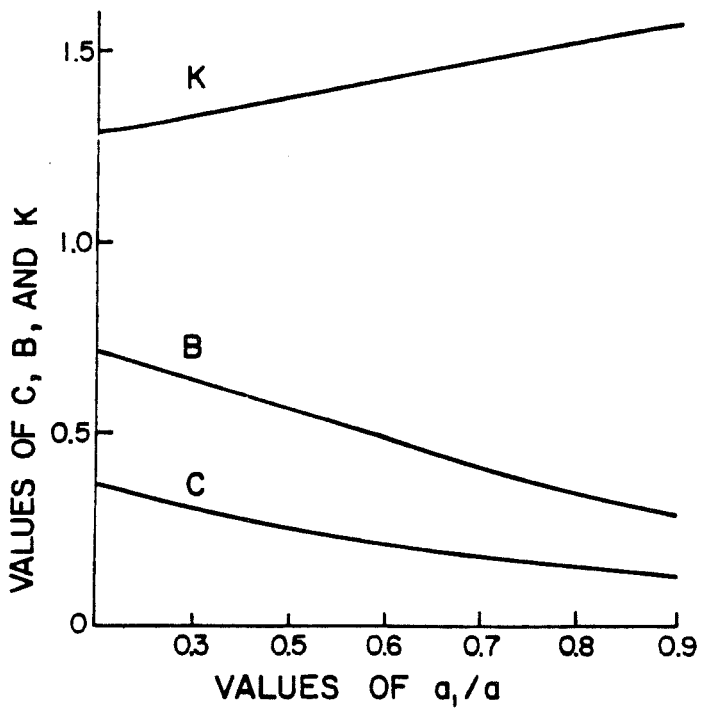

Fig. 1.9 Values of coefficients B, C, and K for Rhodes and Turner Equations (from Ref. #7)

and the total bursting tensile force can be expressed as

$$T = CP$$

where

B and C are parameters which vary with the ratio a_1/a and have been determined by experiment. (See Figure 1.9 for values.)

The distribution of tensile stress in the longitudinal direction (along the tendon path) can be approximated by a triangle, as shown in Figure 1.10. If a permissible tensile stress is specified the theoretical length requiring reinforcement can be limted to the shaded length in figure 1.11. With the concrete resisting part of the tensile force, the tension T_R to be resisted by the reinforcement is given by:

$$T_R = T [1 - (f_t / f_n)^2]$$

where

f_t = the permissible tensile stress.

Zielinski and Rowe [8] found that the strains which occur in end blocks prior to cracking correspond to apparent tensile strength in excess of the splitting tensile strength of the concrete. The ratio of apparent strength to splitting strength is a function of the ratio a_1/a and is denoted by the coefficient K (see Fig 1.9). The permissible tensile stress f_t is therefore assumed to be equal to 0.8Kr, in which r is the tensile splitting strength of the concrete. Tensile stresses greater than f_t must be resisted by the reinforcement, at a working strss f_s of 20,000 psi for mild steel bars or 30,000 psi for hot-rolled deformed bars. The area of reinforcement A_s, required in each

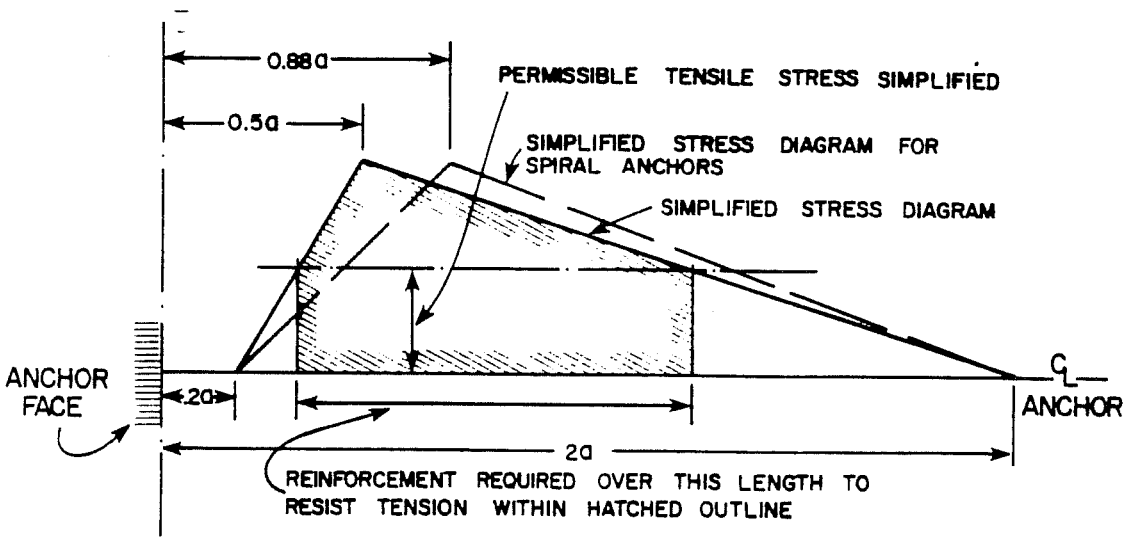

Fig. 1.10 Approximate bursting stress distribution (from Ref. #7)

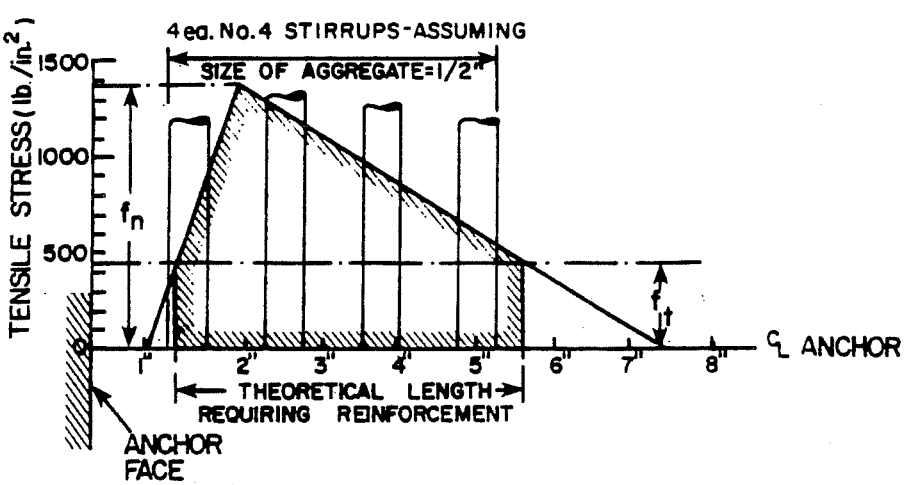

Fig. 1.11 Placement of reinforcement (from Ref. #7)

direction, in any prism containing a single anchorage is

$$A_s = T_R / f_s$$

If the tensile splitting strength for concrete is not available, Rhodes and Turner recommend the relationship

$$r = 0.5\, u^{0.75}$$

where

u = cube compressive strength.

Rhodes and Turner's design equations have been the most specific method reviewed thus far for the design of reinforcement based upon experimental study.

1.5.4 ACI. The American Concrete Institute Building Code, ACI 318-83 [9], requires reinforcement of the tendon anchorage zone to resist excessive anchorage zone stresses; however, it provides little guidance in computing these stresses or designing an effective reinforcing system. Section 18.13 of ACI 318-83 states:

> 18.13.1 - Reinforcement shall be provided where required in tendon anchorage zones to resist bursting, splitting, and spalling forces induced by tendon anchorages. Regions of abrupt change in section shall be adequately reinforced.
> 18.13.2 - End blocks shall be provided where required for support bearing or for distribution of concentrated prestressing forces.
> 18.13.3 - Post-tensioning anchorages and supporting concrete shall be designed to resist maximum jacking force for strength of concrete at time of prestressing.
> 18.13.4 - Post-tensioning anchorage zones shall be

designed to develop the guaranteed ultimate tensile strength of prestressing tendons using a strength reduction factor ø of 0.90 for concrete.

The Commentary [9] for section 18.13 suggests the following formulas from the PTI Post-Tensioning Manual [10] to size tendon anchorages based on permissible bearing stresses when experimental data or more refined analysis are not available:

(1) Immediately after tendon anchorage:

$$f_b = 0.8\, f'_{ci} \sqrt{A_2/A_1 - 0.2} \leq 1.25\, f'_{ci}$$

(2) After allowance for prestress losses:

$$f_b = 0.6\, f'_c \sqrt{A_2/A_1} \leq f'_c$$

where

A_1 = bearing area of anchor plate of post-tensioning tendons

A_2 = maximum area of the portion of the anchorage surface that is geometrically similar to, and concentric with, the area of the anchor plate of the post-tensioning tendons.

f_b = permissible concrete bearing stress under the anchor plate of post-tensioning tendons with the end anchorage region adequately reinforced.

The Commentary does note that "the actual stresses are quite complicated around post-tensioning anchorages," but no recommendations are made for satisfying the reinforcement requirements for the bursting and spalling forces induced by single or several closely-spaced anchorages.

1.5.5 PTI. As stated in previous section, the PTI Post-Tensioning Manual [10] provides the same equations as ACI to size tendon anchorages based on permissible bearing stresses. However, PTI adds the comment that special reinforcement, required for the performance of the anchorage, shall be indicated by the tendon supplier. This statement reflects the current trend in the post-tensioning industry in that anchorage zones are extremely complex to analyze and, in most cases, it is easier and more accurate to verify a newly developed proposed anchorage zone design by actual testing.

In contrast to ACI, PTI does address bursting and spalling stresses. Section 6.2.7 (2) states:

> Horizontal and vertical reinforcement should be placed in front of the anchor plate to resist bursting and spalling stresses in the concrete. The amount and location of the reinforcement depends on the size, number and location of anchor plates with respect to size of the concrete section, and other variables. Often nominal reinforcement will suffice for bursting stresses. In other cases, detailed design of anchorage zone reinforcement will be required. Procedures for design of bursting reinforcement are discussed in Section 5.4.1

Section 5.4.1 of the PTI Post-Tensioning Manual presents Leonhardt's design equation for computing the reinforcement required to resist the tensile splitting force in the anchorage zone which was previously developed in section 1.5.2 of this report.

PTI also references a recent comprehensive investigation of post-tensioned girder anchorage zones by Stone and Breen [2] for additional information on the design of single strand unbonded tendon anchorages. Stone and Breen's design provisions will be reviewed in Section 1.5.8.

1.5.6 AASHTO. The 1983 AASHTO [11] Specification contained the most conservative anchorage zone design provisions reviewed. In Section 9.15.2.4 of the specification, AASHTO limits the allowable anchorage bearing stress at service load to 3000 psi but not to exceed 0.9 f'_{ci}. In reference to bursting stresses, Section 9.21.1 of the 1983 AASHTO Specification states:

> In post-tensioned members, a closely spaced grid of both vertical and horizontal bars shall be placed near the face of the end block to resist bursting stresses. Amounts of steel in the end grid should follow recommendations of the supplier of the anchorage. Where such recommendations are not available the amount of steel in the grid shall be designed and shall consist of at least No. 3 bars on 3 inch centers in each direction placed not more than 1-1/2 inches from the inside face of the anchor bearing plate.

The AASHTO Specification, like ACI, gives designers little guidance in computing bursting or spalling stresses independently from the manufacturers recommendation.

1.5.7 CEB - FIP. The Comité Euro-International du Béton (CEB) and the Federation Internationale de la Precontrainte (FIP) [12] provide an admissible bearing stress formula similar to the one used by ACI and PTI. Depending upon the coefficient of safety for concrete, γ_c, the CEB allowable bearing stress can be substantially higher than the ACI-PTI provision.

$$F_{R_{du}} = f_{cd}\sqrt{A_{cl} / A_{cd}} \leq 3.3\, f_{cd} A_{cd}$$

where

$f_{cd} = f_{ck}/\gamma_c$

f_{ck} = characteristic strength of concrete under compression

γ_c = coefficient of safety applicable to concrete

A_{cd} = the loaded area

A_{cl} = the largest area which is geometrically similar to A_{cd}, with the same center of gravity, lying totally within A_c, in the plane of A_{cd} .

$F_{R_{du}}$ = ultimate resisting force for design

In computing the anchorage zone transverse reinforcement, the CEB-FIP recommends the expression developed by Leonhardt. In general the CEB-FIP code recommends:

> The determination of the additional reinforcement may be based on the theory of elasticity or on the equilibrium and compatibility of a rational internal system of forces. In both cases, the method used must be proven experimentally .

1.5.8 Stone and Breen. An extensive analytical and experimental study of the behavior of post-tensioned girder anchorage zones with single large tendons was recently completed by Stone and Breen [3] at the University of Texas at Austin. The results of this comprehensive investigation were published in the March-April 1984 issue of the PCI Journal [13]. Stone and Breen have developed a design equation that predicts the cracking load for thin web anchorage zones without supplementary anchorage reinforcement. The design equation considers variables such as tendon inclination and eccentricity common to post-tensioned girders but the equation also applies to single

unbonded tendon anchorages as well. Stone and Breen's equation was developed from a comprehensive regression analysis of experimental test data and three dimensional finite element method analyses.

Since the equations include terms involving tendon inclination and eccentricity not generally found in post-tensioned slabs, a simplied form of this equation can be written as:

$$P_{cr} = t\{(f_{sp}/24)(38a - 120) - 7\} + 39a' + (f_{sp}/5)\{166 - 975(a'/t)^2\} - 9.1$$

where

$2a$ = section height, in.

$2a'$ = width of anchor plate (assumed square), in.

t = section thickness, in.

f_{sp} = split cylinder tensile strength, ksi (may be conservatively estimated in psi as $6.5\sqrt{f'_c}$)

P_{cr} = cracking load for section with plate anchor, without supplementary anchorage reinforcement, kips

Figure 1.12 defines the geometric variables, 2a, 2a' and t. Since the equation is based on empirical results, the following limitations restrict the application of the above equation:

1. Thin prismatic web sections are assumed where $0.05 \leq t/2a \leq 0.25$
2. Multiple tendons anchored in the same web sections are not covered.
3. The anchorage is assumed to be square.

Although not verified experimentally, Stone and Breen's equation can be extended to cover (1) multiple anchorages across thick

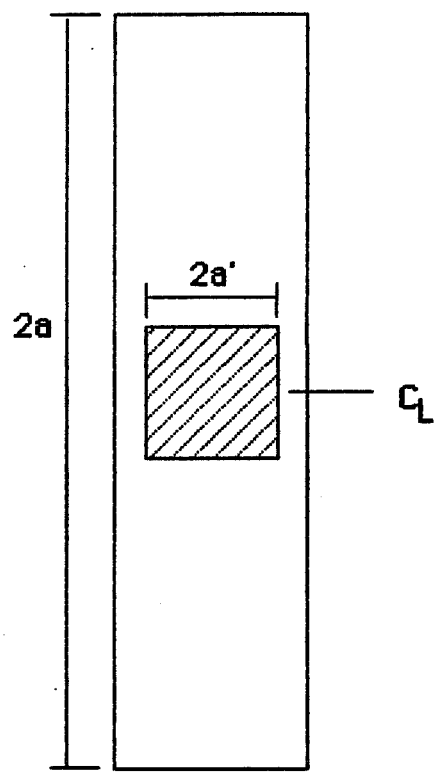

Fig. 1.12 Geometric Variables used in Stone & Breen's Equation

web sections and (2) rectangular anchor plates oriented such that $2a' \leq 2a$ as illustrated in Figure 1.13. To apply the design equation for these cases, replace the value t in the equation with 2g which equals twice the edge distance or the distance between the anchors.

The design equation can also be modified to account for the expected rise in cracking and ultimate loads for anchorage zones with supplementary reinforcement. For a reinforced anchorage zone with adequate supplementary spiral reinforcement and no tendon eccentricity, the cracking and ultimate load can be predicted, respectively, by

$$P'_{cr} = 2.03\, P_{cr}$$
$$P_{ult} = 3.18\, P_{cr}$$

In Chapter Four, the accuracy of the design provisons reviewed in this section will be compared with the experimental values obtained in the test program described in Chapter Two.

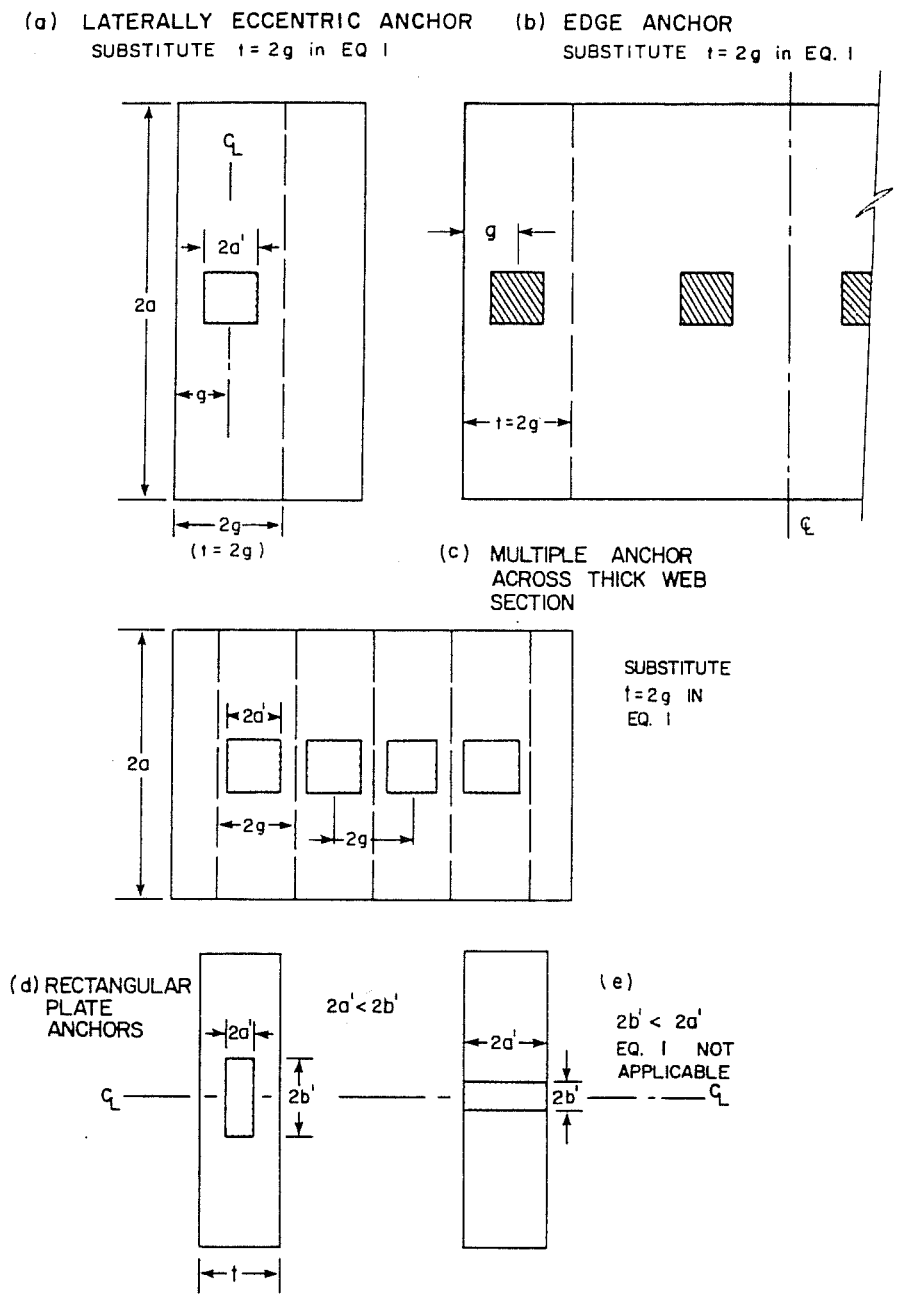

Fig. 1.13 Special cases for Stone and Breen Equation (from Ref. #13)

CHAPTER 2

EXPERIMENTAL PROGRAM

2.1 Introduction

The direct bearing of a large prestress force on the edge of a concrete slab results in a complex state of stress in the immediate vicinity of a tendon anchorage. The complexity of the stress state increases with the interaction of several closely-spaced anchorages. To study anchorage zone behavior of thin post-tensioned bridge decks, an experimental program was developed to test full scale anchorage zone models. This experimental program focused on a strength comparison between a bridge-deck slab anchorage zone with a single anchorage to one with several closely-spaced anchorages.

In general, the term post-tensioned slab can be used to refer to post-tensioned building slabs, parking garage slabs or bridge deck slabs. In this specific study of bridge decks, a careful distinction between bridge deck slabs and building slabs is required. Bridge deck slabs contain substantially larger amounts of conventional bonded reinforcement than commerical building slabs. Both types of slabs transfer static dead and live loads to support points through flexure however, bridge decks are also subject to moving loads, large temperature induced deformations, freezing and thawing cycles, and attacks on the reinforcement by corrosive agents. These additional demands on bridge decks required larger quantities of bonded reinforcement and larger clear cover requirements. Since more reinforcement and concrete cover tend to increase the strength of the anchorage zone, the results of this bridge-deck test program may not

be applicable to all types of post-tensioned slabs. Again, extreme caution is advised in applying the results of this study to slabs other than heavily reinforced bridge decks.

2.2 Description of Test Specimens and Materials

2.2.1 Specimen Variables and Dimensions. The proposed bridge deck design of the Texas Department of Highways and Public Transportation's Colorado River Bridge in LaGrange, Texas served as the prototype in developing twelve full scale anchorage models. Previous finite element analyses performed by Stone [2] on post-tensioned girders indicated that the anchorage zone stresses were sufficiently localized in the region surrounding the anchorage. Thus, for testing purposes, only a small section of the slab is required to be constructed to accurately model the localized behavior of anchorage zones. Typically, in this investigation, length of the test specimens were approximately equal to four or five times the longest dimension of the anchorage.

The twelve test specimens can be categorized into three groups as shown in Figure 2.1. The first group was planned to examine the performance of the center anchorage when two adjacent, previously stressed anchorages are present (Figure 2.1a). The second group has the same width as the first, but was planned to examine the performance of the center anchorage without adjacent anchorages (Figure 2.1b). Similar to the second group, the third group was planned to examine the performance of a single anchorage but now in a slab of width equal to the spacing of the anchorages in the first group (Figure 2.1c).

The controlled test parameters within each specimen group included type of tendon anchorage and amount of anchorage zone reinforcement. There are several types of post-tensioning anchorages, produced by a variety of manufacturers, used for prestressing thin

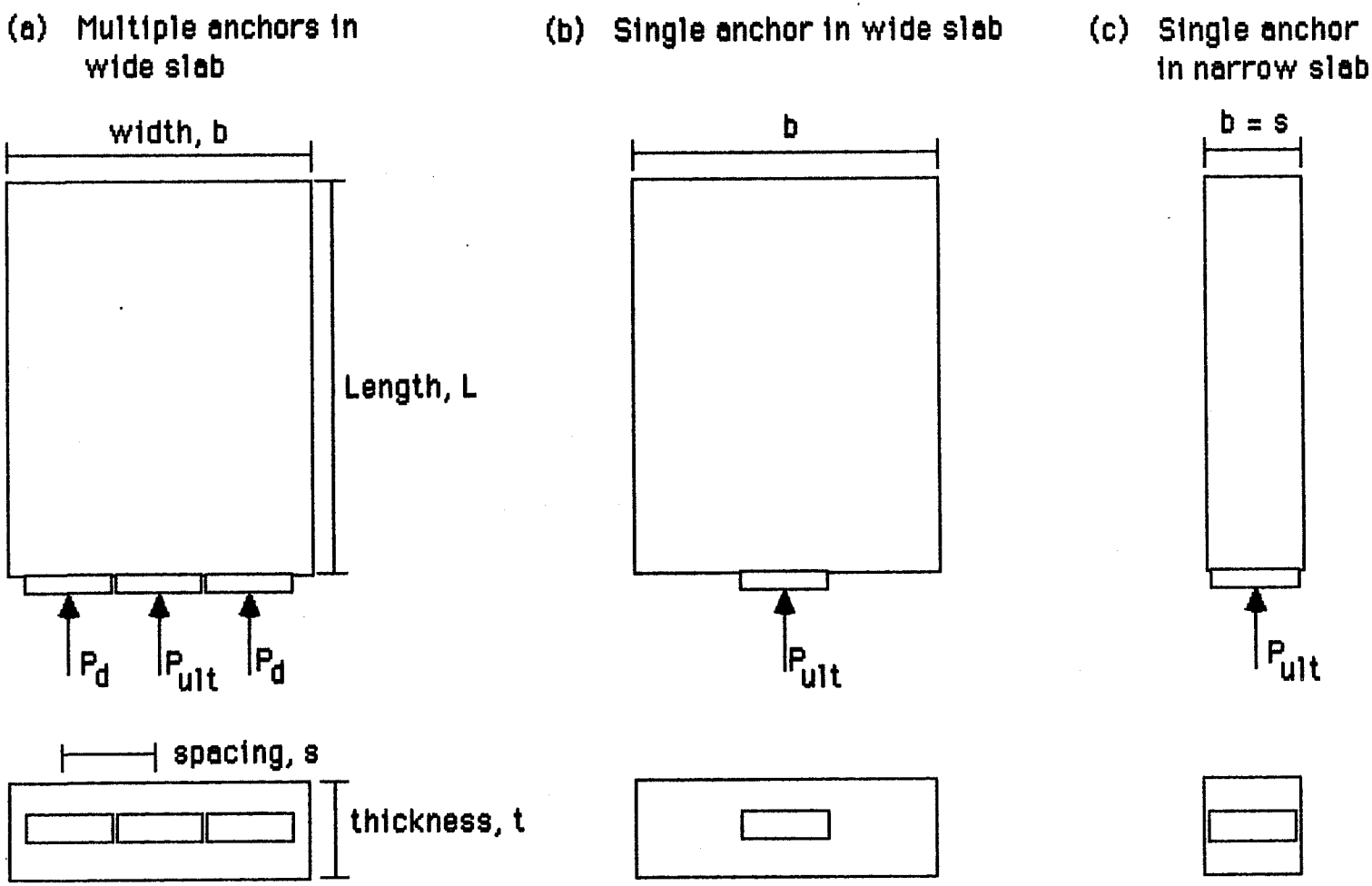

Figure 2.1 Test Specimen Groups

slabs. Two anchorages manufactured by the VSL Corporation were used in this test program; the monostrand and multistrand anchorage. Six test specimens were post-tensioned with monostrand anchorages and six with multistrand anchorages. Details of the monostrand and multistrand anchorages are given in Sections 2.2.3 and 2.2.4, respectively.

In addition to typical bridge deck reinforcement, all of the specimens contained two # 4 reinforcing bars, directly behind the anchor, as minimum anchorage zone reinforcement. However, half of the specimens also contained additional spiral reinforcement to determine if the performance of the anchorage zone could be enhanced by confining the compressed concrete laterally within column-like spiral reinforcement. Details of the bridge deck and anchorage zone reinforcement are given in Sections 2.26 and 2.27, respectfully.

The slab specimens were eight inches thick; the same thickness as the prototype bridge deck. All other dimensions and test program variables for each specimen are listed in Table 2.1 and illustrated in Figure 2.2. To identify each specimen, an alphanumeric sequence was used to indicate specimen anchorage type, number of anchors and specimen width. The alphanumeric sequence is illustrated by the following examples:

1) MO-1NS where MO = monostrand anchorage
1 = specimen contains one anchorage
N = narrow width specimen
S = spiral reinforcement is provided

2) MU-3W where MU = multistrand anchorage
3 = specimen contains three anchorages
W = wide width specimen
(blank) = no spiral reinforcement

Table 2.1 Test Specimen Dimensions and Parameters

Specimen	Specimen Length	Specimen Width	Number of Anchorages	Spiral Reinforcement
MO-1N	2'-0"	5"	1	No
MO-1NS	2'-0"	5"	1	Yes
MO-1W	2'-0"	1'-8"	1	No
MO-1WS	2'-0"	1'-8"	1	Yes
MO-3W	2'-0"	1'-8"	3	No
MO-3WS	2'-0"	1'-8"	3	Yes
MU-1N	3'-9"	1-6"	1	No
MU-1NS	3'-9"	1-6"	1	Yes
MU-1W	3'-9"	4'-0"	1	No
MU-1WS	3'-9"	4'-0"	1	Yes
MU-3W	3'-9"	4'-0"	3	No
MU-3WS	3'-9"	4'-0"	3	Yes

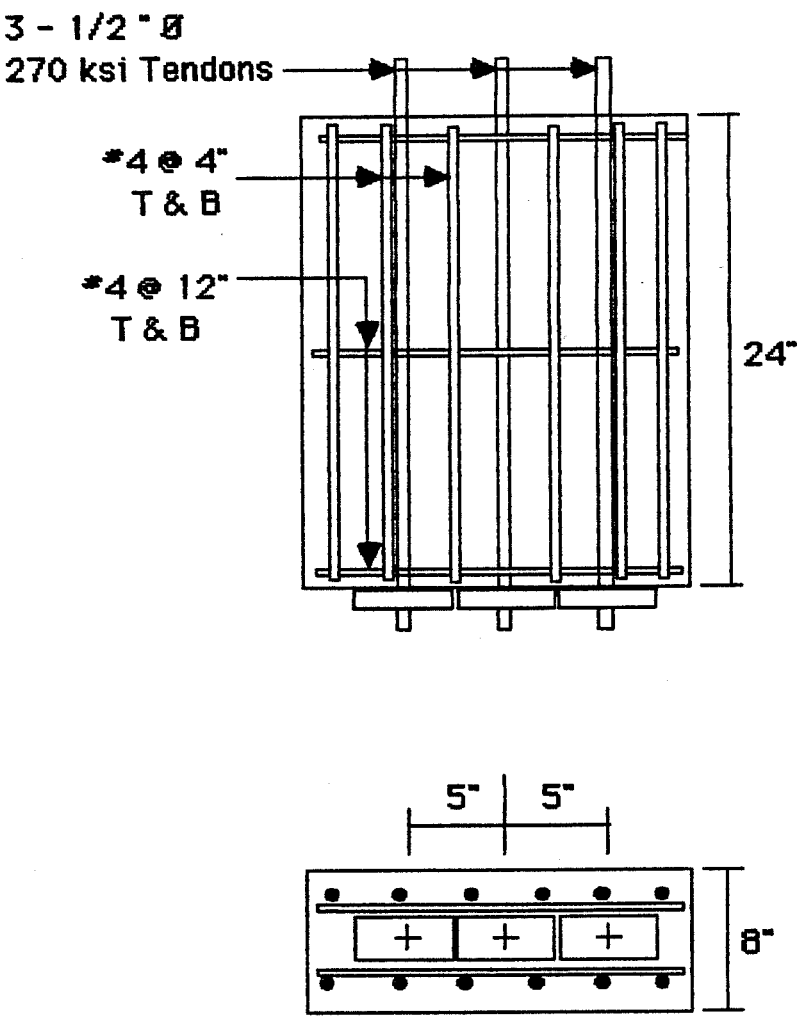

Fig. 2.2a Monostrand anchorage specimens

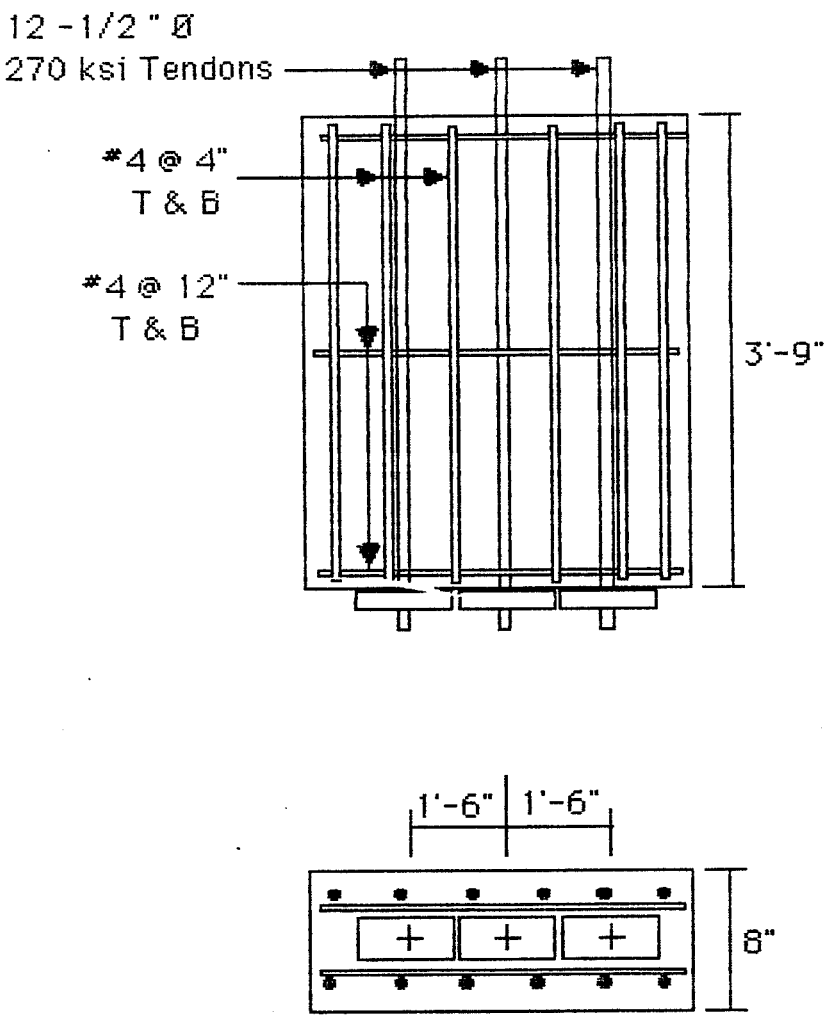

Fig. 2.2b Multistrand anchorage specimens

2.2.2 Concrete. The concrete mix used in fabricating the test specimens was Texas Department of Highways and Public Transportation Class "S" with a maximum aggregate size of 3/4 in. The mix was designed with five sacks of Type III Portland Cement per cubic yard of concrete for a concrete compressive strength of 3600 psi at 28 days. To insure adequate concrete consolidation around the anchor zone reinforcement, internal vibrators were used during the casting of the specimens. The concrete compressive strength was monitored using 6 x 12 inch cylinders and tested in accordance with ASTM C39, "Test Method for Compressive Strength of Cylindrical Concrete Specimens."

The monostrand and multistrands specimens were cast at different times from different concrete batches. One week after casting, the slab specimens were removed from a polyethylene cover, the forms stripped, and the specimens prepared for the post-tensioning procedure. The small size of the monostrand specimens allowed post-tensioning and testing to failure to be performed on the same day. The average compressive strength of the monostrand specimens during testing was 4100 psi. The larger multistrand specimens were post-tensioned 11 days and tested 14 days after casting at an average concrete strength of 3350 psi and 3600 psi, respectively.

2.2.3 Monostrand Anchorage. The monostrand anchorage system consists of an end anchor and a single grease coated prestressing strand in a protective plastic tube as shown in Figure 2.3. The dimensions of the monostrand anchor are shown in Figure 2.4a and Figure 2.4b illustrates a typical slab construction detail.

The monostrand anchorage system is designed for an unbonded system. A polyethylene tube covering the prestressing strand prevents contact between concrete and the strand. The prestressing strand is coated with a heavy grease as shown in Figure 2.4c which protects the strand from corrosion, and prevents any permanent bond between the

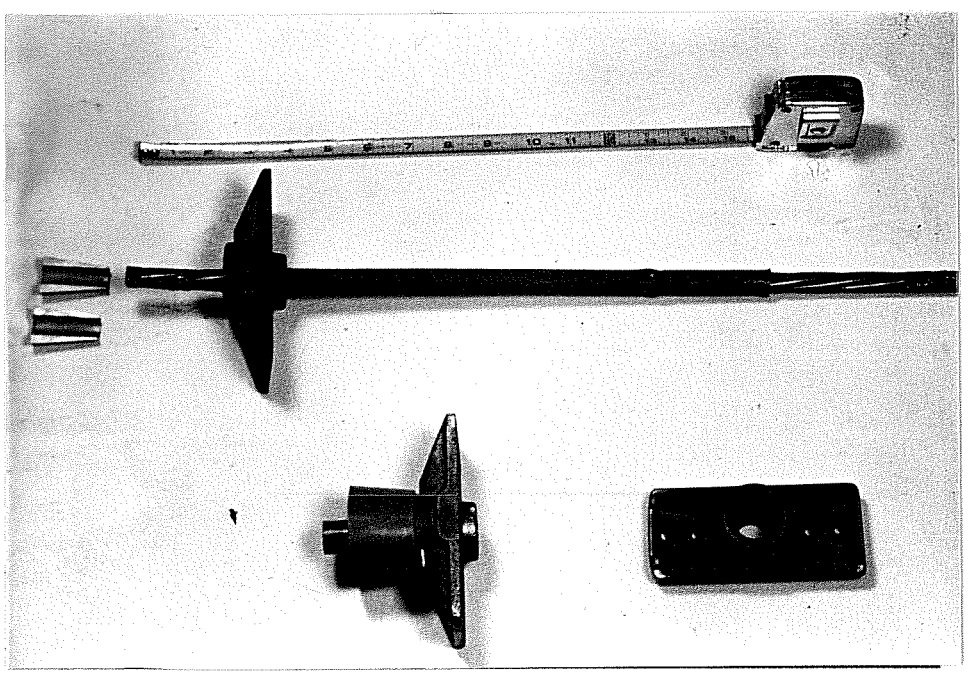

Fig. 2.3 Monostrand anchorage system

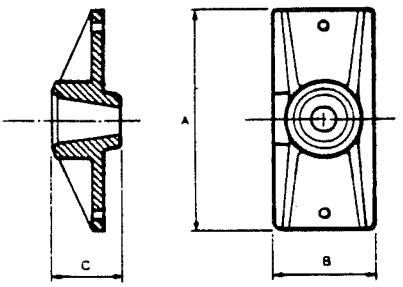

A	B	C	Bearing Area
5.00 in.	2.25 in.	1.50 in.	11.25 in.sq.

(a) Monostrand anchorage dimensions

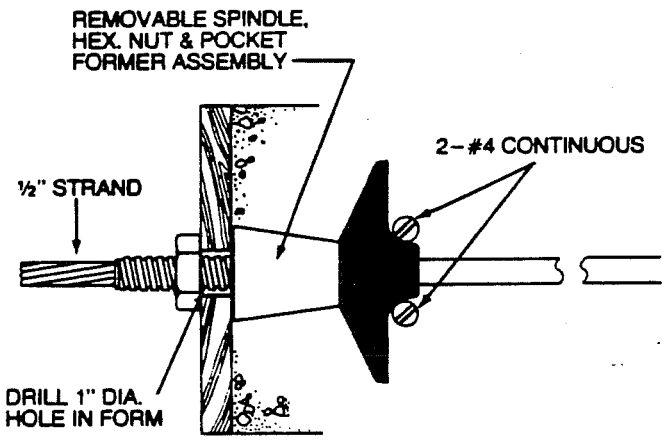

(b) construction detail

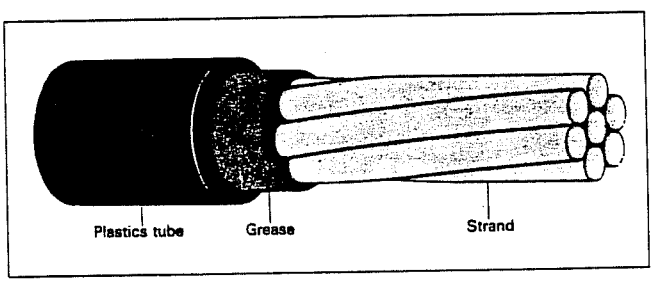

(c) Monostrand detail

Fig. 2.4 Details of monostrand anchorage system (from VSL Catalog)

tube and the strand. The protective sheathing and corrosion preventive coating are governed by requirements in Section 4 and 5 of the Specification for Unbonded Single Strand Tendons developed the Post-Tensioning Institute [14].

There are many advantages of the monostrand anchorage system. During stressing, the grease reduces friction losses between the strand and the tightly fitting tube. Also the monostrand system is less labor intensive than the multistrand system since grouting operations and hardware are not required in the unbonded system. Finally, during construction of the slab, the rather flexible plastic covered strands may be easily threaded through congested areas and are draped in negative and positive moment regions.

There are also disadvantages to the monstrand system. More closely-spaced anchorages are required to provide continuous prestressing in a slab since only one strand can be anchored at each end anchorage. Also, the prestressing strands are vulnerable to corrosion if the plastic ducts are damaged before the concrete is cast. Since the strand is anchored only at the ends in an unbonded system, damage, such as corrosion, to the end achorages could jeopardize the structural integrity of the slab by releasing all of the prestress force in the strands. Thus, complete encapsulation of the end anchorage is required for corrosion protection. The watertight encapsulation requirements are outlined in Section 3(e) of the Specification for Unbonded Single Strand Tendons [14].

2.2.4. Multistrand Anchorage. An alternative to the monostrand system of anchoring one strand at each anchorage is the mulistrand system. The larger multistrand anchorage accommodates four tendons as shown in Figure 2.5a. The sizes of the multistrand and monostrand anchorages can be visually compared in Figure 2.5b and the actual dimensions of a multistrand anchorage are given in Figure 2.6. Figure 2.7 shows one of the test specimens with three multistrand

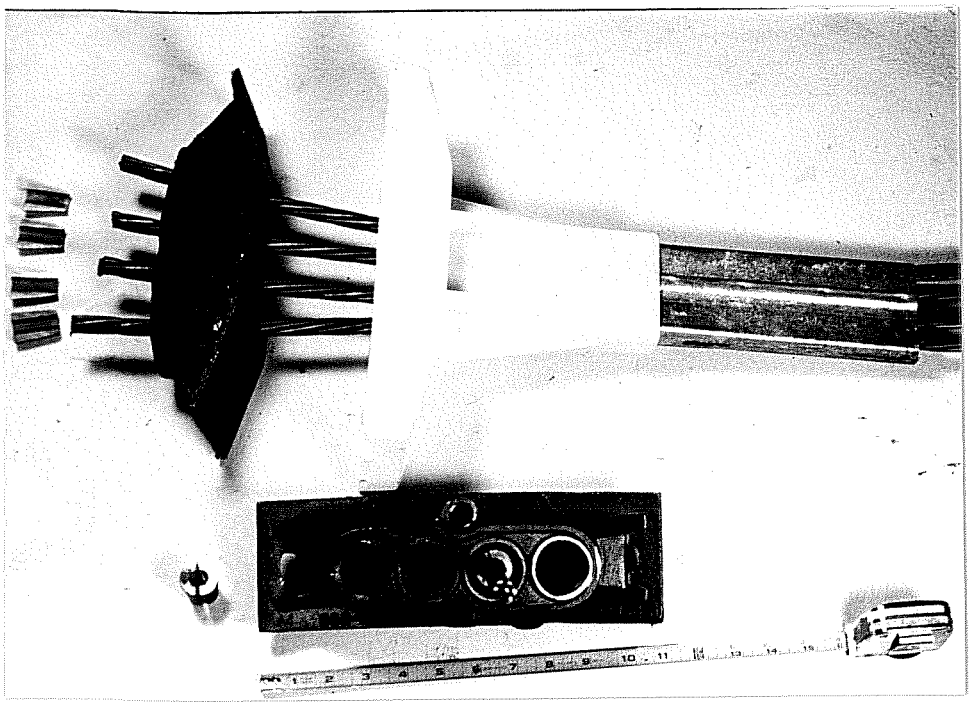

(a) Multistrand anchorage system

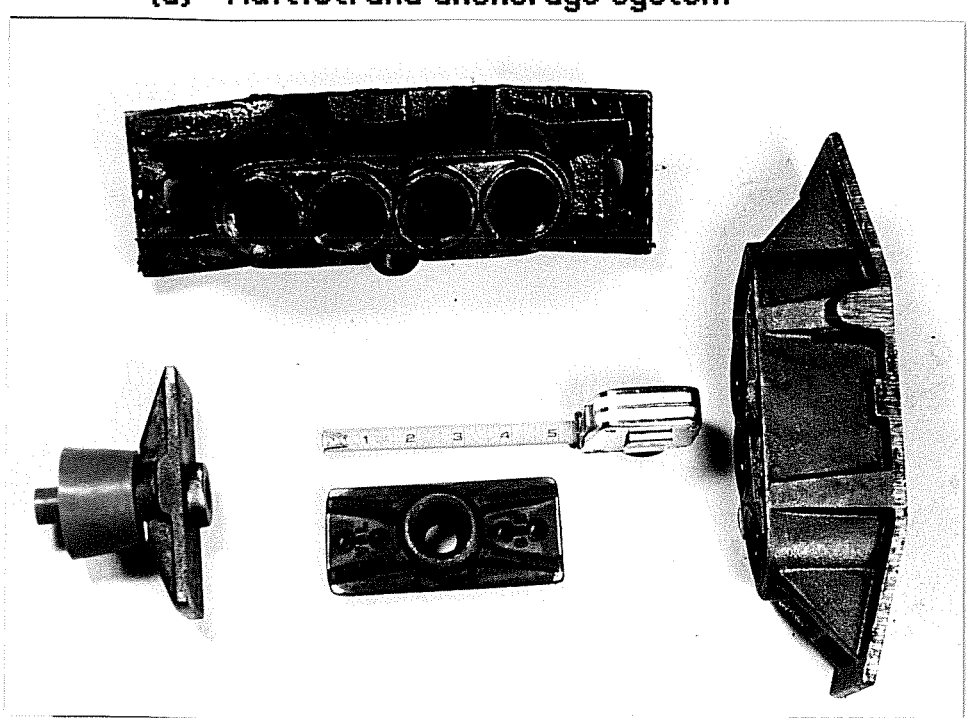

(b) Size comparison of monostrand and multistrand specimens

Fig 2.5 Multistrand anchorage system

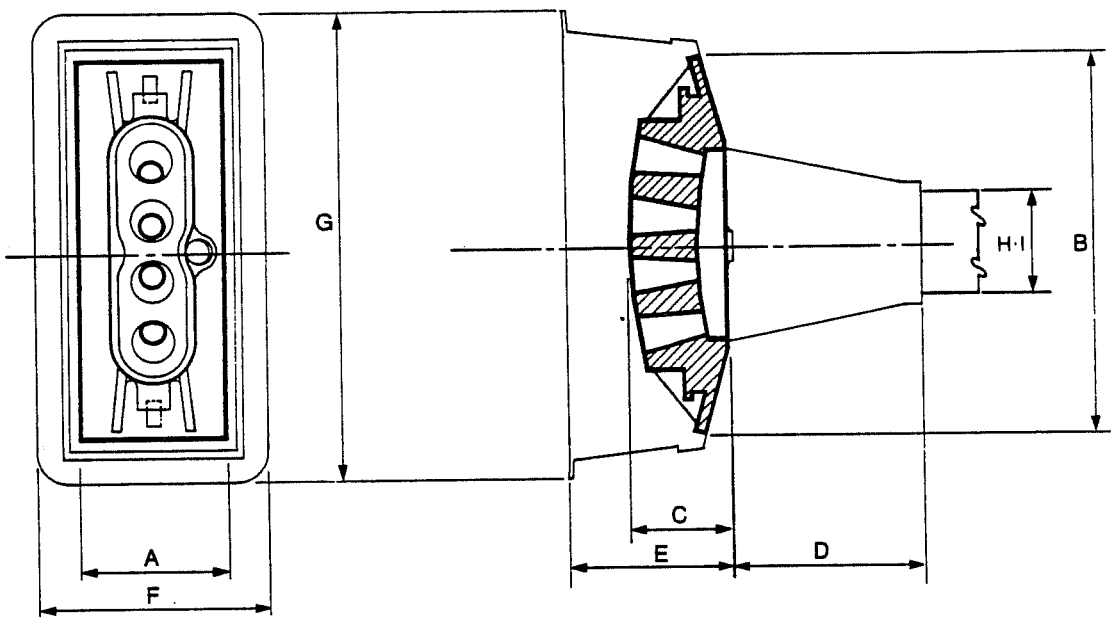

Anchorage Type	VSL SO5-4	SO6-4
A	3.50	3.50
B	11.00	11.00
C	2.87	2.87
D	6.25	6.25
E	5.00	5.00
F	5.62	5.62
G	13.00	13.00
H	3.00	3.00
I	1.00	1.00
J	24.00	24.00
K	4.00	4.00
L	2.50	2.50

Dimensions in inches.

Fig. 2.6 Multistrand anchorage dimensions (from VSL Catalog)

Fig. 2.7 Test specimen with three multistrand anchorages

anchorages. In contrast to the monostrand system, the multistrand system is a bonded system. The four tendons are enclosed in a galvanized metal duct which is filled with grout after the stressing operations are completed.

There are many advantages in using bonded tendons. Several will be enumerated. First, the layer of grout acts as an additional barrier to protect the tendons from corrosion. Second, bonded beams have an ultimate strength 10 to 30% higher than equivalent unbonded beams [15]. Third, during construction only the pocket formers and tendon ducts need to be in place when the concrete is cast. Construction time can be saved by installing the tendons and anchorages during concrete curing which is considered slack time in the construction schedule. Also installation during this time protects the tendons and anchorages from damage and corrosion during the concrete placement.

Constructability of bonded systems present two disadvantages. In congested areas, the large rigid ducts are difficult to place. Also, additional labor and costs may be associated with grouting the tendons.

2.2.5 Prestressing Strand. The prestressing strand used throughout the test program was 1/2 in. diameter, 270K Grade, seven-wire strand, conforming to the ASTM A-416 Specifications. For calculations involving the prestressing strand, a modulus of elasticity of 27500 ksi and nominal area of 0.153 sq. in. were used.

2.2.6 Slab Reinforcement. The size and spacing of the steel reinforcement in the test specimens was determined directly from the prototype bridge deck. In general, the main reinforcement in bridge decks is placed perpendicular to the flow of traffic. In the test specimens, this direction is parallel to the post-tensioning tendons. The main reinforcement was #4 deformed bars spaced 4 inches on

center, top and bottom. Figure 2.8a shows the layout of the reinforcing steel in a multistrand specimen. Perpendicular to the main reinforcement, #4 bars at 12 inch on center spacing were provided top and bottom for temperature, shrinkage and crack control. The reinforcing bars were placed at a depth of 2 inches to maintain the concrete cover requirement. In contrast to the prototype, Grade 60 steel reinforcement was used in the test specimens in place of Grade 40. This considerable amount of conventional reinforcement differs from the practice usually found in post-tensioned building slabs.

2.2.7 Anchorage Zone Reinforcement. When the localized tension stresses in the anchorage zone exceed the tensile capacity of the concrete, the concrete cracks. Additional steel reinforcement can be added in the form of deformed bars or spirals to the anchorage zone to contain the tension stresses.

All of the test specimens contained two # 4 reinforcing bars, directly behind the anchor, as minimum anchorage zone reinforcement as shown in Figure 2.4b for a monostrand specimen and in Figure 2.8b for a multistrand specimen. However, half of the specimens also contained additional spiral reinforcement as shown in Figures 2.9a and 2.9b for a multistrand specimen and in Figure 2.10 for a monostrand specimen. The spirals were formed using 1/4 in. diameter smooth Grade 60 steel rods. Figure 2.11 shows the details of the spiral reinforcing for both the monostrand and multistrand anchorages.

2.3 Post-Tensioning Procedure

This section describes the manner in which the outer anchorages of the three-anchorage specimens were post-tensioned. Figures 2.12a and 2.12b show a completed monstrand and multistrand specimen, respectively. The post-tensioning of the center anchorage of

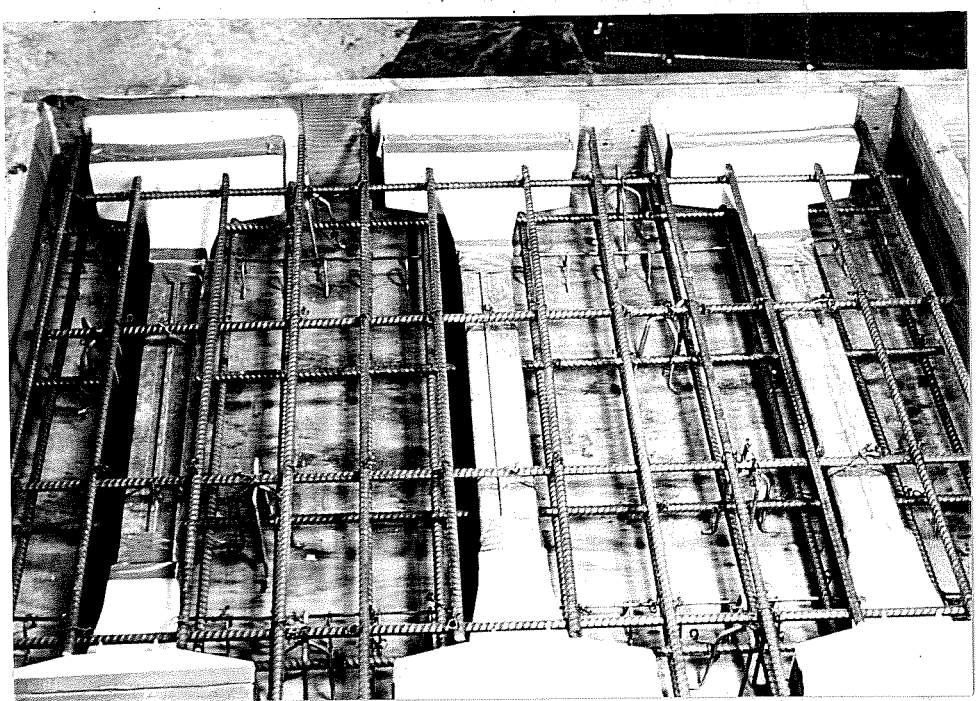

(a) Slab reinforceing steel for multistrand specimen

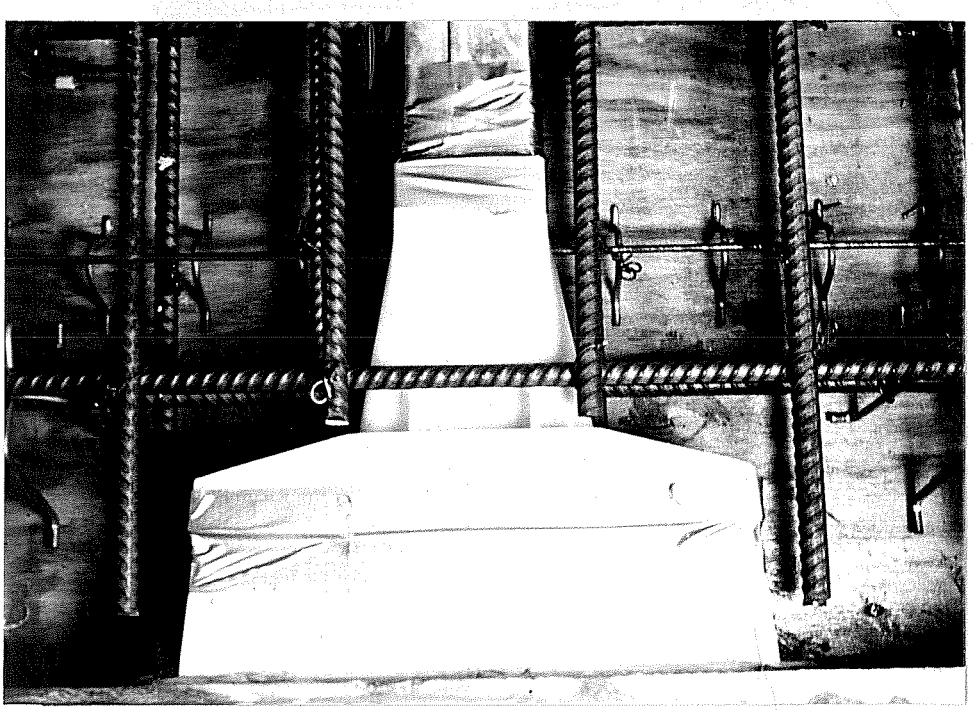

(b) Anchorage zone reinforcement for multistrand specimen

Fig 2.8 Reinforcing steel for multistrand anchorage specimen

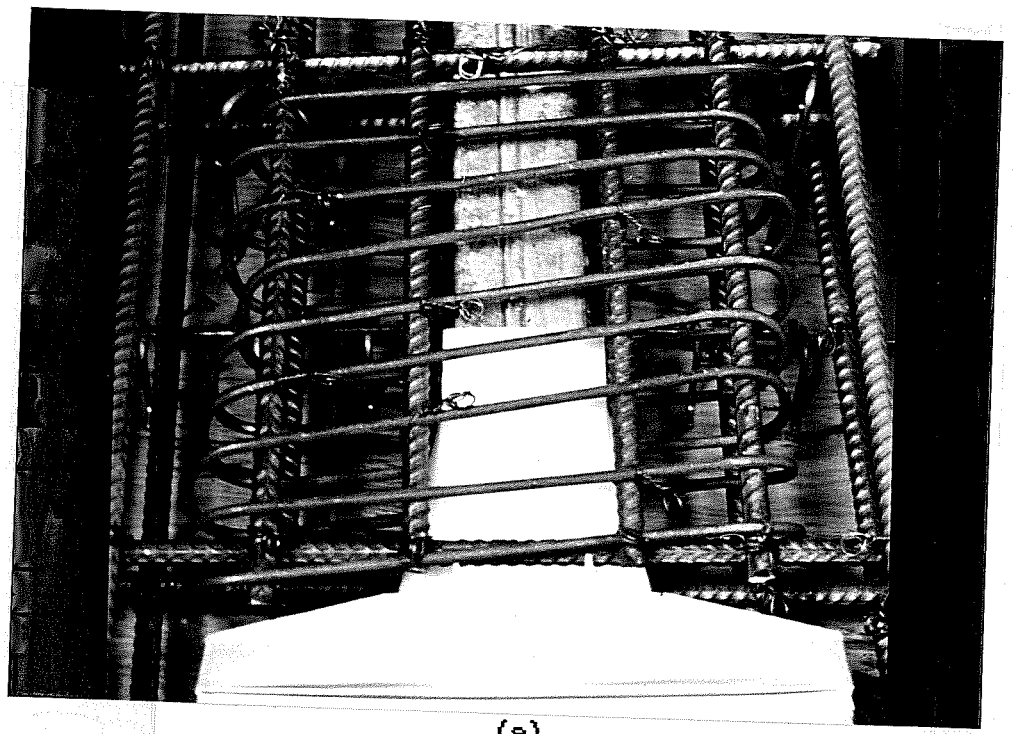

(a)

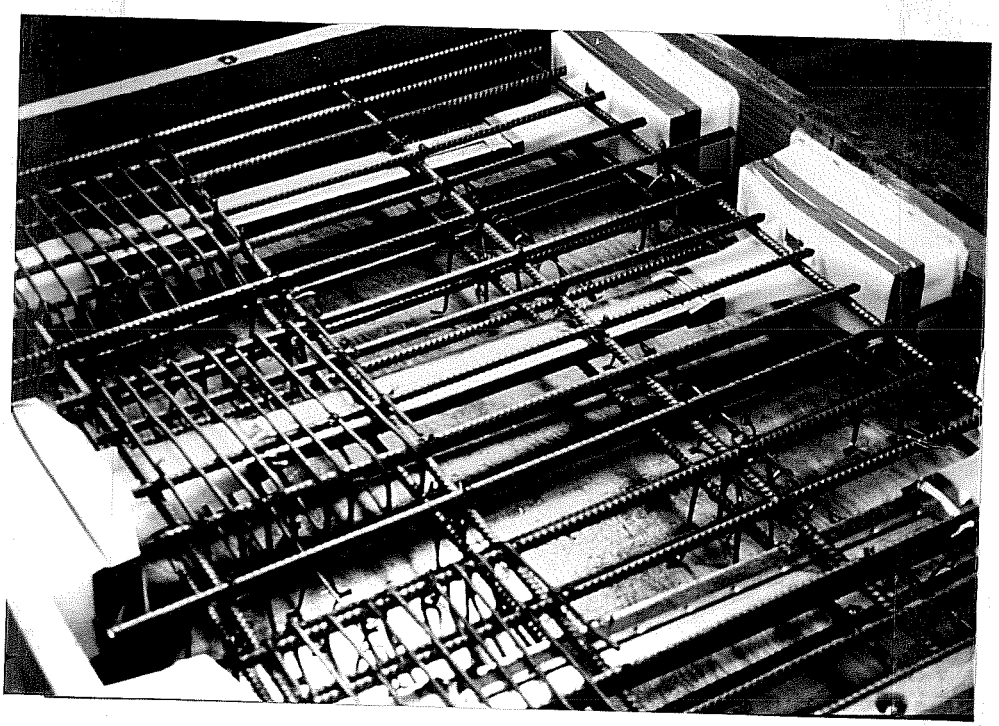

(b)

Fig 2.9 Spiral reinforcement for multistrand anchorage specimen

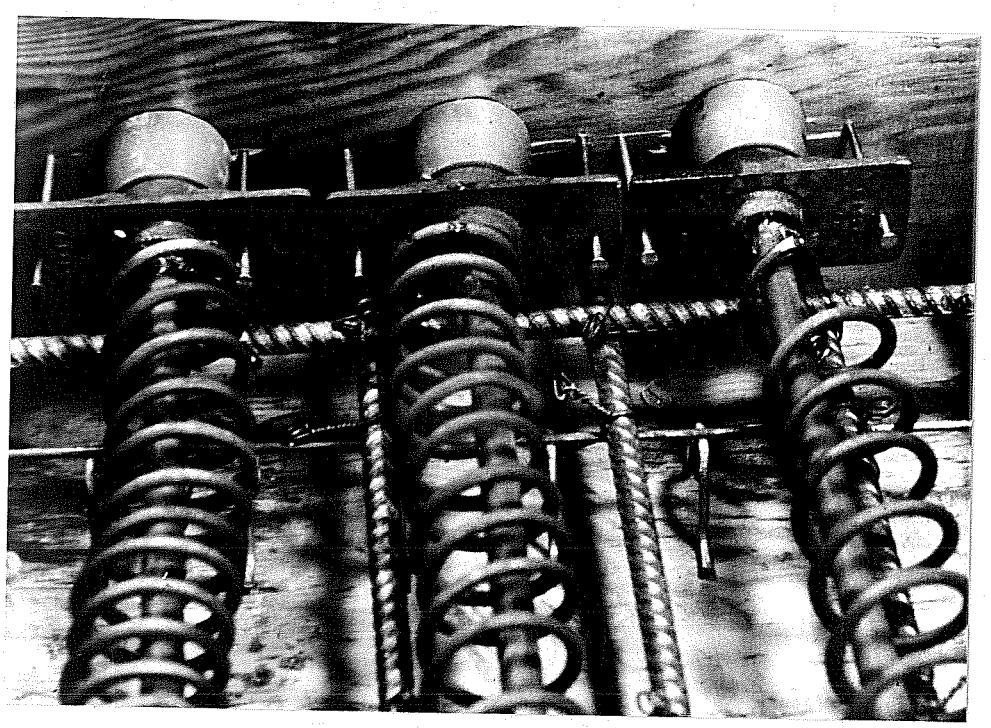

Fig. 2.10 Spiral reinforcement for monostrand anchorage

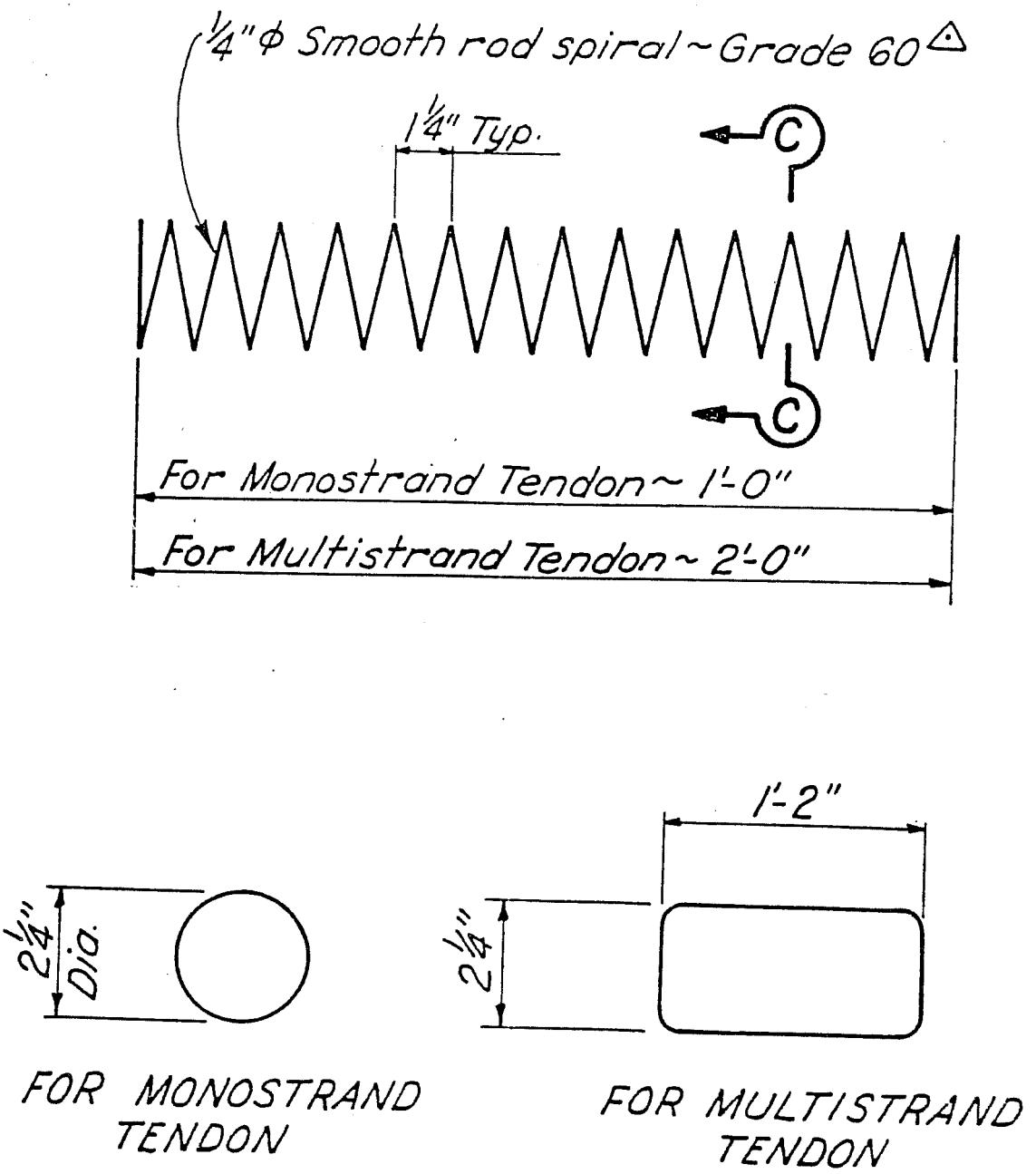

Fig. 2.11 Details of spiral reinforcement for monostrand and multistrand anchorages

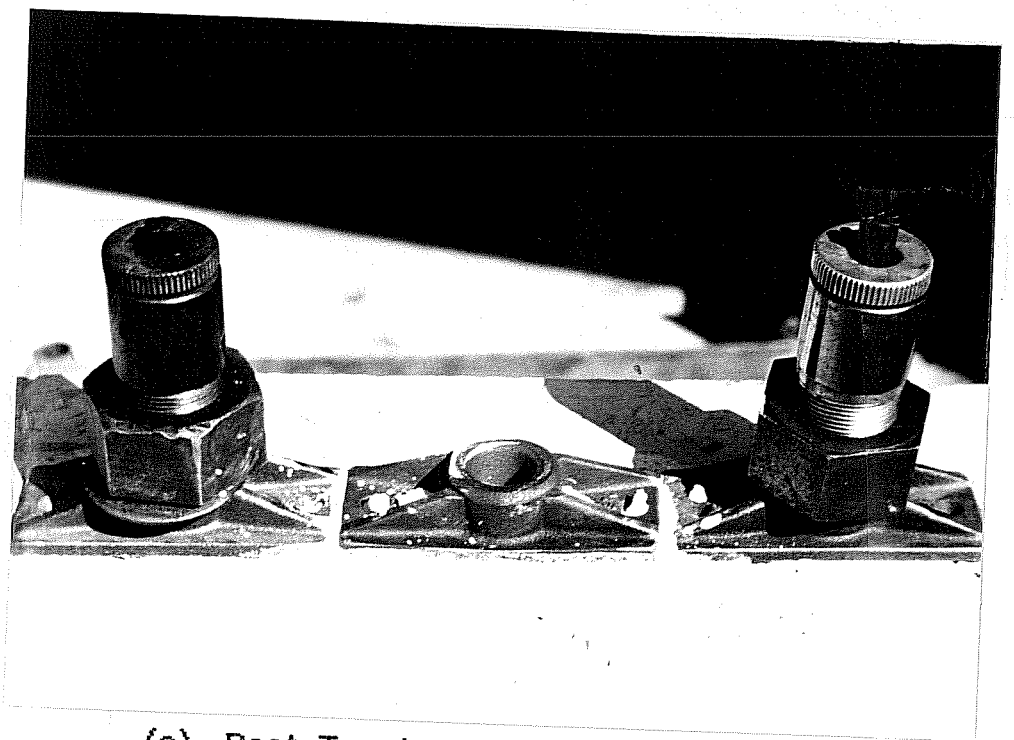

(a) Post-Tensioned monostrand specimen

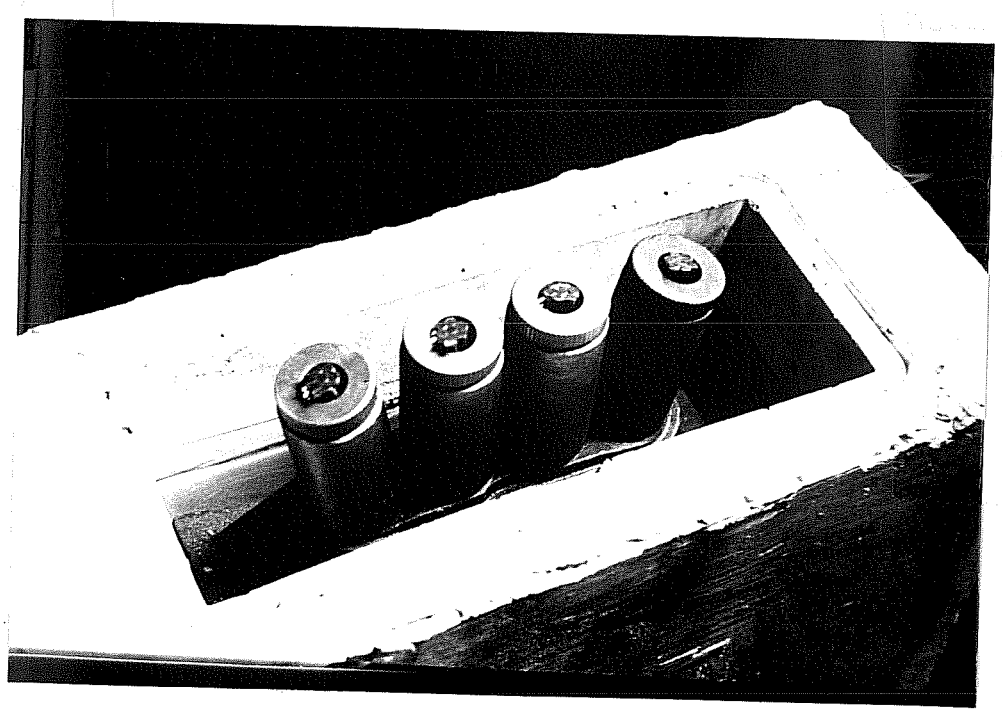

(b) Post-Tensioned multistrand specimen

Fig 2.12 Post-Tensioned specimens

the three-anchorage specimens and of the single anchorage specimens will be discussed in Section 2.4.1, the Loading System.

The ACI Building Code [9] limits the tensile stress in post-tensioning tendons immediately after anchorage to $0.70f_{pu}$. In an effort not to exceed this allowable stress, the jacking force applied to the test specimen tendons was limited to this level also. For 1/2 inch strands, this results in an equivalent force of 28.9 kips/strand.

Each strand in the outer anchorages was stressed individually using a 20 ton centerhole hydraulic ram as shown in Figure 2.13a. The load was applied slowly using a hand pump and monitored using a load cell connected to a strain indicator as shown in Figure 2.13b. The load cell and strain indicator were previously calibrated using a universal testing machine. As a precautionary measure the pressure gauge for the ram was also monitored. The pressure reading on the dial gauge was multipled by the area of the ram head to compute the applied force.

Since the specimen lengths were relatively short, special efforts were made to minimize wedge seating losses. Special screw chucks shown in Figure 2.14 were used. For the monostrand specimens, the strands were stressed to 28.9 kips. Then the screw chuck was hand tighten to remove any slack between the wedges and the strand before the ram pressure was released. The procedure was repeated until the screw did not require any adjustment upon restressing of the strand to 28.9 kips. The strands were never restressed more than twice.

When the stressing was complete the excess strand was ground off as shown in Figure 2.15. In cutting the strand, the strand reached high enough temperatures to glow red. The magnitude of any losses of prestress in the strand due to this heating and cooling is not known, but is assumed to be negligible since this is localized outside the anchor and not within the stressed region.

The close spacing of the strands in the multistrand anchorages prevented the wide screw chucks from being used on the multistrand specimens. Further deviations in the stressing procedure

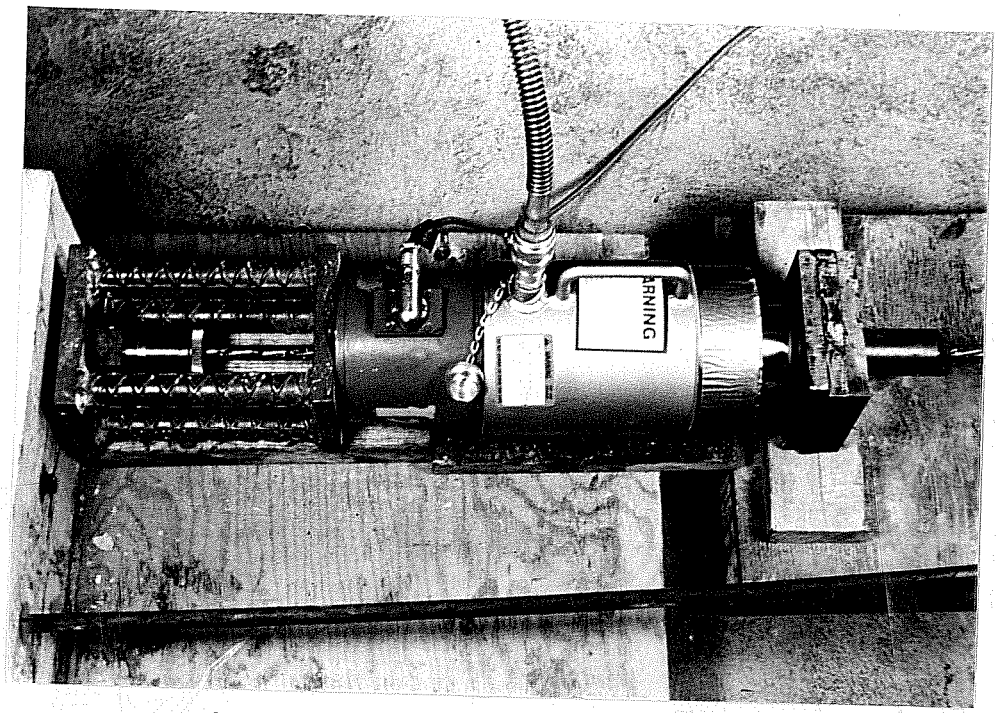

(a) Post-Tensioning hydraulic ram

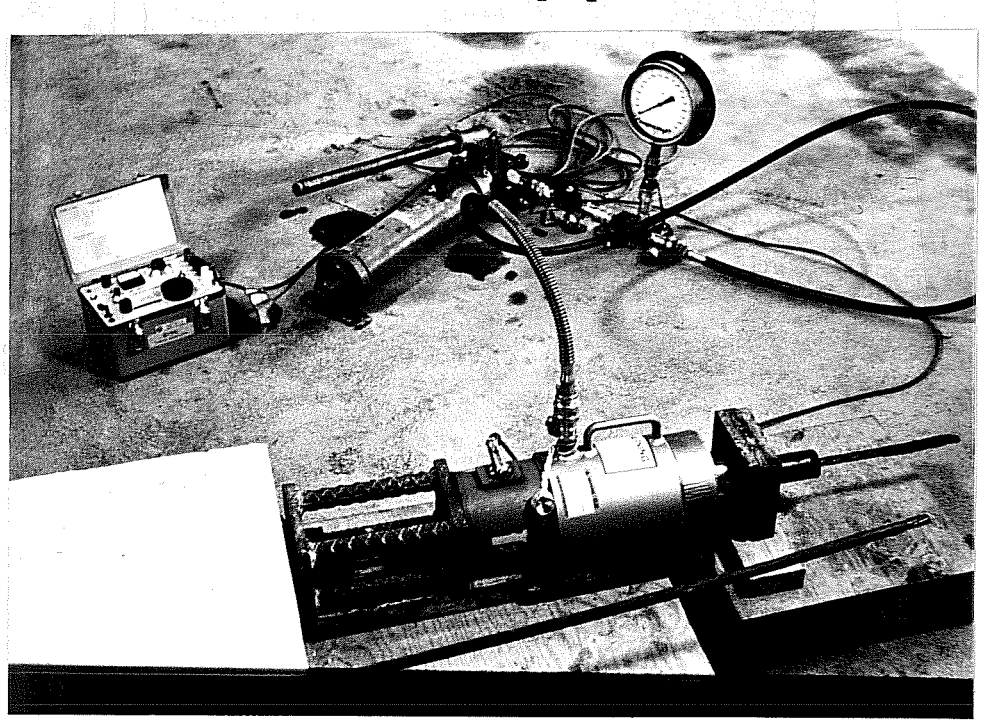

(b) Post-Tensioning set-up

Fig 2.13 Post-Tensioning set-up for monostrand specimens

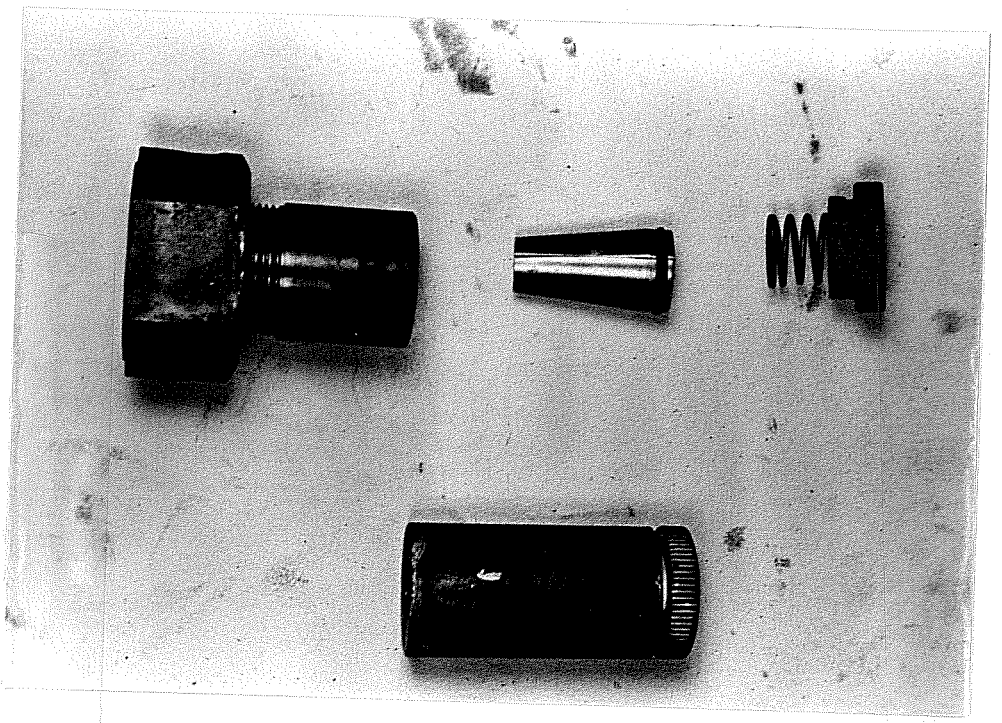

Fig. 2.14 Special screw chucks

Fig. 2.15 Cutting off excess strand after post-tensioning

were caused by the curved surface of the multistrand anchor as shown in Figure 2.16. The curved surface caused the strands to exit the anchorage at an angle thus preventing use of the 90 degree stressing chair used in post-tensioning the monostrand anchorage.

Figure 2.17 shows the stressing setup used for the multistrand specimens. Since the anchorage is free to move in the plastic pocket a straight chuck was used to bear against the anchorage on one end and provide a flat surface for the stressing chair on the other end. An additional ram was required to force the wedges in to the chuck to seat them before the 28.9k force was released. The procedure was repeated twice to reduce the seating losses. Two completed strands of a multistrand anchorage are shown in Figure 2.18.

To minimize losses due to creep and shrinkage in the concrete and relaxation in the strands, the monostrand specimens were tested the same day of post-tensioning and the multistrand specimens were tested within three days of post-tensioning.

The exact stress in the strands at the time of testing was not known. It is recommended for future research that improved instrumentation be attached to the individual strands to monitor the prestress in the strands. An attempt to use strain gauges on a multistrand tendon failed during the stressing of the tendon. The failure is attributed to the large movement of the strand during stressing and the friction forces of the adjacent strands and metal duct.

2.4 Testing Procedures

2.4.1 Loading System. The goal of post-tensioning is to precompress the concrete before service and dead loads are applied. This is commonly accomplished using internal tendons anchored at the ends of the slab. Figure 2.19a shows the stretched tendons exerting a compressive force on the slab through the end anchorage.

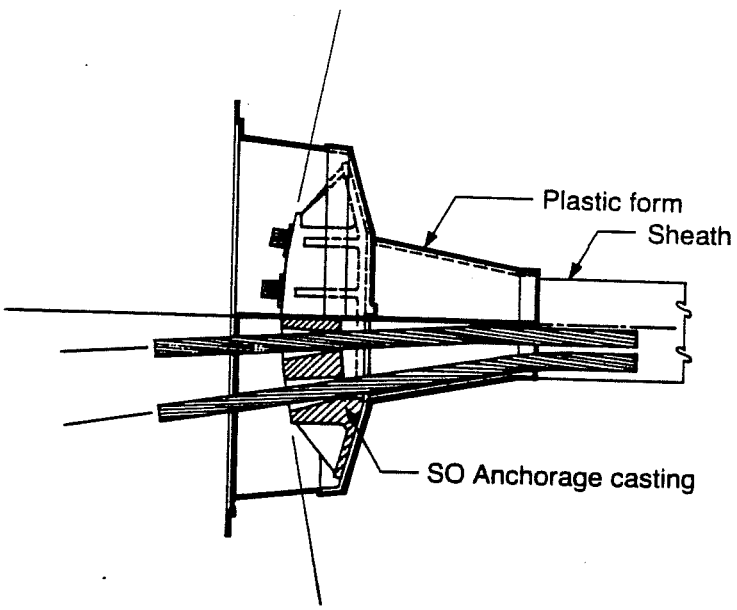

Fig. 2.16 Curved surface of multistrand anchorage (From VSL Catalog)

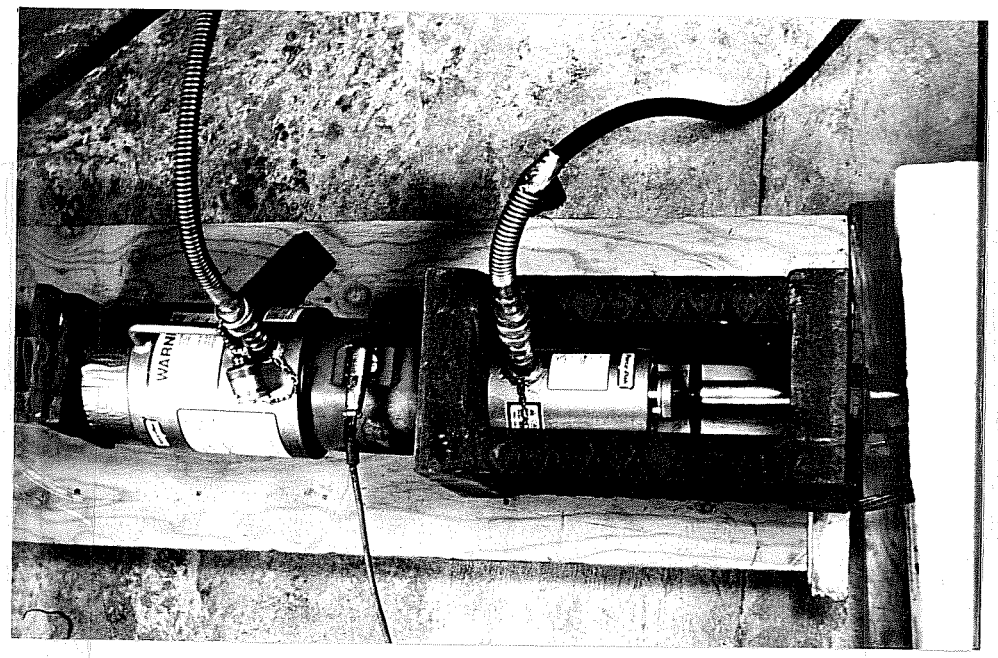

Fig. 2.17 Stressing setup for multistrand specimens

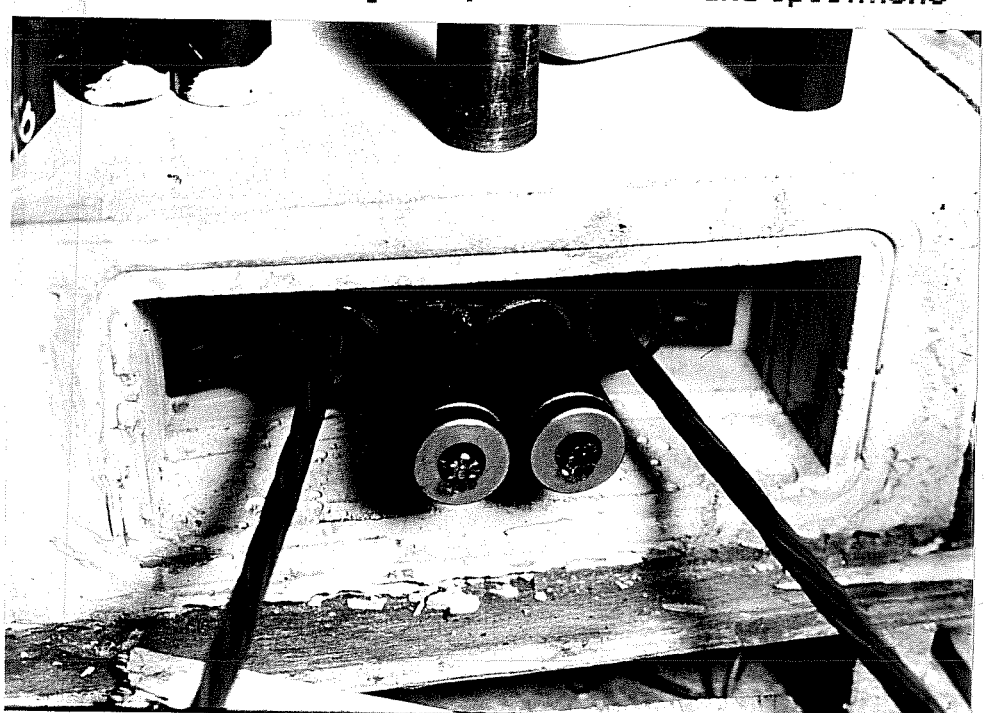

Fig. 2.18 Two completed post-tensioned strands of a multistrand anchorage

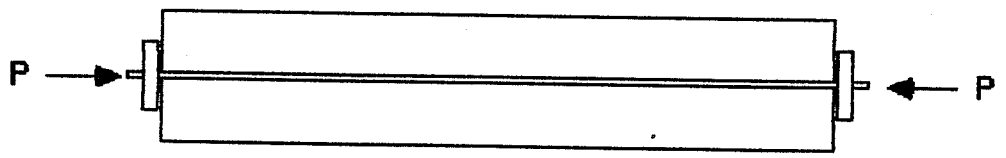

(a) Tendon applies compressive force

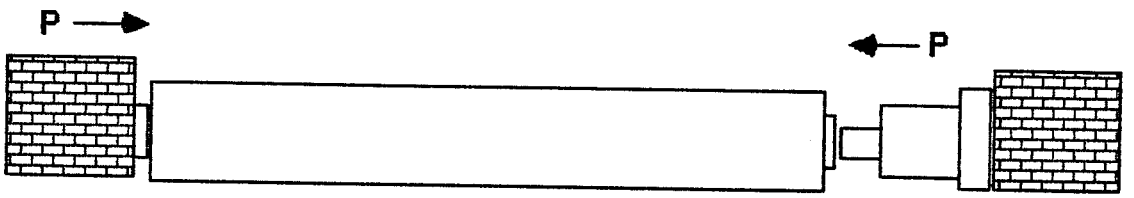

(b) External jack applies compressive force

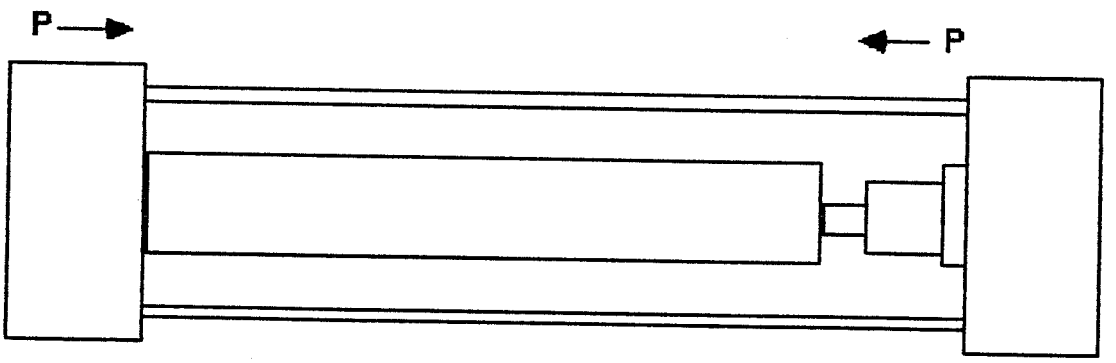

(c) Testing machine applies compressive force

Figure 2.19 Different methods of applying post-tensioning compressive force

Alternatively, an equivalent compressive force can be applied through external sources such as a jack between two abutments or applied through the loading head of a testing machine as shown in Figures 2.19b and 2.19c, respectfully.

The advantages of using a calibrated testing machine to apply the precompressive force in a laboratory environment is two fold. First, the applied force can be more accurately controlled and monitored than with a hydraulic jack and load cell. Second, and most importantly the magnitude of the applied force is not limited to the strength of the prestressing strand. Previous tests performed on anchorage zones [Stone] found that the strands could fail before the capacity of the anchorage zone was reached. In order to estabish factors of safety, it is important to know the ultimate capacity of anchorage zone. This can only be determined if tendon failure is precluded.

For this test program, the precompression force was applied directly to the anchorage using a 600 kip capacity testing machine. Figure 2.20a shows the testing of a monostrand specimen in the testing machine. A thin layer of hydrostone was used to provide an even bearing surface at the bottom of the specimen. The size of the multistrand specimens prohibited the use of the same testing machine. Figure 2.20b shows the multistrand specimen in a larger 600kip machine.

On typical construction sites, each tendon is stressed individually. To replicate this procedure for the specimens with three anchorages, the tendons in the outer two anchorages were post-tensioned to normal design levels first as described in Section 2.3, then the center anchorage was loaded to ultimate in the testing machine. The single anchorage specimens were loaded to ultimate directly in the testing machine.

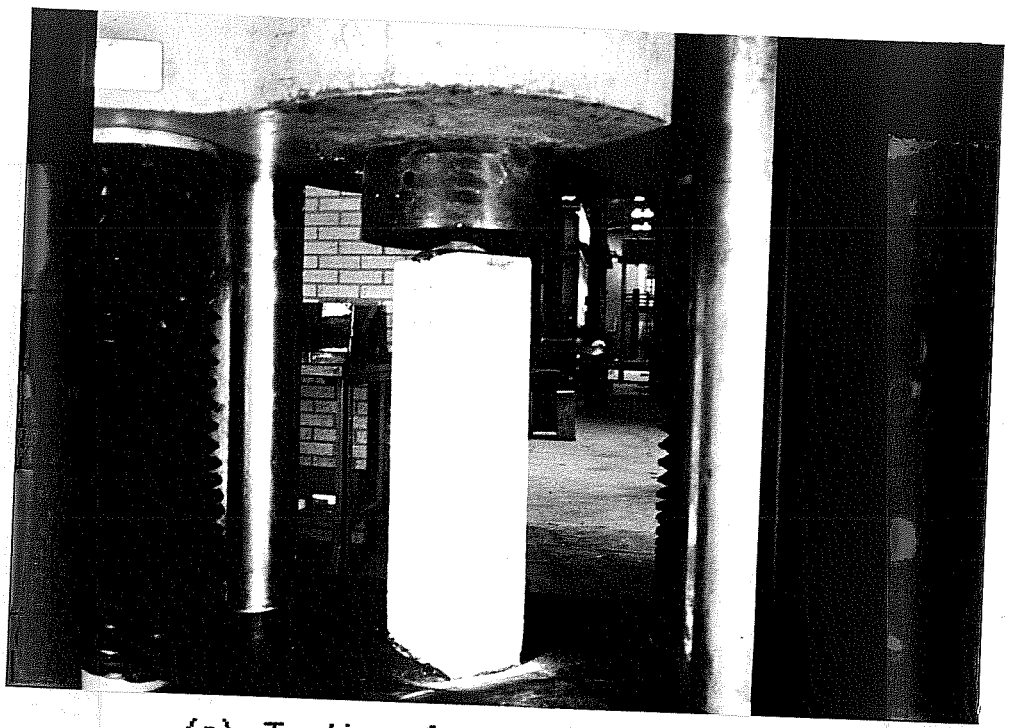

(a) Testing of a monstrand anchorage

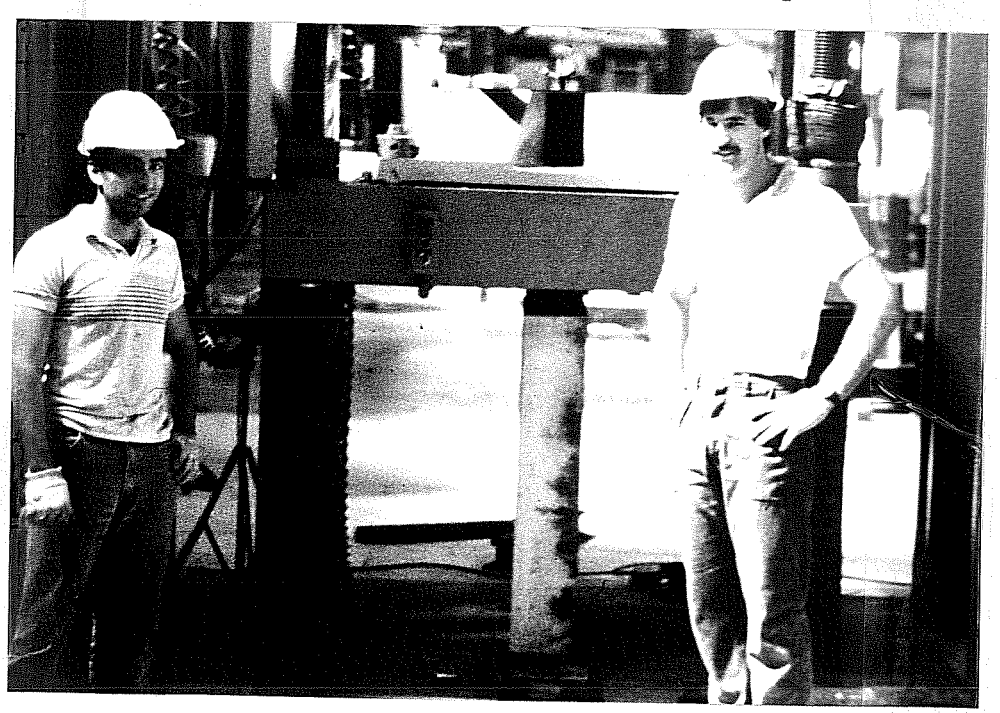

(b) Testing of a multistrand specimen

Fig 2.20 Loading system for test specimens

2.4.2 Intrumentation. A Demec mechanical extensometer was used to measure transverse surface strains along the tendon path. The Demec points were placed with a 2 inch gage length at 2 inch intervals along the tendon path as shown in Figure 2.21. The magnitude of the surface strains in the concrete was found to be too small to be measured accurately by the extensometer. The strain data collected during testing yielded irregular results. After the monostrand specimen test series the use of the Demec points was discontinued.

2.4.3 Test Procedures. Prior to loading the specimens, initial instrumentation readings were recorded. The load was then applied in 10 kip increments. At each load stage Demec readings were recorded and the specimen was examined for cracks in the anchorage zone. When the first cracks appeared, the cracking load and crack location were recorded. The crack progation was monitored with each increment of load. The increments of applied load were reduced to better define the failure point. The ultimate failure of the specimen was considered to have occurred when it was no longer possible to increase the applied load on the specimen.

Fig. 2.21 Demec instrumentation

CHAPTER 3

TEST RESULTS

3.1 Introduction

The results of the monostrand and multistrand anchorage test series are presented in this chapter. The primary test variable was the influence of closely-spaced anchorages on the performance of post-tensioned bridge deck anchorage zones. Secondary variables included the effects of spiral anchorage zone reinforcement and specimen width on anchorage zone performance. The cracking and ultimate load capacity of the anchorage zones were used to compare results within each test series.

3.2 Monostrand Anchorage Series

Six test specimens with monostrand anchorages were loaded to failure to observe the behavior and to determine the cracking and ultimate load capacity of the anchorage zones. Details of the specimen geometry and test procedures are given in Chapter Two. The cracking and ultimate load were defined as the applied compressive force causing first anchorage zone cracks visible by the unaided eye and the maximum compressve force the anchorage zone resisted before failure, respectively.

3.2.1 Anchorage Zone Failure Mechanism. The initial stages of cracking for the monostrand anchorage specimens can be generalized for all six specimens tested. However, the final anchorage zone failure mechanism differed for the single anchorage and multiple anchorage specimens.

The failure sequence for the single anchorage specimens is summarized in Figure 3.1a through 3.1d. The basic stages were as follows:

Stage 1. Initial longitudinal cracking occurs along the tendon path on the top and bottom surfaces of the bridge deck.

Stage 2. With increased load, the tendon path crack extends both towards the loaded face and away from it.

Stage 3. Cracks form on the loaded face perpendicular to the tendon path cracks.

Stage 4. The perpendicular cracks propagate to the edges of the specimen and a non-explosive failure occurs.

Superimposing the crack pattern with the location of the heavy bridge deck reinforcement as shown in Figure 3.2. provides insight into the anchorage zone behavior. The heavy bridge deck reinforcement acts to control the width of the tendon path crack. However, lack of reinforcement in the perpendicular direction allows the perpendicular cracking to propagate uncontrolled until the slab is split in two by the wedge action of the anchorage.

The presence of previously stressed tendons changes this behavior in the specimens with three closely-spaced anchors as shown in Figure 3.3a through 3.3 d. The difference in failure sequence stages 3 and 4 were as follows:

Stage 3. Inclined cracks extend from the four corners of the center anchorage and propagate to the bridge deck face. (The compression regions produced by the previously stressed anchorages force the

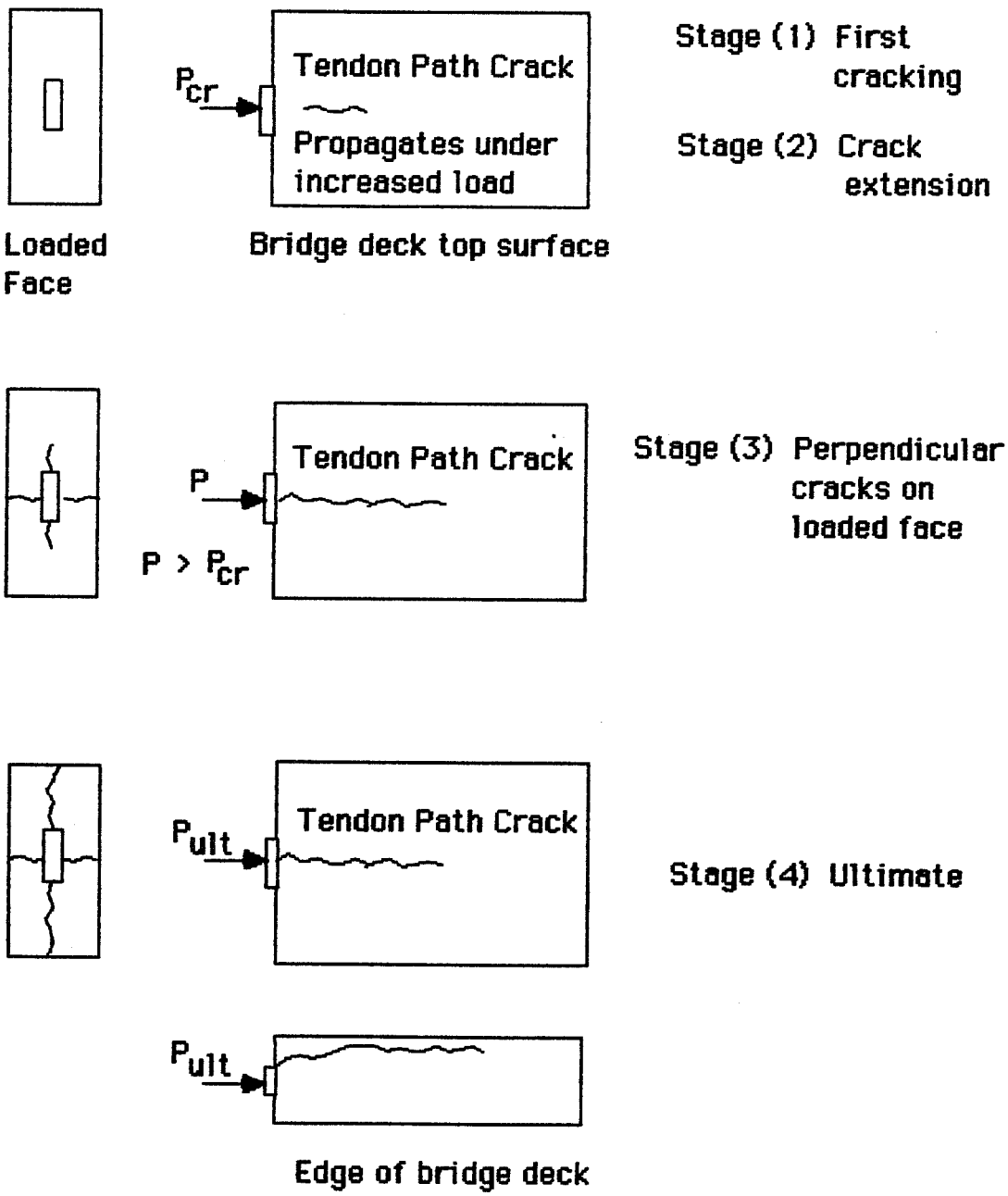

Fig. 3.1a Failure sequence for single monostrand anchorage specimens

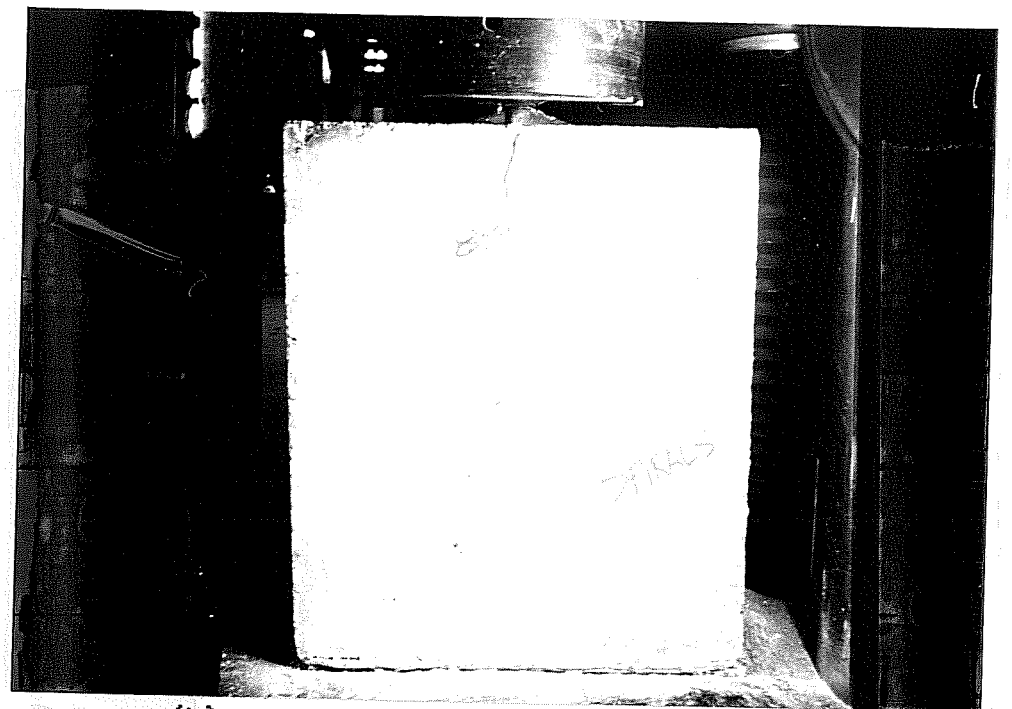

(b) Stage 1 and 2 - Tendon path crack

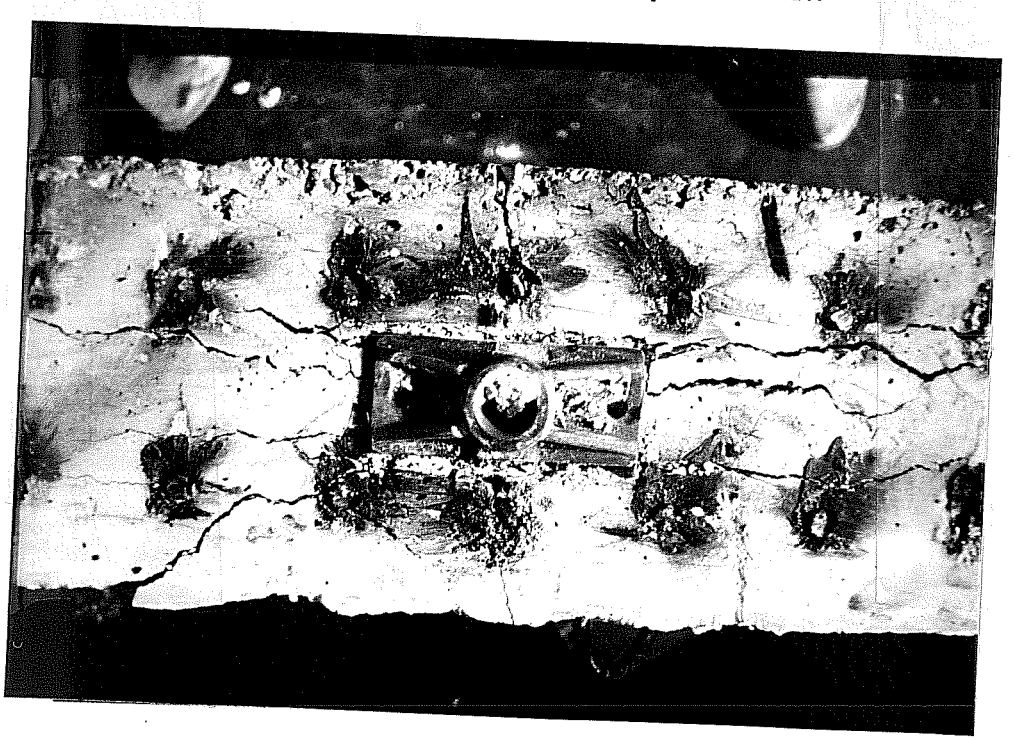

(c) Stage 3 -cracks on loaded face

Fig 3.1 Failure sequence for single monostrand anchorage specimens

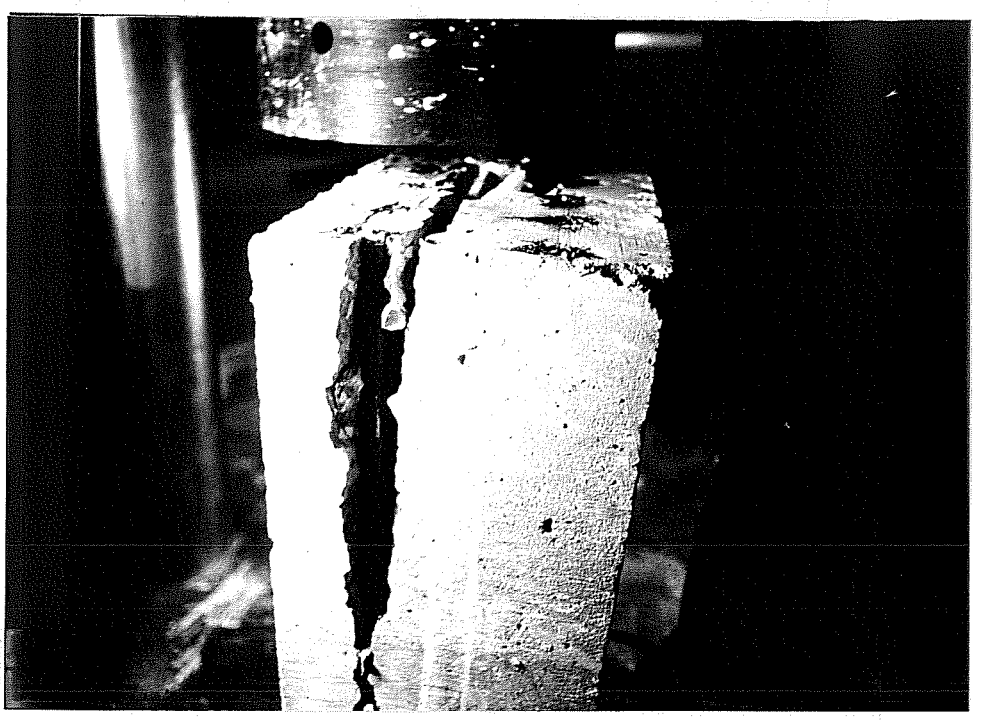

(d) Stage 4 -Perpendicular cracks split specimen

Fig 3.1 Failure sequence for single monostrand anchorage specimens

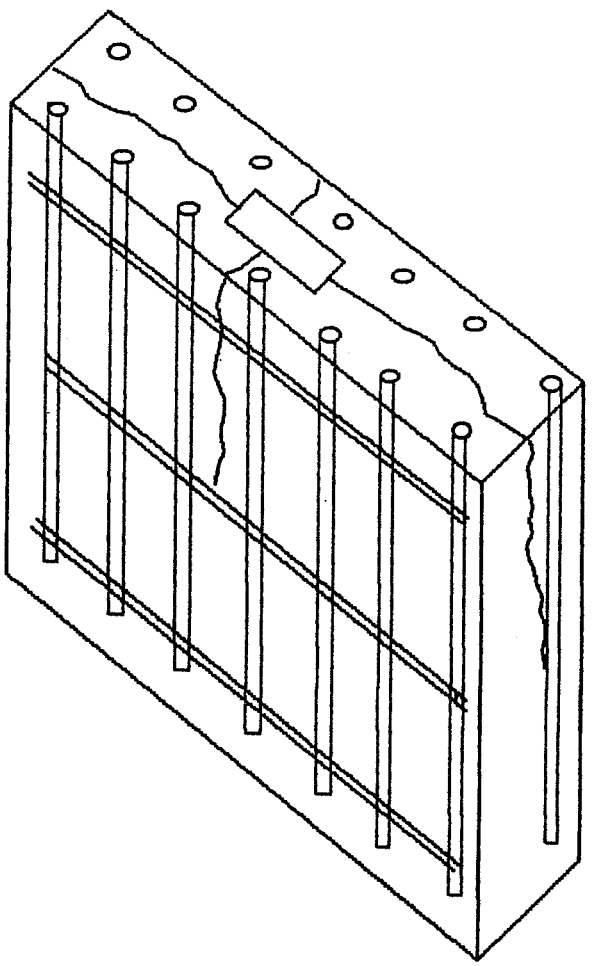

Fig. 3.2 Crack pattern of single monostrand anchorage specimens superimposed with bridge deck reinforcement

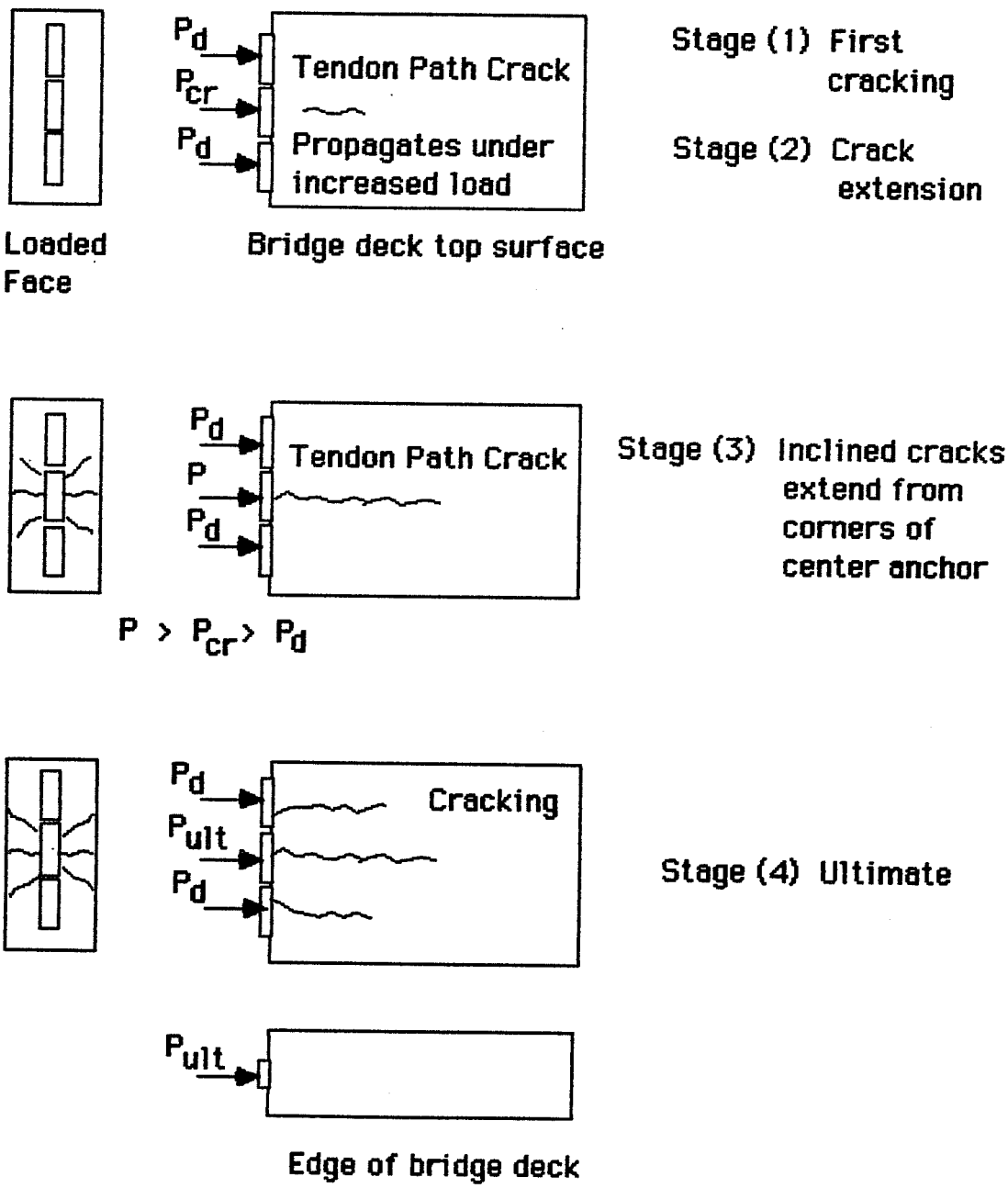

Fig. 3.3a Failure sequence for closely-spaced monostrand anchorage specimens

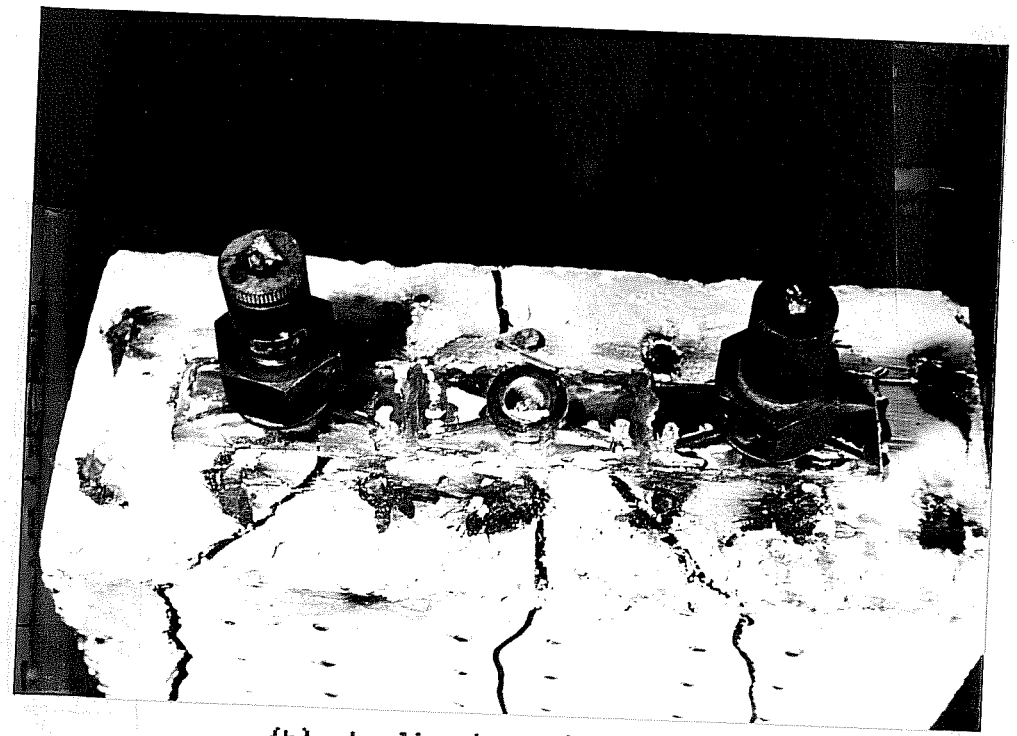

(b) Inclined cracks at anchor

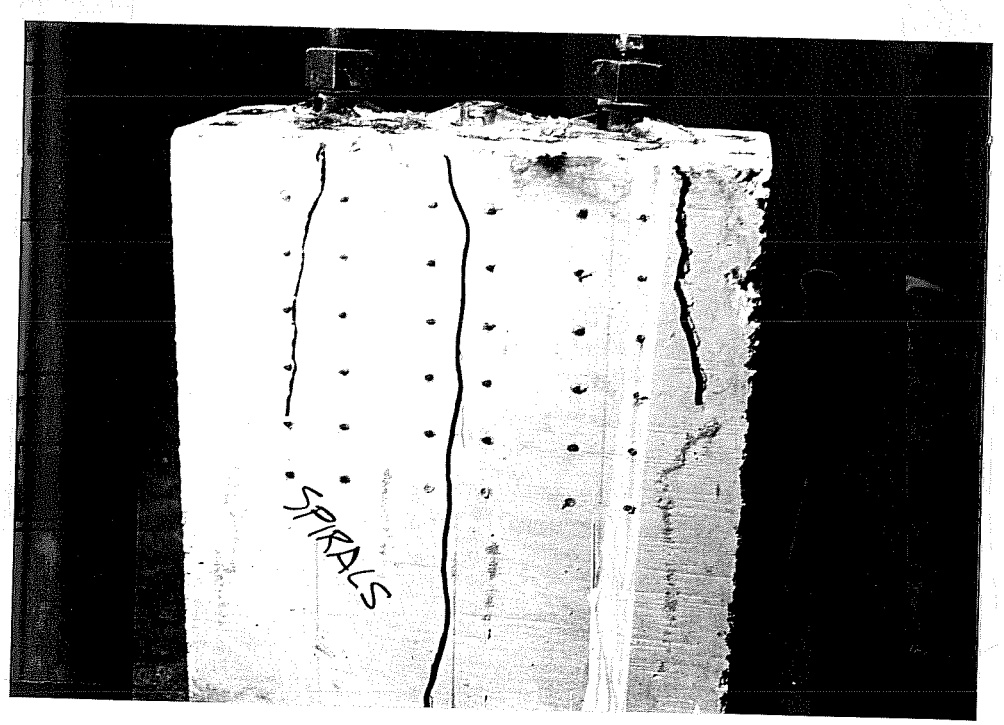

(c) Inclined cracks propagate

Fig 3.3c Failure sequence for closely-spaced monstrand anchorage specimens

diagonal cracks to the face of the slab.)

Stage 4. The inclined cracks reach the top and bottom surfaces of the bridge deck and propagate away from the loaded face.

Again by superimposing the crack pattern with the heavy reinforcement and the previously stressed anchors as shown in Figure 3.4, the resulting crack pattern becomes more apparent.

3.2.2. Effect of Closely-Spaced Anchorages. To identify each specimen, an alphanumeric sequence was used to indicate specimen anchorage type, number of anchors and specimen width. The alphanumeric sequence is illustrated by the following examples:

1) MO-1NS where MO = monostrand anchorage
1 = specimen contains one anchorage
N = narrow width specimen
S = spiral reinforcement is provided

2) MU-3W where MU = multistrand anchorage
3 = specimen contains three anchorages
W = wide width specimen
(blank) = no spiral reinforcement

The cracking and ultimate load capacity results for the six monostrand anchorage specimens are shown in Figure 3.5. Test specimens MO-3W and MO-3WS were 20 inches wide with three monostrand anchorages and specimens MO-1W and MO-1WS were of the same width but had only one monostrand anchorage. Table 3.1 illustrates the increase in the cracking and ultimate loads for the closely-spaced anchorage specimens.

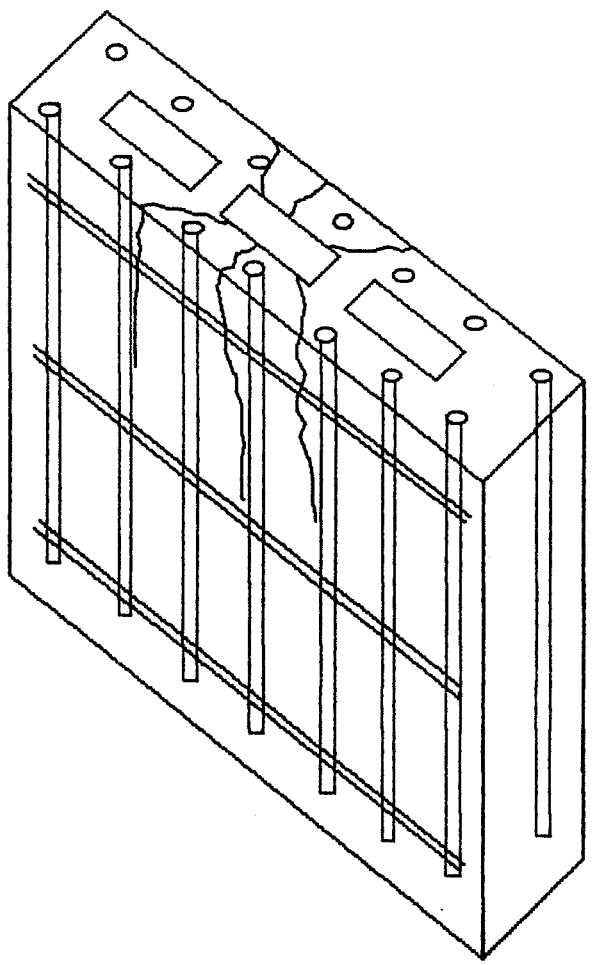

Fig. 3.4 Crack pattern of closely-spaced monostrand anchorage specimens superimposed with bridge deck reinforcement

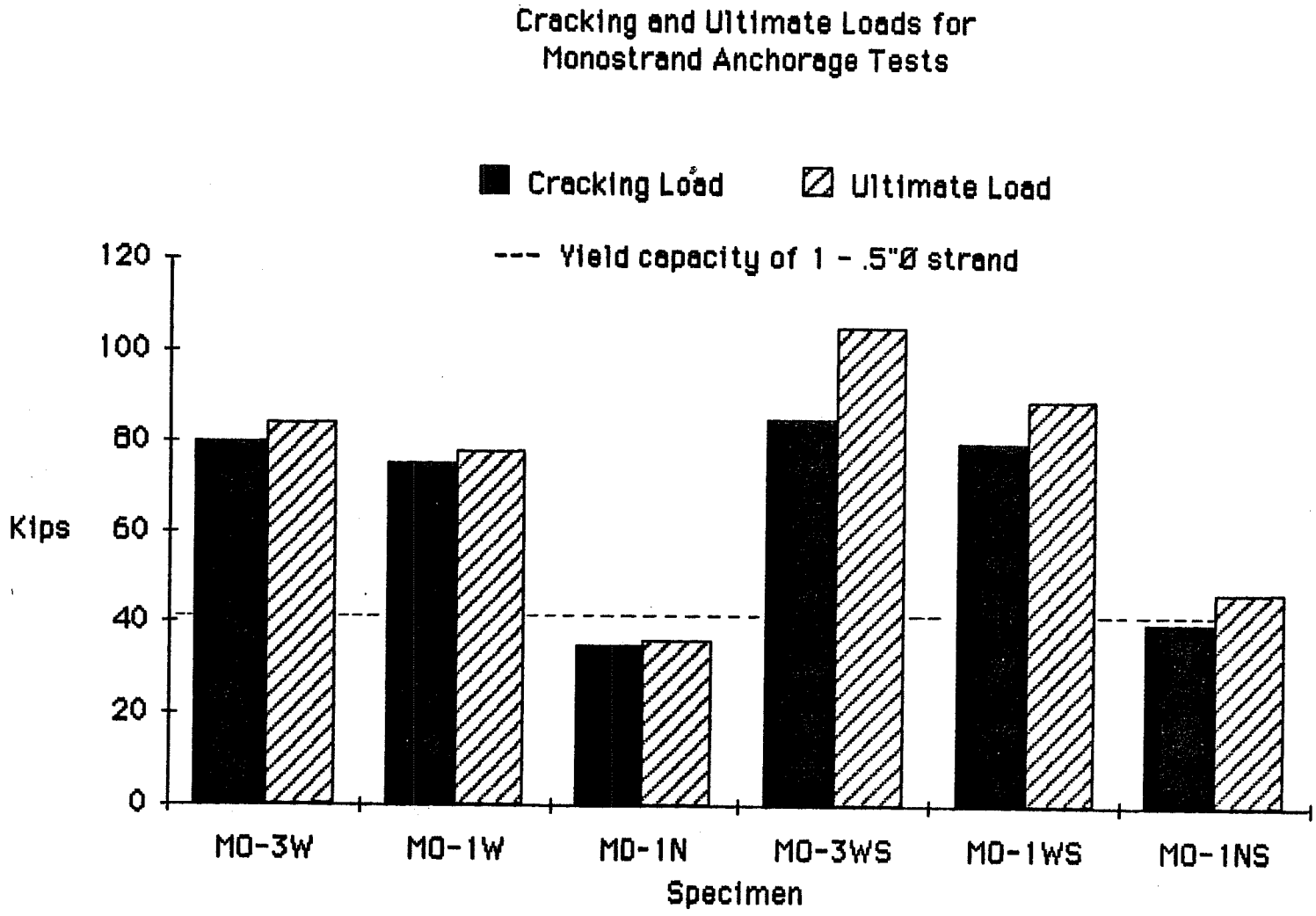

Fig. 3.5 Cracking and ultimate loads for monostrand anchorage tests

TABLE 3.1 Increase in Cracking and Ultimate Load for Closely-Spaced Monostrand Anchorage Specimens

Specimen	Cracking Load (Kips)	Ultimate Load (Kips)
Without Spirals		
MO-1W	75	78
MO-3W	80	84
% Increase	6.7%	7.7%
With Spirals		
MO-1WS	80	89
MO-3WS	85	105
% Increase	6.2%	18%

TABLE 3.2 Ratio of Cracking Load to Tendon Ultimate Strength for the Monostrand Anchorage Specimens

Specimen	Cracking Load (Kips)	Ultimate Strength of Tendon * (Kips)	Factor of Safety
MO-1W	75	41.3	1.8
MO-1WS	80	41.3	1.9
MO-3W	80	41.3	1.9
MO-3WS	85	41.3	2.1

* 1/2" Diameter 270 Ksi prestressing strand

A gain in cracking and ultimate load of 6.2% to 18% is evident between the multiple and single anchorage specimens of the same width. These results show that previously stressed closely-spaced anchorages do not increase the tension splitting stresses of the center anchorage but actually tend to reduce it . This favorable result is due to the precompression of the center anchorage zone, B, during the stressing of the outer anchorages, A and C, as illustrated in Figure 3.6. Thus, the tension splitting stresses now must overcome this initial precompression, in addition to the tensile stress of the concrete, before a tendon path crack can occur when anchor B is stressed (P_B).

In light of this precompression effect, it becomes advantageous to use a prestressing sequence in which the anchorages are stressed in an alternating fashion. First, every other anchorage would be stressed to precompress the adjacent anchorage zone, then the remaining anchorages are stressed. Also it is important to start the stressing at the middle of the slab to reduce the possibility of end edge splitting. This does not require any additional stressing but does reduce the possibility of cracking when the concrete has minimal strength and maximum prestressing force before losses.

Another favorable result from the monostrand anchorage tests is shown in Table 3.2. The ratio of the actual cracking load of the anchorage zones to 100% of the ultimate capacity of a 1/2 inch prestressing strand ranged from 1.8 to 2.1. The actual factor of safety may be more if prestressing force is 0.8 x 41.3 kips at initial stressing. The ultimate capacity of the 1/2 inch strand is also illustrated in Figure 3.5 with a dashed line. Thus for this particular bridge deck design and conventional reinforcement present, it is more likely the prestressing strand will yield before damage to the anchorage zone can occur.

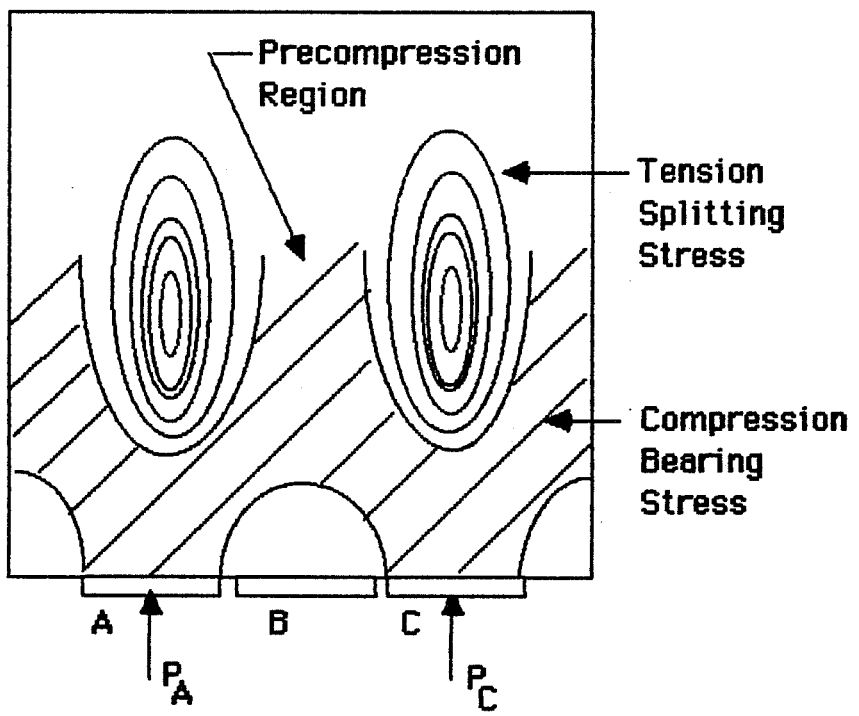

Fig. 3.6 Precompression of center anchorage zone during stressing of outer anchorages

3.2.3 Effect of Spiral Reinforcement. Test specimens M0-1NS, M0-1WS, and M0-3WS contained additional anchorage zone reinforcement in the form of confining spirals. Details of the spiral reinforcement are given in Section 2.2.7. Spiral reinforcement is used in post-tensioned anchorage zones for two reasons. First, to confine the concrete in a manner similar to a spirally reinforced column, and second, to reduce the crack width of the tendon path cracks thus providing reserve strength between cracking and ultimate. Without spiral reinforcement a shear cone forms behind the anchorage after the concrete fails in shear as illustrated in Figure 3.7. The shear cone acts like a wedge and splits the concrete like a steel wedge splits firewood. Providing spiral reinforcement tends to confine the concrete behind the anchorage and delay the formation of the shear cone. This confining effect, similar to a reinforced concrete column with spiral reinforcement, was verified during the test program as evident in Figure 3.8.

The test results for the spirally reinforced specimens are summarized in Table 3.3. The increase in cracking load with the addition of spiral reinforcement ranged from 6.2% to 14.3%. The increase in ultimate load was 14 to 30%. In general, the percentage increase was not as high as initally expected. Three possible reasons could be that: (1) Since the slab is heavily reinforced, the anchorage zone may be overly-reinforced and no ductility is provided. The spirals do not become effective until sufficient stress is reached in the steel. Perhaps that level is not reached until failure has already occurred. (2) Since the slab thickness was much larger than the width of the anchorage, the spalling of the concrete outside the spiral may have produced the failure before the confined concrete could resist the applied compression. (3) The spirals were not large enough. The diameter of the spirals used was only 2.25 inches. The clear cover

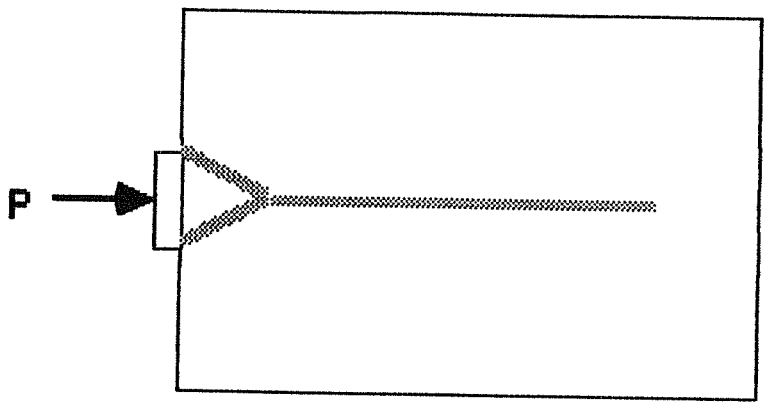

Fig 3.7 Shear Cone acting like a wedge to split the concrete

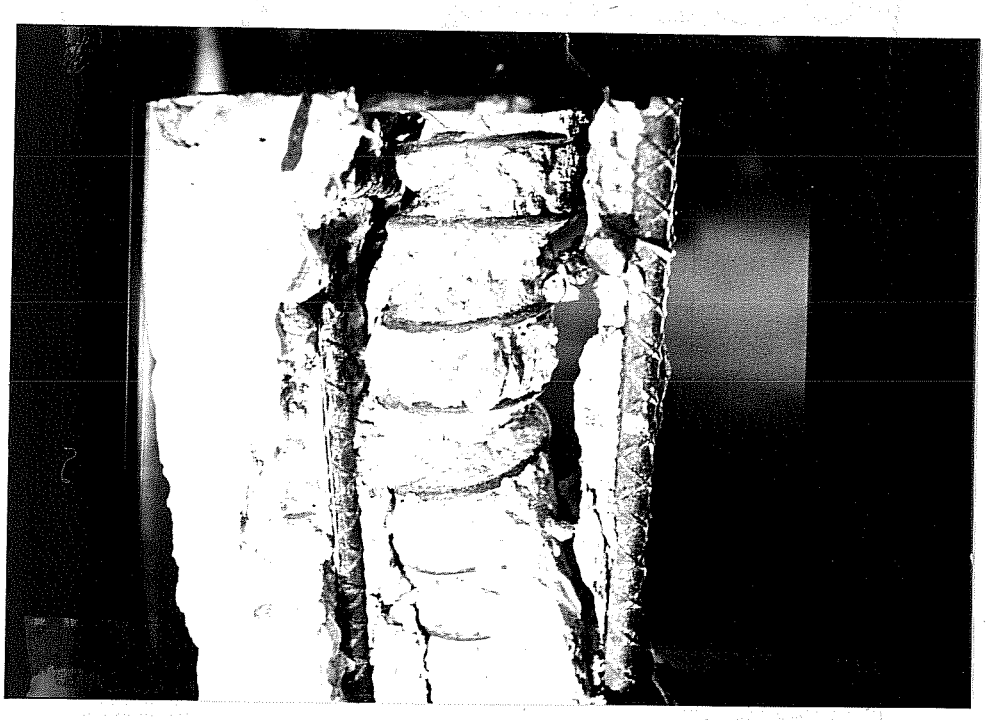

Fig. 3.8 Spiral reinforcing acts to confine the concrete similar to a tied column

TABLE 3.3 Increase in Cracking and Ultimate Load with Spiral Anchorage Zone Reinforcement for Monostrand Specimens

Specimen	Cracking Load (Kips)	Ultimate Load (Kips)
MO-1N	35	36
MO-1NS	40	47
% Increase	14.3%	30%
MO-1W	75	78
MO-1WS	80	89
% Increase	6.7%	14.1%
MO-3W	80	84
MO-3WS	85	105
% Increase	6.2%	25%

TABLE 3.4 Effect of Specimen Width on Cracking and Ultimate Load Capacity for Monostrand Specimens

Specimen	Cracking Load (Kips)	Ultimate Load (Kips)
MO-1N	35	36
MO-1W	75	78
% Increase	114%	117%
MO-1NS	40	47
MO-1WS	80	89
% Increase	100%	89%

requirements would have allowed four inch diameter spirals. A larger spiral could maximize the volume of concrete confined thus increasing compression capacity.

Also it is important to note that the spiral reinforcement does cause congestion in the anchorage zone. If there is too much congestion, it is difficult to get good consolidtion of the concrete and honeycombing behind the anchorage could possibly cause premature failure of anchorage zone.

3.2.4. Effect of Specimen Width. Test specimens MO-1N and MO-1NS were 5 inches in width (the width of a single monstrand anchorage) and the other four speciments were 20 inches in width. The test results for the effect of specimen width are summarized in Table 3.4. The small width specimens failed at much lower loads because the 5 inch width of specimen is smaller than the 8 inch slab thickness. Thus, initial cracks formed on the sides of the specimens and not on the bridge deck face. With no reinforcement tieing the layers of reinforcement together as illustrated in Figure 3.9, the spalling stresses increased without resistance until failure as shown in Figure 3.10 for Specimen MO-1NS.

This test variable shows that a minimum edge distance for the anchorage is required to prevent premature failure of the bridge deck and that the layers of reinforcement should be tied at the edge of the slab to avoid splitting.

3.3. Multistrand Anchorage Series.

Six test specimens with multistrand (four strands) anchorages were loaded to failure to observe the behavior and to determine the cracking and ultimate load capacity of the anchorage zones. Details of the specimen geometry and test procedures are given in Chapter Two.

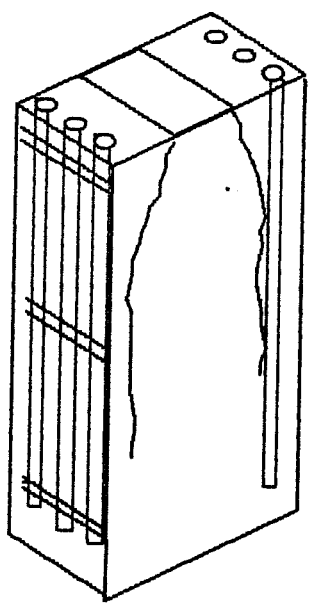

Fig 3.9 Crack pattern of the narrow, single monostrand anchorage specimens superimposed with bridge deck reinforcement

Fig 3.10 Typical failure of a narrow width specimen

3.3.1. Anchorage Zone Failure Mechanism. In contrast to the monostrand anchorage test specimens, both the single and multiple multistrand anchorage specimens tended to exhibit the same sequence of failure. This failure sequence is summarized in Figure 3.11. The basic stages are as follows:

Stage 1. Almost simultaneously, an initial longitudinal crack occurs along the tendon path and inclined cracks form to the right and left of the longitudinal crack. When these cracks occur the load apparatus registers a large drop in applied load.

Stage 2. Upon reapplication of load but still considerably below the inital cracking level, the longitudinal and inclined cracks propagate.

Stage 3. With continued loading, inclined cracks form on the loaded face radiating from the corners of the anchorage pocket.

Stage 4. Applied load regains original cracking load but does not go any higher. Failure is not explosive.

3.3.2. Effect of Closely-Spaced Anchorages. The cracking and ultimate load capacity results are shown in Figure 3.12 for the six specimens containing multistrand (four strands) anchorages . Table 3.5 shows the increase in anchorage zone capacity for the specimens with closely-spaced anchorages.

A gain in cracking and ultimate load of 5% is evident between specimens MU-1W and MU-3W. For specimens MU-1WS and MU-3WS, the cracking load decreased 5% but the ultimate load increased 5%. Even though these gains are not as high as the monostrand anchorage specimens, the results show that closely-spaced anchorages do not tend to increase the tension splitting stresses of the center anchorage.

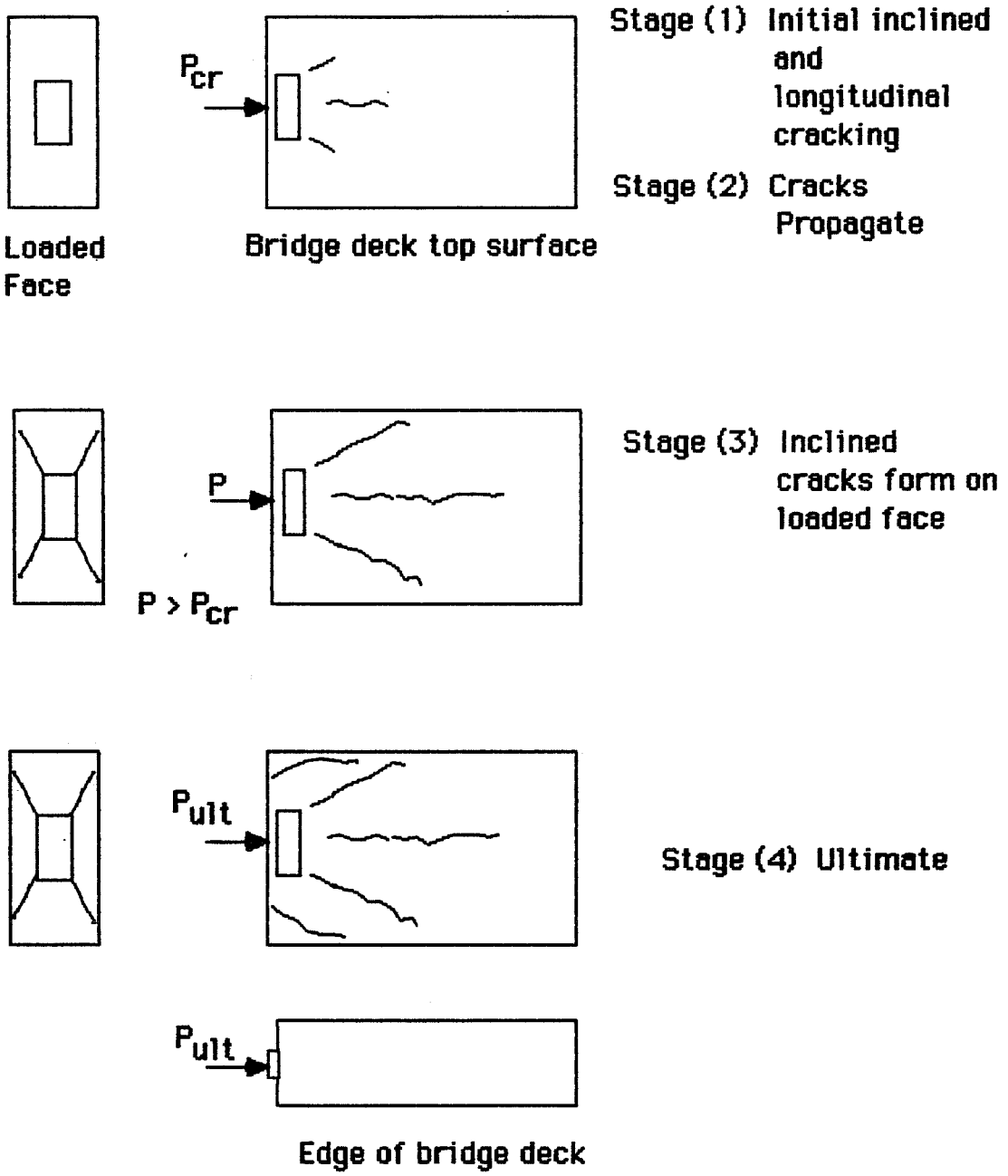

Fig. 3.11a Failure sequence for single and closely-spaced multistrand anchorage specimens

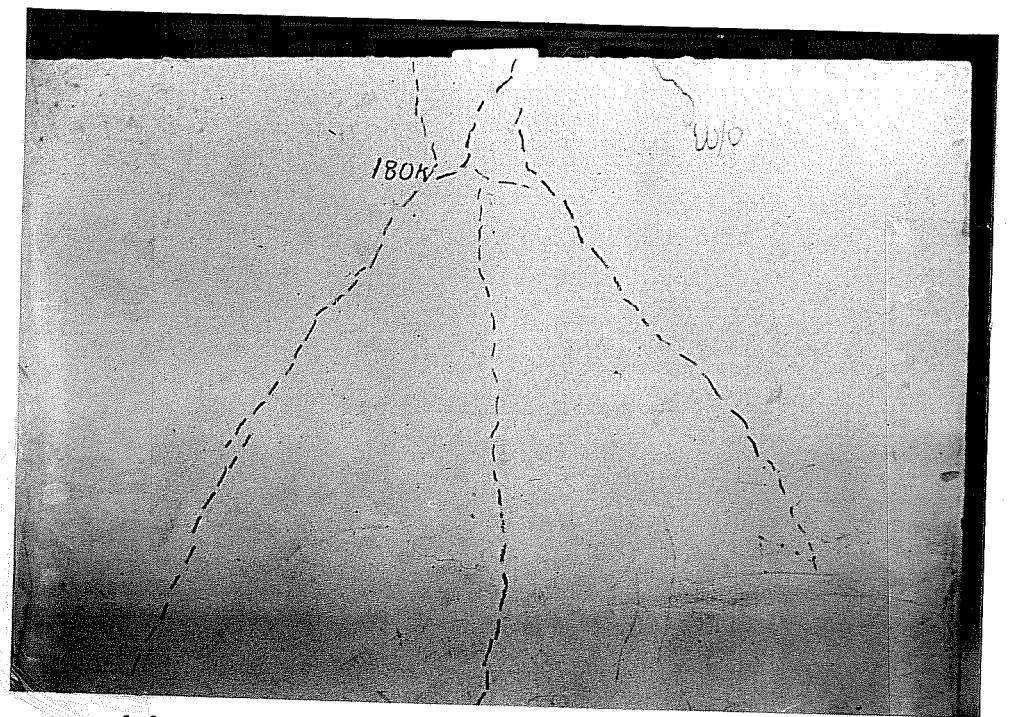

(b) Stage 2 - Longitudinal and diagonal cracks

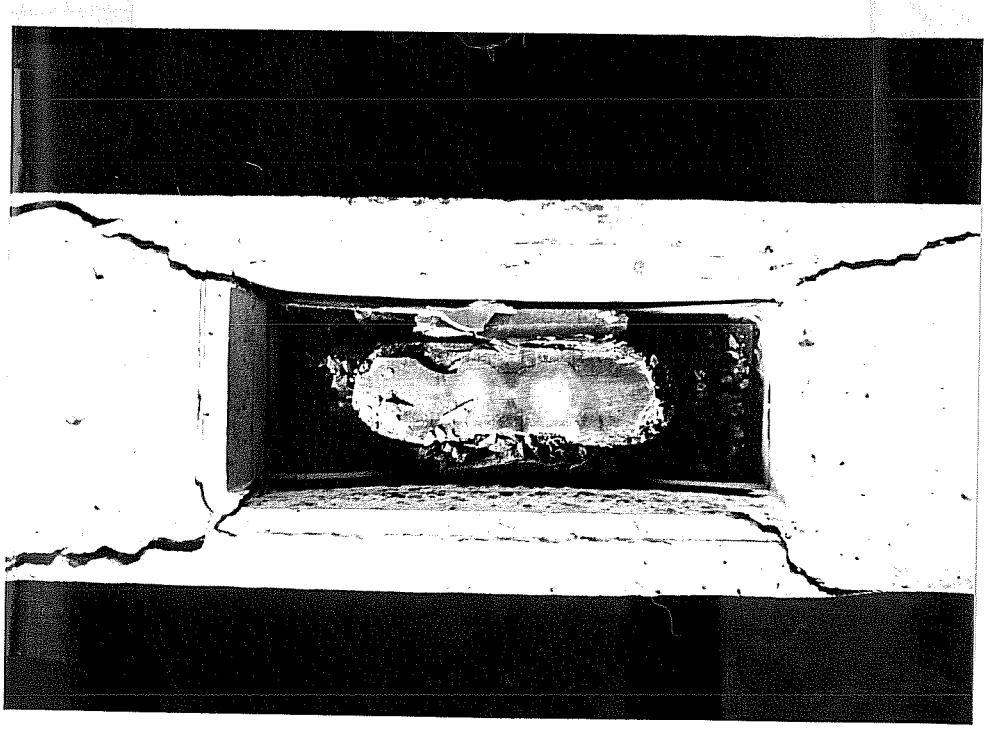

(c) Stage 3 -diagonal cracking on loaded face

Fig 3.11 Failure sequence for single and closely-spaced multistrand anchorage specimens

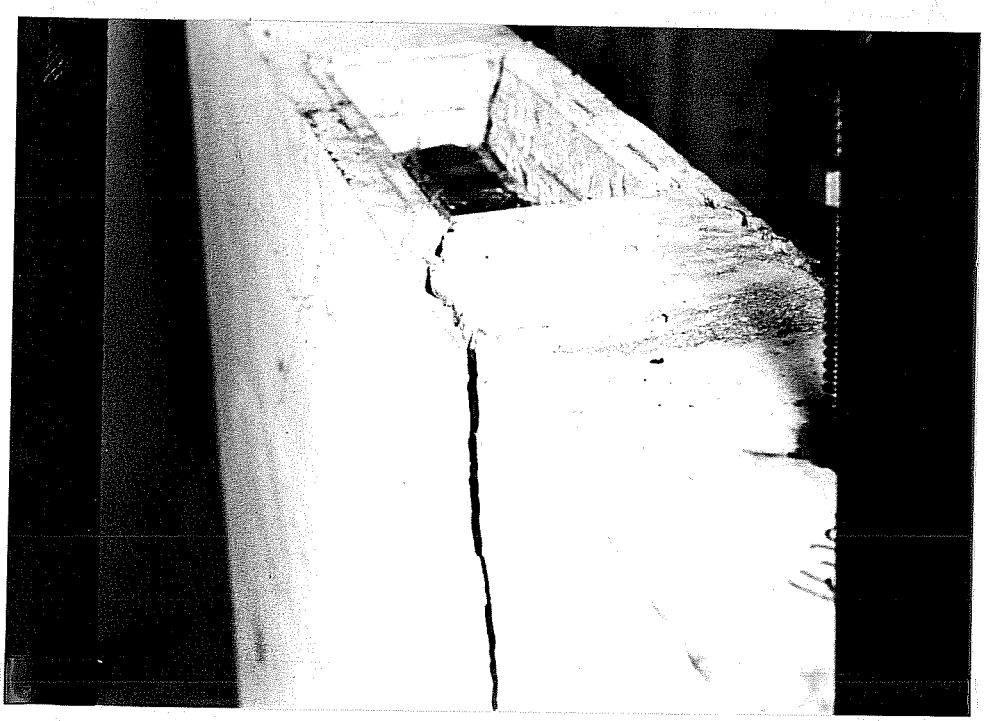

(d) Stage 4 - Propagation of inclined cracks

Fig 3.11 Failure sequence for single and closely-spaced multistrand anchorage specimens

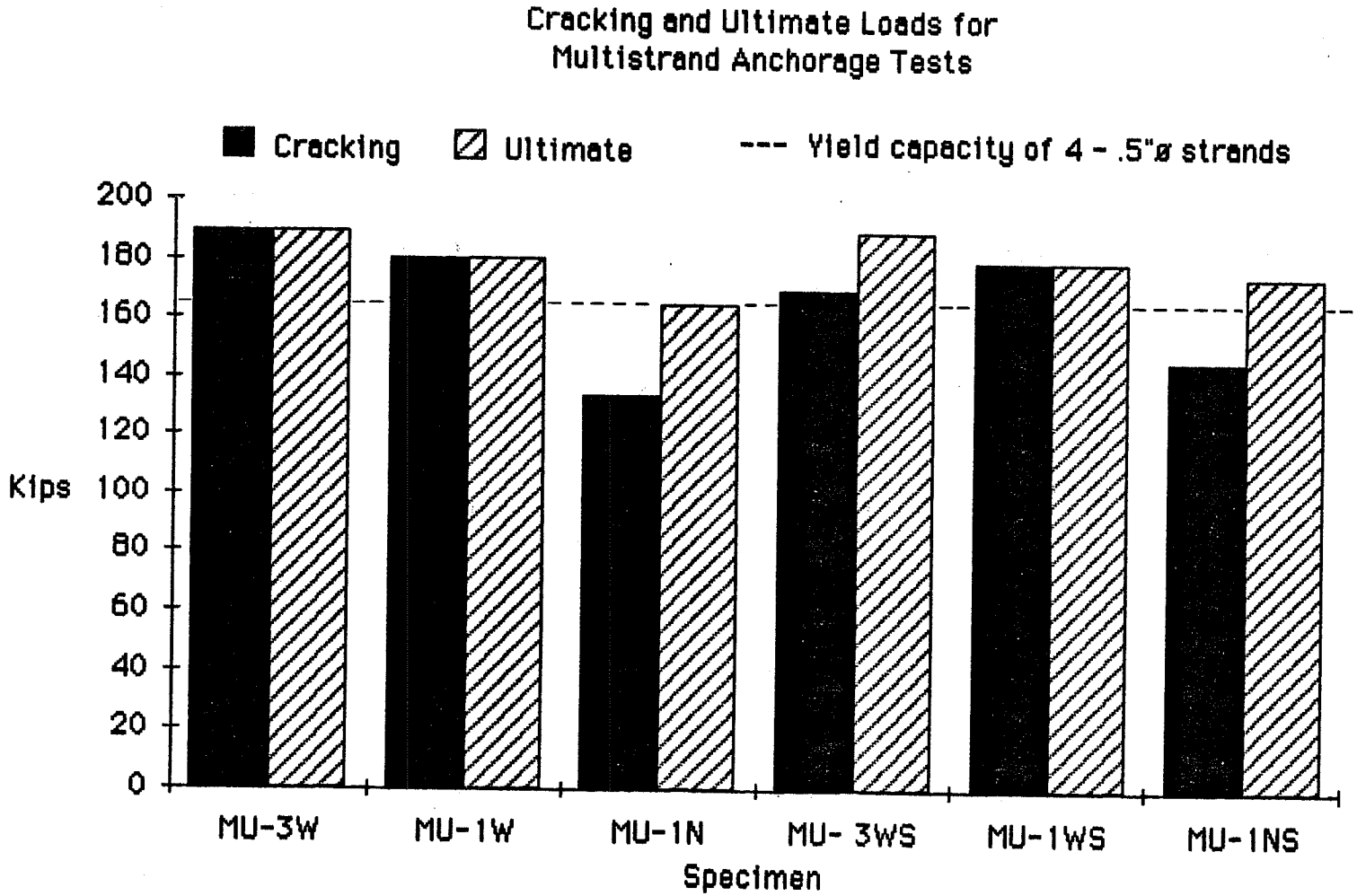

Fig. 3.12 Cracking and ultimate loads for multistrand anchorage tests

TABLE 3.5 Increase in Cracking and Ultimate Load for Closely-Spaced Multistrand Anchorage Specimens

Specimen	Cracking Load (Kips)	Ultimate Load (Kips)
Without Spirals		
MU-1W	181	181
MU-3W	190	190
% Increase	5%	5%
With Spirals		
MU-1WS	180	180
MU-3WS	170	190
% Increase	(5%)	5%

TABLE 3.6 Ratio of Cracking Load to Tendon Ultimate Strength for the MUltistrand Anchorage Specimens

Specimen	Cracking Load (Kips)	Ultimate Strength of Tendon * (Kips)	Factor of Safety
MU-1W	181	165.2	1.10
MU-1WS	181	165.2	1.10
MU-3W	190	165.2	1.15
MU-3WS	170	165.2	1.03

* 4 - 1/2" Diameter 270 Ksi prestressing strands

This is probably due to the precompressing of the center anchorage zone during the stressing of the outer anchorages.

Also Table 3.6 shows the factors of safety for the actual cracking load compared to 100% of the ultimate load for four -1/2 inch prestressing tendons. The actual factor of safety may be more if prestressing force for each tendon is 0.8 x 41.3 kips at initial stressing. Thus for this particular bridge deck design and conventional reinforcement present, a marginal factor of safety insures the prestressing strand would yield shortly before the anchorage zone cracks.

3.3.3. Effects of Spiral Reinforcement. Test specimens Mu-1NS, MU-1WS, and MU-3WS contained additional anchorage zone reinforcement in the form of confining spirals. Details of the spiral reinforcement are given in Section 2.2.7. The test results for the spirally reinforced specimens are summarized in Table 3.7.

In contrast to the monostrand anchorage specimens, the multistrand anchorage specimens did not show any significant increase in strength with the additional spiral reinforcement. In fact, the cracking load actually decreased 12% for specimen MU-3WS compared to MU-3W. The same reasons apply as stated in Section 3.2.2.

3.3.4. Effects of Specimen Width. Test specimens MU-1N and MU-1NS were 18 inches in width and the other four specimens were 45 inches in width. The test results for the effect of specimen width are summarized in Table 3.8. Again the smaller width specimens failed at much lower loads. Figure 3.13 shows the spalling failure of a small width specimen. This test variable shows that a minimum edge distance for the the anchorage is required to prevent premature failure of the bridge deck. It is recommended that a minimum clear distance

TABLE 3.7 Increase in Cracking and Ultimate Load with Spiral Anchorage Zone Reinforcement for Multistrand Specimens

Specimen	Cracking Load (Kips)	Ultimate Load (Kips)
MU-1N	134	165
MU-1NS	146	175
% Increase	8.9%	6%
MU-1W	181	181
MU-1WS	180	180
% Increase	0%	0%
MU-3W	190	190
MU-3WS	170	190
% Increase	(12%)	0%

TABLE 3.8 Effect of Specimen Width on Cracking and Ultimate Load Capacity for Multistrand Specimens

Specimen	Cracking Load (Kips)	Ultimate Load (Kips)
MU-1N	134	165
MU-1W	181	181
% Increase	35%	10%
MU-1NS	146	175
MU-1WS	180	180
% Increase	23%	3%

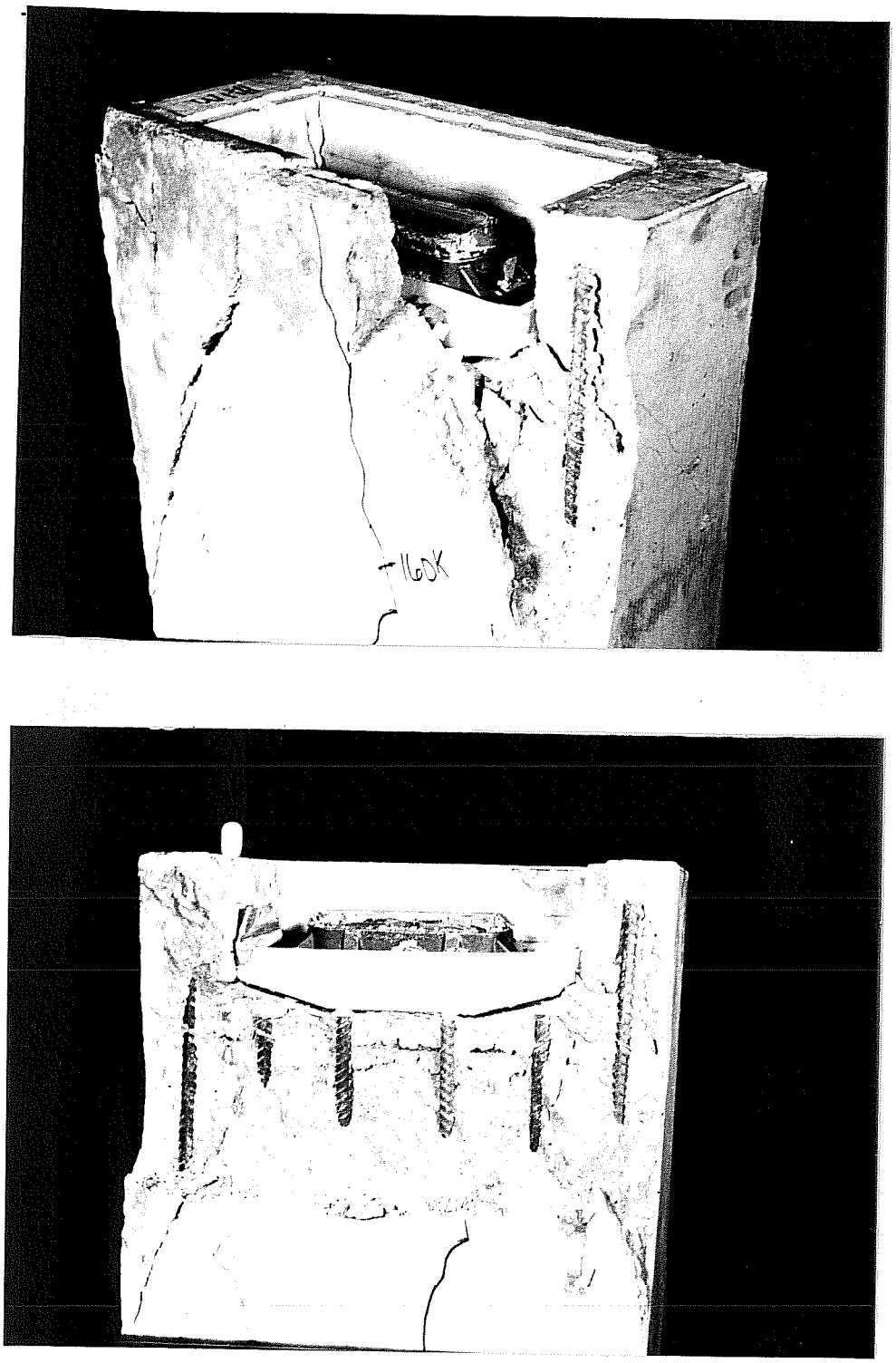

Fig. 3.13 Spalling failure of narrow width specimen MU-1N

equal to at least half of the slab thickness be provided and that the top and bottom layers of reinforcement should be tied at the edge of the slab to avoid splitting.

3.4 Summary of Test Results

The experimental results of the twelve full-scale anchorage zone specimens can be summarized as follows:

1. The previously-stressed adjacent anchorages had a favorable effect on increasing the performance of the anchorage zone of the specimens with closely-spaced anchors.
2. The addition of spiral reinforcement in the anchorage zone did not significantly increase the cracking and ultimate capacity of the test specimens.
3. The narrow width specimens failed at lower loads than the wider width specimens.

CHAPTER 4

DESIGN INDICATIONS

4.1 Comparison of Test Results to Design Provisions

In this section the actual test cracking loads are compared to values predicted by Leonhardt [6], Rhodes and Turner [7], Stone and Breen [2], ACI and PTI, and AASHTO's design provisions. It must be noted that these design provisions were originally developed for post-tensioned girders. This section discusses the applicability of these provisions to post-tensioned bridge decks only and does not address beams or girders.

4.1.1 Leonhardt. Leonhart [6] developed the following expression for computing the total splitting force due to bursting stresses (see Section 1.5.2):

$$Z = .3F(1 - a/h)$$

While not intended for specific use in this fashion, this equation may be used to predict cracking loads by substituting the concrete tensile strength for the total splitting force, Z. In addition, it was assumed:

1. the anchorage zone reinforcement is not effective until after the concrete cracks

2. $Z = f_r \times A_{effective}$

3. $f_r = 7.5\sqrt{f'_c}$, ACI Code [9] recommendation for concrete modulus of rupture

4. $A_{effective}$ = slab thickness x h/2

The effective area assumption was based on Leonhardt's suggestion that the reinforcement required to resist the splitting force be distributed within the distance of h/2 of the anchorage location as shown in Figure 4.1. However, since Leonhardt's model is only two dimensional it must be interpreted two ways to determine the smallest load at which cracking will occur. Thus, h can be either the thickness of the slab or the width of the slab specimen. Since, in general, the thickness of the slab was less than the width, the smallest cracking load was computed when the effective area was assumed equal to

$$A_{effective} = (\text{slab thickness})^2 / 2$$

A comparison of the calculated cracking load by this method for the single anchorage specimens and the actual cracking load from test data is listed in Table 4.1 and illustrated in Figure 4.2. It must be noted that Leonhardt's equation is not applicable to several closely-spaced anchorages.

This interpretation and use of Leonhardt's equation predicts cracking for the wide monostrand anchorage specimens within twenty percent of the actual values. However, for the case which best matchs Leonhardt's original assumption, a concentrically applied force spread over the entire width of the member, this interpretation of Leonhardt's equation overestimates the cracking load for specimens MO-1N and MO-1NS by 86% and 63%, respectively. For the multistrand specimens Leonhardt's equation underestimates the cracking load by 58 to 112%. In general, the results predicated by Leonhardt's equation are too scattered to recommend broad use of this equation for predicting anchorage zone cracking loads.

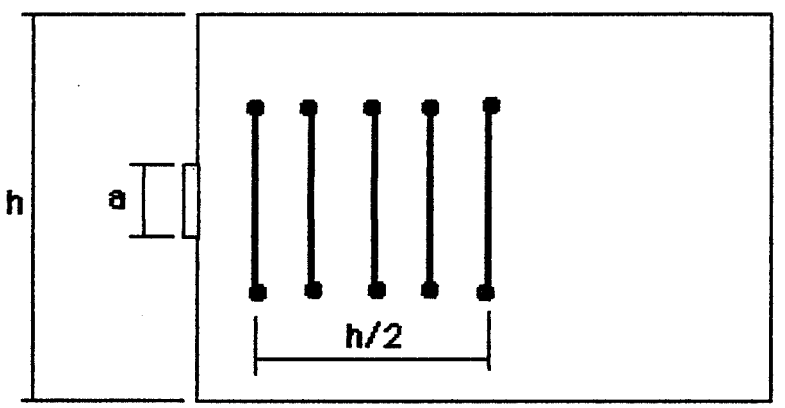

Fig. 4.1 Leonhardt's suggested distribution of anchorage zone reinforcement

Table 4.1 Leonhardt's calculated versus actual cracking load

Specimen	Calculated Cracking Load	Actual Cracking Load	P_{act}/P_{cal}
MO-1N	65	35	0.54
MO-1NS	65	40	0.62
MO-1W	68	75	1.10
MO-1WS	68	80	1.18
MU-1N	85	134	1.58
MU-1NS	85	165	1.94
MU-1W	85	181	2.13
MU-1WS	85	180	2.12

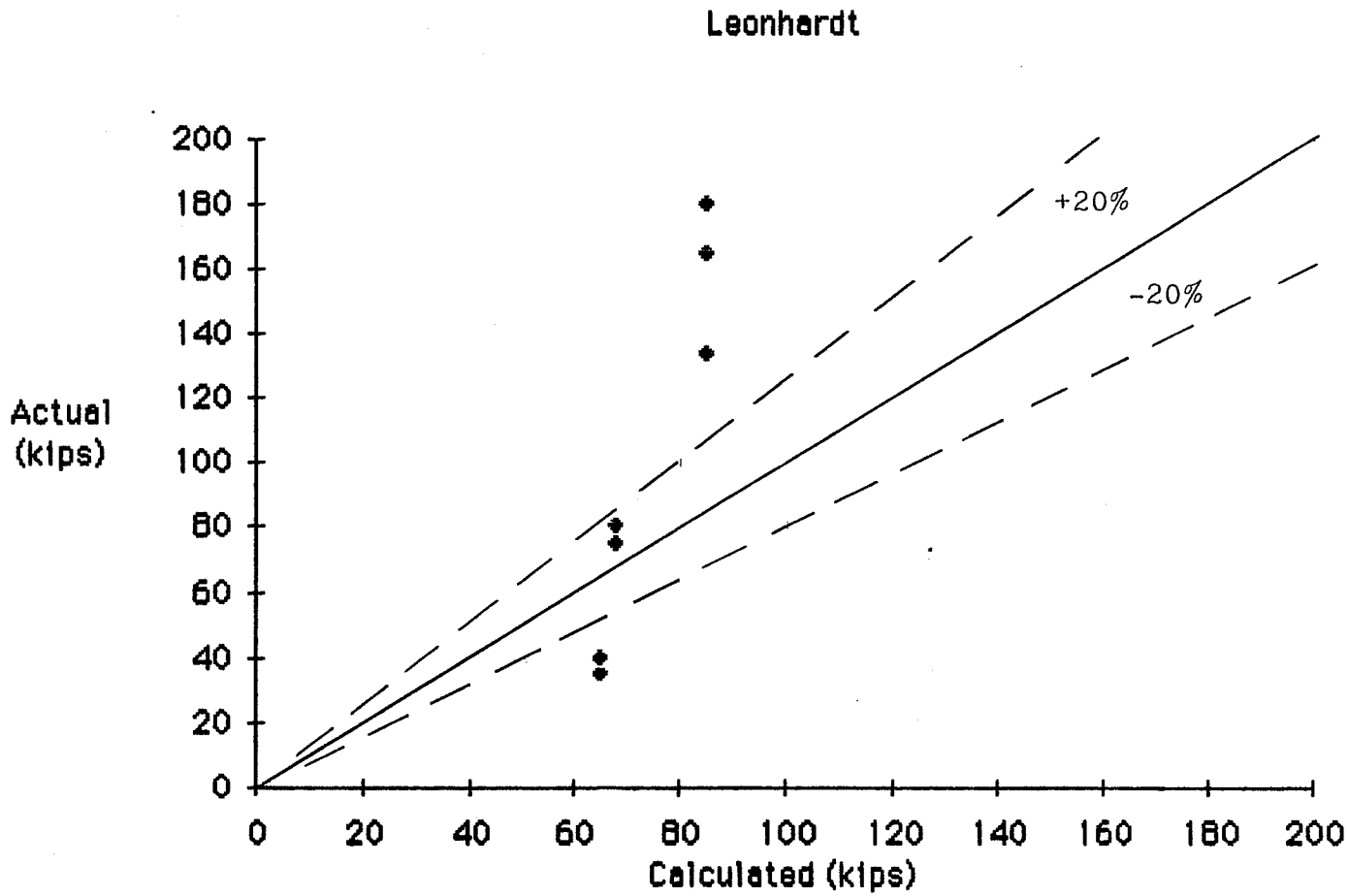

Fig. 4.2 Leonhardt's calculated cracking load vs. actual cracking load

4.1.2 Rhodes and Turner. Rhodes and Turner [7] developed an expression similar to Leonhardt's for the total splitting force, T:

$$T = CF$$

where

C is determined from Figure 1.8

F is the applied prestress force.

Rhodes and Turner also derived a direct expression for the maximum tensile bursting stress, f_n:

$$f_n = B\,F/A_c$$

where

B is determined from Figure 1.8

A_c is the area of the anchorage minus the area of the tendon.

Substituting ACI's modulus of rupture, f_r, for f_n, the predicted cracking value can be determined.

A comparison of the cracking load predicted by this method and the actual cracking load from test data is listed in Table 4.2 and illustrated in Figure 4.3. In general, Rhodes and Turner's equation predictions tended to be overly conservative. The cracking load for the closely-spaced anchorage specimens were too conservative by 154 to 431%. However, for the single wide-width monostrand anchorage specimens, MO-1W and MO-1WS, Rhodes and Turner's equation predictions were unconservative by 30 and 25%, respectively. Since Rhodes and Turner's design equation does not accurately predict results for the closely-spaced anchorage specimens and does not yield constitent results for single anchorage specimens, it is not recommended for the design of post-tensioned bridge decks.

Table 4.2 Rhodes and Turner's calculated versus actual cracking load

Specimen	Calculated Cracking Load	Actual Cracking Load	P_{act}/P_{cal}
MO-1N	15	35	2.33
MO-1NS	15	40	2.67
MO-1W	100	75	0.75
MO-1WS	100	80	0.80
MO-3W	16	80	5.00
MO-3WS	16	85	5.31
MU-1N	73	134	1.84
MU-1NS	73	165	2.26
MU-1W	150	181	1.21
MU-1WS	150	180	1.20
MU-3W	67	190	2.84
MU-3WS	67	170	2.54

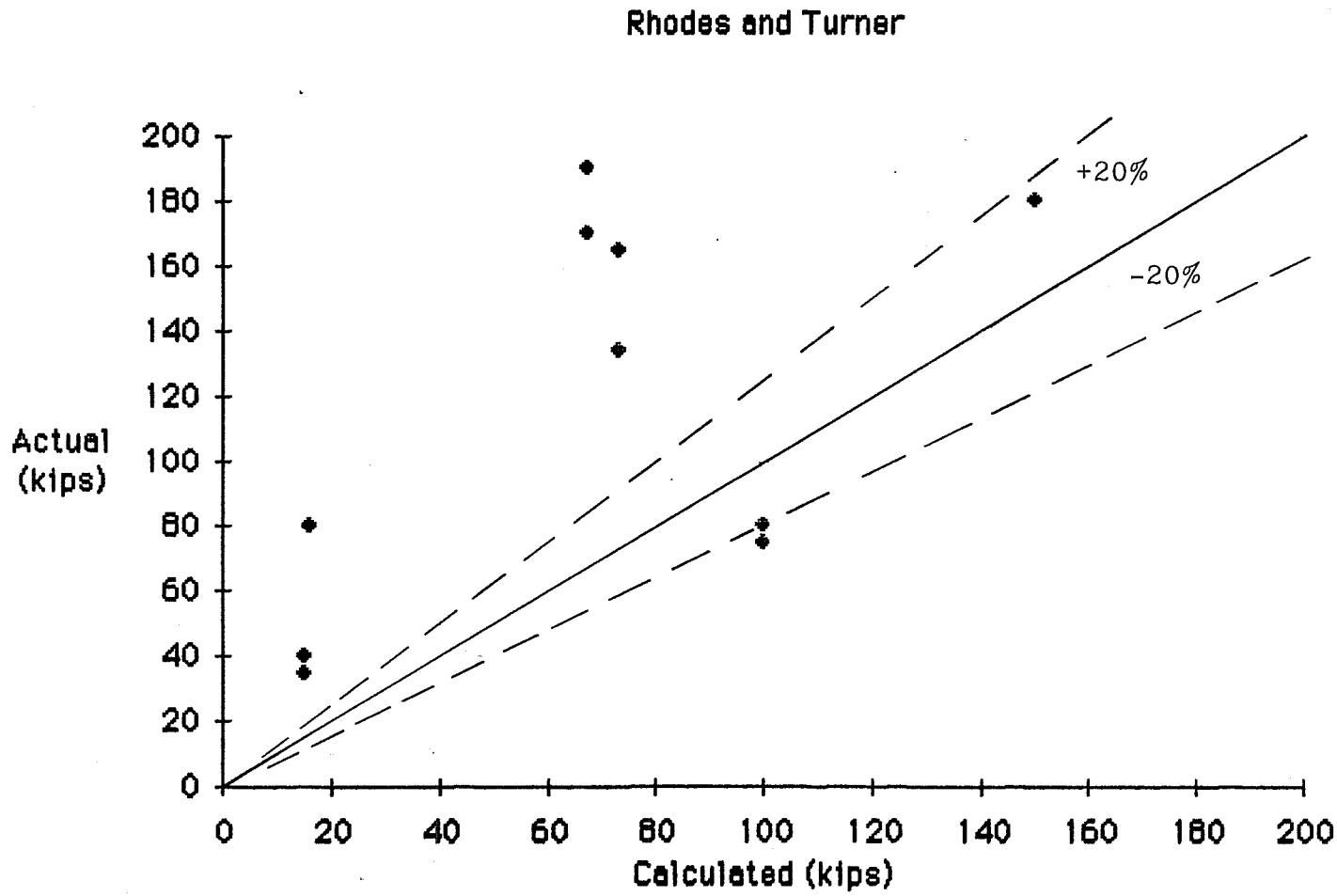

Fig. 4.3 Rhodes and Turner calculated cracking load vs. actual cracking load

1.4.3 Stone and Breen. Stone and Breen's design equation [2] (see Section 1.5.8) calculates the cracking load, P_{cr}, directly:

$$P_{cr} = t\{(f_{sp} / 24)(38a - 120) - 7\} + 39a' + (f_{sp} / 5)\{166 - 975(a' / t)^2\} - 9.1$$

Stone and Breen's test program found that the presents of supplemental reinforcement did increase that cracking load and they accounted for this expected rise by modifying the results of above equation as follows:

$$P'_{cr} = 1.61\, P_{cr} \qquad \text{(For orthogonal reinforcement)}$$

$$P'_{cr} = 2.03\, P_{cr} \qquad \text{(For spiral reinforcement)}$$

Stone and Breen's equation is the only design provision which adequately addresses closely-spaced anchorages. Although not specifically verified in their study, they indicate that a conservative solution should be obtained by replacing the value of t in the above equation with the value 2g which equals twice the edge distance or the distance between the anchorages as shown in Figure 4.4. Also illustrated in Figure 4.4 is the provision for rectangular anchorages where $2a' < 2b'$ and $2a' > 2b'$. Stone and Breen note that for the $2a' < 2b'$ case their design equation should yield conservative results; however, for rectangular anchorages where $2a' > 2b'$, their equation does not apply. Thus, the cracking loads for specimens MO-1N and MO-1NS can not be computed with this method.

A comparison of the cracking load calculated by this method and the actual cracking load from test data is listed in Table 4.3 and illustrated in Figure 4.5. Since Stone and Breen's equation was derived based on empirical results, they limit their design equation to the cases verified by their test results (see Section 1.5.8). This limitation

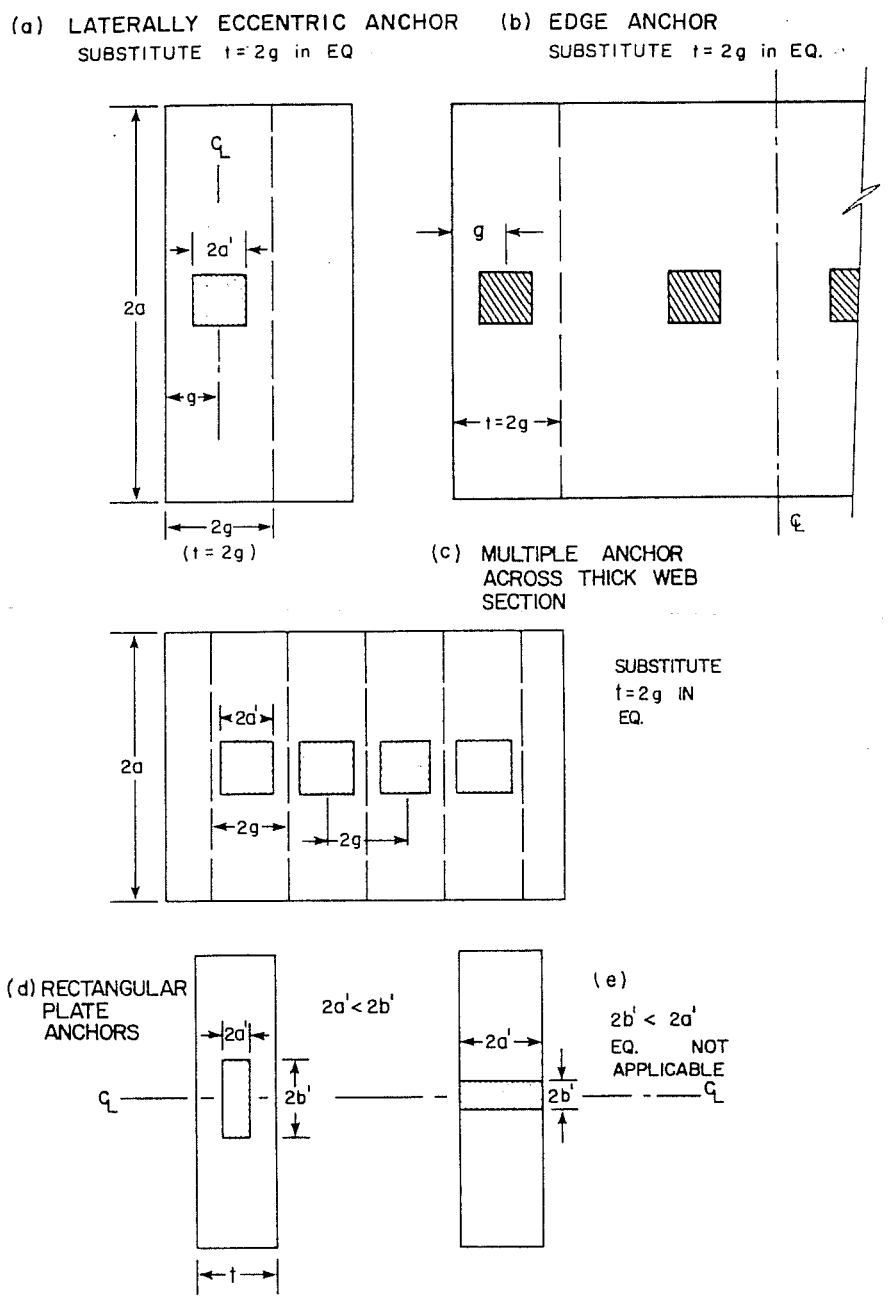

Fig. 4.4 Special cases for Stone and Breen Equation (from Ref. #13)

Table 4.3 Stone & Breen calculated versus actual cracking load

Specimen	Calculated Cracking Load	Actual Cracking Load	P_{act}/P_{cal}
MO-1N	N.A.	35	N.A.
MO-1NS	N.A.	40	N.A.
MO-1W	46	75	1.63
MO-1WS	58	80	1.38
MO-3W	80	80	1.00
MO-3WS	101	85	0.84
MU-1N	67	134	2.00
MU-1NS	84	165	1.96
MU-1W	180	181	1.01
MU-1WS	234	180	0.77
MU-3W	152	190	1.25
MU-3WS	192	170	0.89

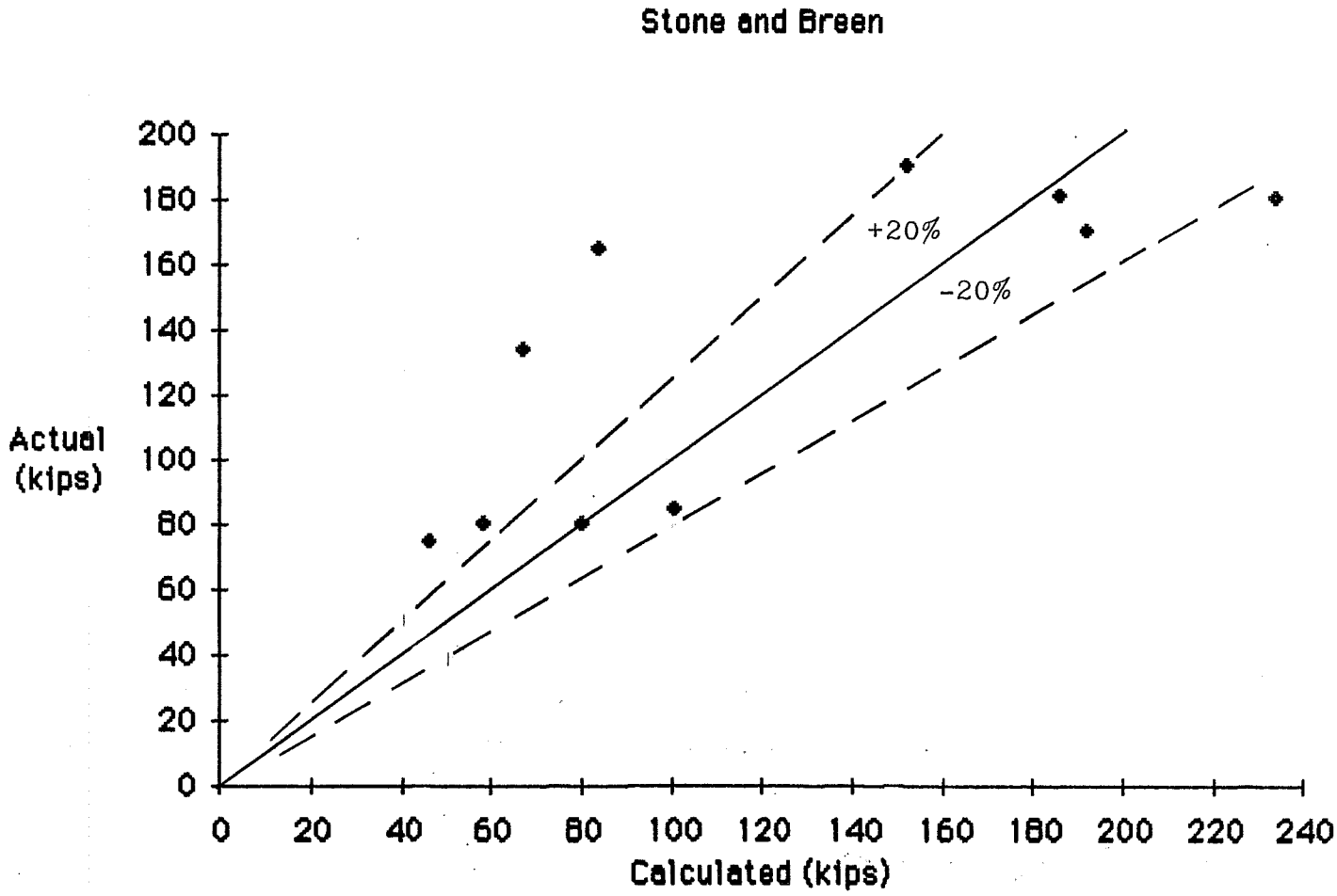

Fig. 4.5 Stone and Breen calculated cracking load vs. actual cracking load

was exceeded in some cases to compute the results in Table 4.3. It also should be noted Stone and Breen's notation can be interpreted in two ways; 2a can be equal to the width of the specimen or the thickness of the slab. Negative cracking loads result when 2a is the slab thickness. The negative values were disregarded as falling outside the limits of the empirical equation and only the results where 2a equal the specimen width were considered.

Overall, Stone and Breen's provisions predict the cracking load for the closely-spaced anchorage specimens better than any of the other provisions discussed thus far. This may be a result of Stone and Breen's effort to include the effects of bearing and spalling stressing in their equation. The expression does overestimate the cracking capacity for the specimens with spiral reinforcement. However, it does provide a reasonable values for orthogonal reinforcement. In general, it is recommended that Stone and Breen's design provisions be used to estimate the cracking load of post-tensioned bridge deck anchorage zones with closely spaced anchorages; but, no increase in P_{cr} should be used to reflect the use of supplement spiral reinforcement.

4.1.4 ACI and PTI. ACI and PTI's design provisions are based on an allowable bearing stress [8] (see Section 1.5.4 and 1.5.5). The permissible bearing stress immediately after tendon anchorage is:

$$f_b = 0.8 f'_{ci} \sqrt{A_2 / A_1} \leq 1.25 f'_{ci}$$

In some cases the allowable bearing stress was controlled by the maximum 1.25 f'_{ci} rule. The cracking load, P_{cr}, was computed by multiplying the allowable bearing stress by anchor plate bearing area.

A comparison of the cracking load calculated by this method and the actual cracking load from test data is listed in Table 4.4 and illustrated in Figure 4.6. The ACI-PTI equation predictions were conservative for all of the specimens except one narrow width

Table 4.4 ACI-PTI Calculated versus Actual Cracking Load

Specimen	Calculated Cracking Load	Actual Cracking Load	P_{act}/P_{cal}
MO-1N	28	35	1.25
MO-1NS	28	40	1.43
MO-1W	52	75	1.44
MO-1WS	52	80	1.54
MO-3W	78	80	1.03
MO-3WS	78	85	1.09
MU-1N	140	134	0.96
MU-1NS	140	165	1.18
MU-1W	140	181	1.29
MU-1WS	140	180	1.29
MU-3W	118	190	1.61
MU-3WS	118	170	1.44

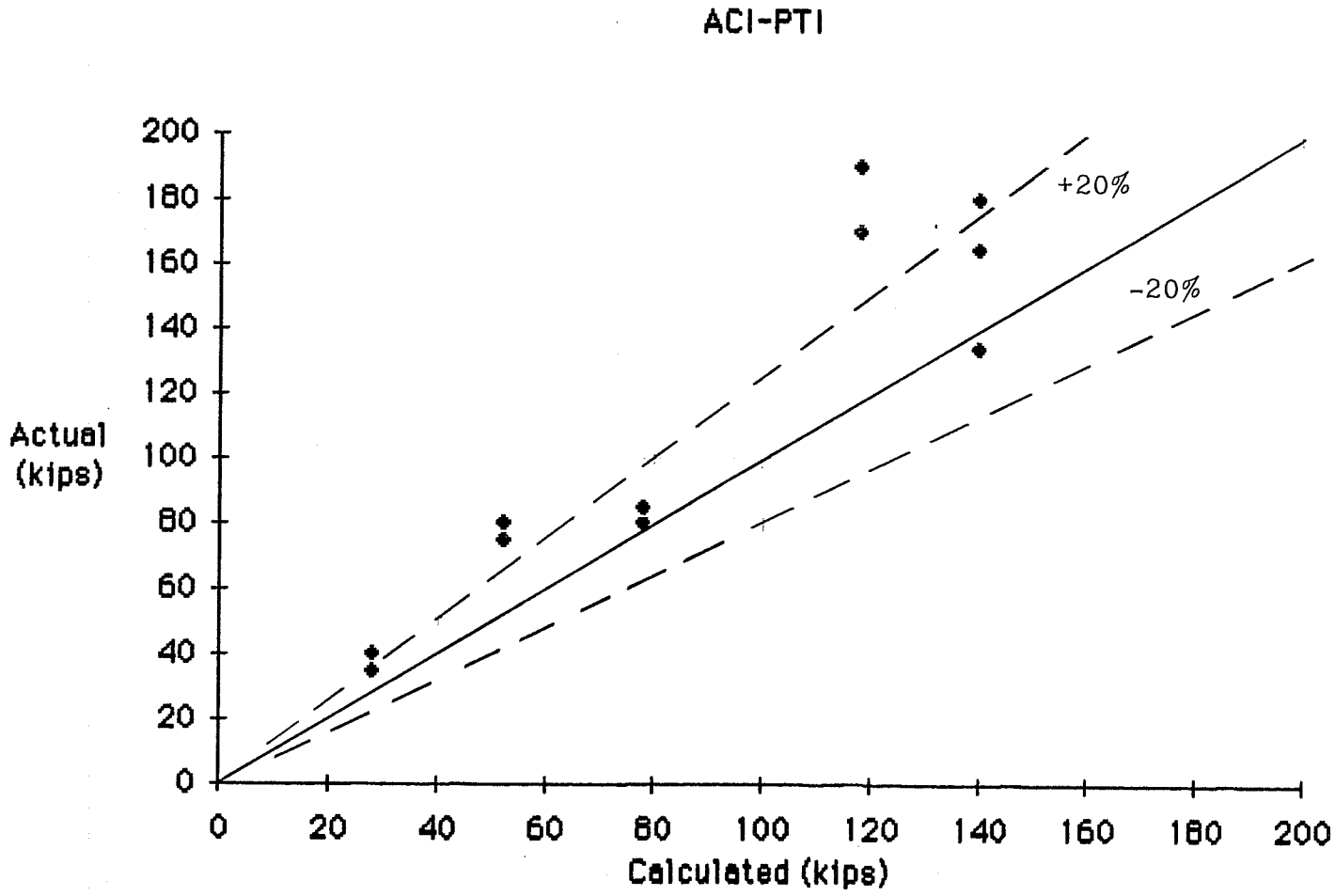

Fig. 4.6 ACI-PTI calculated cracking load vs. actual cracking load

multistrand specimen, MU-1N, which was above 4% the actual value. The majority of the predicted values were within 40% of the actual values. Thus, the ACI-PTI method is recommended as a fast and easy-to-apply method to predict the cracking load for both the single anchorage and closely-spaced anchorage cases.

4.1.5 AASHTO. The AASHTO design provision, like the ACI-PTI equation, is based on an allowable bearing stress. However, the AASHTO Specification is more conservative by limiting the permissible bearing stress to 3000 psi but not more than 0.9 f'_{ci} [11]. The cracking load, P_{cr}, was computed by multiplying the allowable bearing stress by anchor plate bearing area.

A comparison of the cracking load calculated by this method and the actual cracking load from test data is listed in Table 4.5 and illustrated in Figure 4.7. The AASHTO equation predictions were conservative for all of the specimens. However, predicted values were generally overconservative. For the closely-spaced, multistrand anchorage specimens, MU-3W and MU-3WS, the AASHTO provisions were conservative by 304 and 262%, respectively. Thus, the AASHTO method is not recommended as a method to predict the cracking load for post-tensioned bridge decks since it is too conservative.

4.2 Design Recommendations.

Accurate predictions of the cracking behavior of closely-spaced anchorages is essential if the improved durability of post-tensioned bridge decks is to be ensured. If cracks form in the anchorage zone, the advantage of post-tensioning to minimize cracking under service loads is lost. Based on the observed behavior of twelve full scale anchorage zone specimens of an eight inch bridge deck slab and on the comparison of the test results with design provisions, the

Table 4.5 AASHTO calculated versus actual cracking load

Specimen	Calculated Cracking Load	Actual Cracking Load	P_{act}/P_{cal}
MO-1N	33	35	1.06
MO-1NS	33	40	1.21
MO-1W	33	75	2.27
MO-1WS	33	80	2.42
MO-3W	41	80	1.95
MO-3WS	41	85	2.07
MU-1N	93	134	1.44
MU-1NS	93	165	1.77
MU-1W	93	181	1.95
MU-1WS	93	180	1.94
MU-3W	47	190	4.04
MU-3WS	47	170	3.62

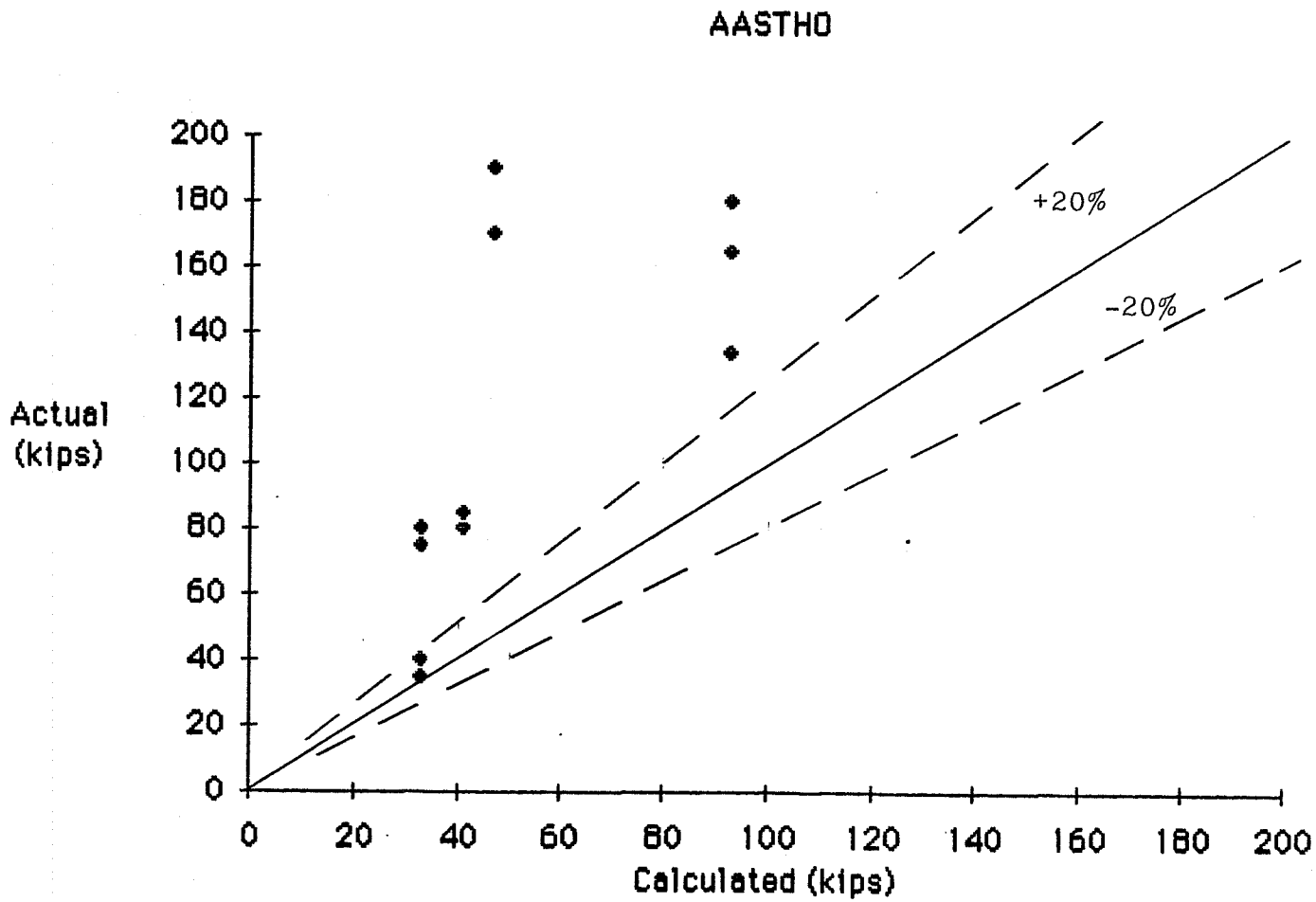

Fig. 4.7 AASHTO calculated cracking load vs. actual cracking load

following recommendations are made in an effort to prevent cracking in post-tensioned bridge deck anchorage zones with closely spaced anchorages:

1. All of the design provisions reviewed were originally developed for post-tensioned girders. Applying these provisions to heavily reinforced and post-tensioned bridge decks yield mixed results. However, the predicted cracking loads based on ACI-PTI's allowable bearing stress provisions were generally conservative for both single and closely-spaced anchorage specimens. Stone and Breen's provision predicted cracking load for the closely-spaced anchorage specimens fairly accurately when the factor for orthogonal reinforcement was used.

2. The width of the anchorage zone influences the post-tensioning cracking load. Thus, for the anchorages located at the end of the slab, a minimum clear distance equal to at least half of the slab thickness should be provided. Also, at the ends of the deck slab, top and bottom slab reinforcement bars in the anchorage zone should be bent and tied to limit the possibility of end-edge cracking.

3. In heavily reinforced bridge decks, additional spiral anchorage zone reinforcement provides only a slight to moderate increase in the cracking or ultimate strength of the anchorage zone.

4. The interaction betwen adjacent, closely-spaced post-tensioned anchorages is favorable. A previously stressed anchor tends to precompress the anchorage zone of an adjacent anchor. Thus it is advantageous to prestress the anchorages in an alternating sequence where every other anchorage is stressed and then the remaining anchorages are stressed. Also to reduce the possibility of end edge splitting, the stressing operations should start at the middle of the slab.

CHAPTER 5

SUMMARY, CONCLUSIONS, AND RECOMMENDATIONS

5.1 Summary

The principle objective of this study was to document the anchorage zone behavior of thin post-tensioned bridge decks with closely-spaced tendon anchorages and to specifically determine if closely-spaced anchorages increase or decrease the cracking and ultimate capacity of post-tensioned bridge deck anchorage zones. The scope was primarily limited to heavily reinforced bridge deck slabs. Many of the study findings may not be applicable to other thin post-tensioned slabs which do not contain the large amounts of conventional bonded reinforcement found in bridge decks. Also the study was also limited to determining trends in the performance of closely-spaced anchorages and not to develop general design provisions for variable slab thicknesses and anchorage spacings.

To study the behavior of post-tensioned bridge deck anchorage zones, an experimental program was undertaken in which twelve full-scale slab anchorage zone specimens were loaded to ultimate capacity. Eight of the specimens contained a single post-tensioning anchorage and four specimens each contained three closely-spaced anchorages. The description of this experimental program and a discussion of the test results were presented in Chapters Two and Three, respectively. A review of the nature of anchorage zone stresses and of current anchorage zone design provisions was presented in Chapter One. In Chapter Four a comparison of the predicted and actual cracking load for the test specimens and recommendations for post-tensioned anchorage zones with closely spaced anchorages were presented.

5.2 Conclusions

In this study, twelve full-scale anchorage zone specimens modeling the behavior of a typical eight inch thick, heavily reinforced and post-tensioned bridge deck were loaded to ultimate capacity. Based on the observed behavior of the limited number of specimens and on a comparison of test data with design provision predictions, conclusions about the anchorage zone behavior of post-tensioned bridge decks with closely-spaced anchorges may be summarized as follows:

1. The interaction between adjacent closely-spaced post-tensioned anchorages is favorable. A previously stressed anchor tends to precompress the anchorage zone of an adjacent anchor and slightly increase its cracking load.

2. In heavily reinforced bridge decks, additional spiral anchorage zone reinforcement provides only a slight to moderate increase in the cracking or ultimate load capacity of the anchorage zone.

3. The width of the anchorage zone influences the post-tensioning cracking load. Thus, for the anchorages located at the end of the slab, a minimum clear distance equal to at least half of the slab thickness should be provided. Also, at the ends of the deck slab, top and bottom slab reinforcement bars in the anchorage zone should be bent and tied to limit the possibility of end-edge cracking.

4. The design provisions reviewed in this study were originally developed for post-tensioned girders. Applying these provisons to heavily reinforced bridge decks yields mixed results. However, in this study, predicted cracking loads based on ACI-PTI's allowable bearing stress provisions were generally conservative for single and closely-spaced anchorages.

5.3 Recommendations for Future Research

Although observed behavior of post-tensioned bridge deck anchorage zones with closely-spaced anchorages was favorable, present design provisions do not provide adequate guidance in predicting the performance of post-tensioned slabs. In general, these design provisions were developed for post-tensioned girders and yield mixed results in slab applications.

It is recommended that future research in this area include an extensive analytical and experimental study of post-tensioned thin slab anchorages zones considering such variables as slab thickness, anchorage eccentricity, anchorage spacing, minimum edge spacing, and the amount and distribution of anchorage zone reinforcement. These results could be used to develop a general equation for predicting cracking loads in post-tensioned slabs. In addition, design provisions for supplemental anchorage zone reinforcement and procedures for calculating its effect on cracking and ultimate loads should be developed. Future research may conclude that in order to accurately predict slab anchorage zone cracking loads, design equations, like Stone and Breen's equation for post-tensioned girders, must include the interaction of bursting, bearing, and spalling stresses instead of treating each individually.

REFERENCES

1. Poston, R. W., "Improving Durability of Bridge Decks by Transverse Prestressing," Ph. D. dissertation, The University of Texas at Austin, December 1984.

2. Stone, W. C., and Breen, J.E., "Design of Post-Tensioned Girder Anchorage Zones," Research Report No. 208-3F, Center for Transportation Research, The University of Texas at Austin, June, 1981.

3. Schlaich, J., "Zum einheitlichen Bemessen von Stahlbetontragwerken," Beton-Und Stahlbetonbau, Verlag Wilhelm, Ernst and Sohn, 1000 Berlin.

4. Guyon, Y., Prestressed Concrete, John Wiley and Sons, Inc., New York, 1953.

5. Guyon, Y., The Limit State Design of Prestressed Concrete, Vol. II: The Design of the Member, Translated by F. H. Turner, John Wiley and Sons, New York, 1974.

6. Leonhardt, F., Prestressed Concrete - Design and Construction, Wilhelm Ernest and Son, Berlin, 1964.

7. Rhodes, B. and Turner, F. H., "Design of End Blocks for Post-Tensioned Cables," Concrete, December 1967.

8. Zielinski, T., and Rowe, R. E., "The Stress Distribution Associated with Groups of Anchorages in Post-Tensioned Concrete Members," Cement and Concrete Association, Research Report No. 13, London, October 1962; No. 9, London, September 1960.

9. American Concrete Institute, Building Code Requirements for Reinforced Concrete and Commentary (ACI 318-83), Detroit, Michigan, 1983.

10. Post-Tensioning Institute, Post-Tensioning Manual, 4th Edition, Phoenix, Arizona, 1985.

11. American Association of State Highway and Transportation Officals, Standard Specifications for Highway Bridges, 13th Edition, Washington, D. C., 1983.

12. Comité Euro-International Du Béton (CEB) and the Féderation Internationale de La Précontrainte (FIP), Model Code for Concrete Structures, English Translation, 1983.

13. Stone, W. C., and Breen, J. E., "Design of Post-Tensioned Girder Anchorage Zones," PCI Journal, Vol. 29, No. 2, March-April 1984, pp. 28-61.

14. "Specification for Unbonded Single Strand Tendons," PCI Journal, Vol. 30, No. 2, March-April 1985, pp. 22 -39.

15. Lin, T.Y., and Burns, N. H., Design of Prestressed Concrete Structures, John Wiley and Sons, Inc., New York, 1981.